

International Association for Gondwana Research



2021 Convention & 18th International Conference on Gondwana to Asia

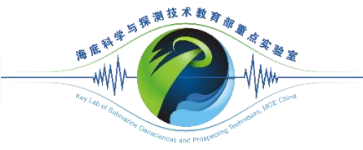
Abstract Volume

Editors

Sanzhong Li¹ and M. Santosh²

¹ Key Lab of Submarine Geosciences and Prospecting Techniques, MOE
Ocean University of China, Qingdao 266100, China

² School of Earth Sciences and Resources, China University of Geosciences Beijing, 29
Xueyuan Road, Beijing 100083, China



青岛海洋科学与技术试点国家实验室
Pilot National Laboratory for Marine Science and Technology (Qingdao)



Organized by

Key Lab of Submarine Geosciences and Prospecting Techniques, MOE
Ocean University of China

Pilot National Laboratory for Marine Science and Technology (Qingdao)

National Natural Science Foundation of China

September 17-21, 2021, Qingdao

International Association for Gondwana Research

2021 Convention & 18th International Conference on Gondwana to Asia

Abstract Volume

Editors

Sanzhong Li and M. Santosh

Published by the International Association for Gondwana Research

Headquarters: Division of Interdisciplinary Science,
Kochi University, Akebono-cho 2-5-1, Kochi 780-8520, Japan

Pages: 99

© 2021, International Association for Gondwana Research

Contents

Carboniferous–Triassic subduction in East Qinling <i>Bader Thomas, Franz Leander, Zhang Lifei, Mullis Joseph, Li Xiaowei</i>	1
Island-arc crustal growth rates along the Izu-Bonin-Mariana subduction system <i>Bai Yongliang, Zhang Diya</i>	3
Generation of andesite through partial melting of basaltic metasomatites in the mantle wedge: insight from quantitative study of Andean andesites <i>Chen Long, Zheng Yong-Fei, Xu Zheng, Zhao Zi-Fu</i>	5
Geochemical and Seismic Tomography Constraints of Two-Layer Magma Chambers beneath the Bimodal Volcanism: A Case Study of Late Cenozoic volcanic rocks from Ulleung Island and Mt. Changbai (Paektu) <i>Chen Shuang-Shuang, Lee Seung-Gu, Simutè Saulè, Fichtner Andreas, Lee Tae Jong, Lee Youn-Soo, Liu Jia-Qi, Gao Rui</i>	6
Origin and accumulation process of crude oil in the Dongsha uplift far from the source rocks in Pearl River Mouth Basin, South China Sea <i>Duan Wei, Tian Jin-Qiang, Li San-Zhong, Long Zulie</i>	8
Maihantewula ophiolitic mélange from the Great Xing'an Range, NE China: Geochronology, geochemistry and tectonic implications for the geodynamic setting <i>Feng Zhiqiang, Liu Yongjiang, Li Weimin, Li Xiaoyu, Jiang Liwei</i>	11
A curious case of continental breakup across an orogenic front <i>Foulger Gillian R.</i>	12
New Paleomagnetic Results from the South Shetland Islands: Implications for the Cretaceous Tectonic Framework of the Antarctic Peninsula <i>Gao Liang, Pei Junling, Zhao Yue, Yang Zhenyu, Riley Teal R., Liu Xiaochun, Zhang Shuanhong, Liu Jianmin</i>	13
Ocean Plate Stratigraphy of a long-lived Precambrian subduction-accretion system: The Wutai Complex, North China Craton <i>Gao Pin, Santosh M., Kwon Sanghoon, Kim Sung Won</i>	15
Reconstructing seepage activities over the past 20000 yrs in the Okinawa Trough: Evidences from methane index and trace metals <i>Guan Hongxiang, Liu Lei, Hu Yu, Sun Zhilei, Wu Nengyou</i>	16
Opening of the West Paleo-Tethys Ocean: Constraints from zircon U-Pb-Hf isotopic and geochemical characteristics of the earliest Devonian meta-mafic rocks in Saualpe basement, Eastern Alps <i>Guan Qingbin, Liu Yongjiang, Neubauer Franz</i>	17
Gravity and Magnetic Characteristics of Micro-blocks in the Subduction System of Southeast Asia <i>Guan Xueting, Jiang Suhua, Li Sanzhong, Wei Dong, Liu Jie, Suo Yanhui, Zhang Jianli</i>	18
A rare earth element and Nd isotopic investigation of Neoproterozoic iron formations: Constraints on Neoproterozoic seawater compositions <i>Hu Jun, Wang He</i>	19
The influence of the magnetic structure complexity of the oceanic crust on the marine magnetic anomalies <i>Hu Yuewei, Zhang Jianli, Jiang Zhaoxia, Li Sanzhong</i>	21
Permian-Triassic A-type and I-type granites in the Schladming Complex, Austroalpine Unit: Constraints on subduction of Paleo-Tethys Ocean in the Eastern Alps <i>Huang Qianwen, Liu Yongjiang, Genser Johann, Neubauer Franz, Chang Ruihong, Yuan Sihua, Guan Qingbin, Yu Shengyao</i>	23
Tsunami origin from focal mechanism solutions of global Tsunami earthquakes <i>Jia Zhongjia, Zhu Junjiang, Ou Xiaolin, Zhang Shengsheng, Chen Ruixue, Zhang Shaoyu</i>	25
The Trials and Tribulations of the Hawaii hot spot model	

<i>Jiang Zhaoxia, Li Sanzhong, Liu Qingsong, Zhang Jianli, Zhou Zaizheng, Zhang Yuzhen</i>	26
Mg isotopic fractionation involving magmatic-hydrothermal transition recorded in the Himalayan granites	
<i>Li Dong-Yong, Teng Fang-Zhen, Xiao Yilin</i>	28
Numerical modeling of the coupling between tectonism and sedimentation: A case from the Yangjiang sag of Northern South China Sea	
<i>Li Fakun, Dai Liming</i>	29
Geochemical and lead isotope compositions of olivine-hosted melt inclusions from Okinawa Trough: Implications for petrogenesis and slab subduction	
<i>Li Xiaohui</i>	30
High-silica rhyolites in the latest stage of massive Cretaceous volcanism in the SE China: insights into modified crustal sources and low-pressure magma chamber	
<i>Li Xi-Yao, Li Sanzhong, Suo Yanhui, Wang Pengcheng, Zhou Jie</i>	31
Disintegration and deformation characteristics of the Keluo Complex in Nenjiang, Heilongjiang Province: Evidence for multistage evolution of Da Hinggan Mountains	
<i>Liang Chenyue, Song Zhiwei, Liu Yongjiang, Zheng Changqing, Neubauer Franz, Chen Long, Liu Xiaojing</i>	32
Microplate identification of mid-ocean ridge system in South America and the eastern Pacific Ocean based on potential field data processing and analysis	
<i>Liu Jie, Li Sanzhong, Jiang Suhua, Suo Yanhui</i>	33
Dynamics of Closure of the Proto-Tethys Ocean: the Southeast Asian Tethys realm	
<i>Liu Junlai, Chen Xiaoyu, Fan Wenkui, Shan Hongshuai, Yan Jiaxin, Ding Xu, Zhao Tianyu, Yu Xinqi, Liu Zhenghong, Xu Zhongyuan</i>	35
The impact of dust on the Neoproterozoic climate	
<i>Liu Peng</i>	36
3D numerical simulation of deep-shallow coupling in pull-apart basins	
<i>Liu Ze, Li Sanzhong, Wang Guangzeng, Ding Xuesong, Wang Pengcheng, Dai Liming, Suo Yanhui, Wajid S., Bukhari Hanif</i>	37
A step-like crustal growth pattern in response to the evolution of supercontinent cycles: Evidence from the eastern Central Asian Orogenic Belt	
<i>Long Xinyu, Tang Jie, Xu Wenliang, Sun Chenyang, Luan Jinpeng</i>	38
Pre-Alpine tectonic evolution of the Eastern Alps: From Prototethys to Paleotethys	
<i>Neubauer Franz, Liu Yongjiang, Dong Yunpeng, Chang Ruihong, Genser Johann, Yuan Sihua</i>	39
Frequency-dependent anisotropy in partially saturated porous rock with multiple sets of meso-scale fractures	
<i>Pang Shuo, Xing Huilin, Stovas Alexey</i>	41
Detrital zircon U-Pb ages, Lu-Hf isotopes and whole-rock geochemical and isotope data from greywacke sandstones of eastern Kazakhstan	
<i>Perfilova A., Safonova I., Aoki S., Komiya T., Wang B., Sun M.</i>	42
Jurassic fold-thrust belts of overriding plate on the northeastern North China record Paleo-Pacific Plate subduction	
<i>Qiu Liang, Yan Dan-Ping, Kong Ruoyan, Mu Hong-Xu, Sun Weihua, Sun Shouheng, Dong Xiaoyu, Ariser Shahnawaz</i>	44
S-type granites in the southern East Kunlun Belt, northern Tibetan Plateau: Petrogenesis and tectonic implications	
<i>Ren Xiang, Dong Yunpeng, He Dengfeng, Sun Shengsi</i>	45
The Tekturmas ophiolite belt of central Kazakhstan: geology and ore potential	
<i>Safonova I.Yu., Antonyuk R.M., Lis S.N., Kasimov A.A., Perfilova A.A., Savinskiy I.A., Kotler P.</i>	46
Tectonic erosion at Pacific-type convergent margins of the Paleo-Asian Ocean: new evidence from Central Asia	
<i>Safonova I.Yu., Perfilova A.A., Savinskiy I.A., Gurova A.V.</i>	48
Reconstruction ocean plate stratigraphy and thrust duplexes of Itmurundy accretionary complex, Northern Balkhash, Central Kazakhstan	
<i>Savinskiy I., Safonova I.Yu., Maruyama S., Perfilova A., Gurova A.</i>	50
Discovery of Middle Jurassic lamprophyre in southeastern Guangxi Province and its tectonic implications	
<i>Shi Yu, Tang Yuan-Lan, Hu Xiu-Mian, Liu Xi-Jun, Wang Yong-Qiang, Sun Yi-Rong</i>	53
Thermal state and evolving geodynamic regimes of the Meso- to Neoproterozoic North China Craton	
<i>Sun Guozheng, Liu Shuwen, Cawood Peter A., Tang Ming, Hunen Jeroen van, Gao Lei,</i>	

<i>Hu Yalu, Hu Fangyang, Li Sanzhong</i>	55
Large-scale asymmetry in thickness of crustal accretion at the Southeast Indian Ridge due to deep mantle anomalies	
<i>Suo Yanhui, Li Sanzhong, Cao Xianzhi</i>	56
Three-dimensional velocity structure near the 2021 M7.3 earthquake sequence in Tohoku, Japan	
<i>Tan Yuyang, Xing Huilin, Pang Shuo, Jin Zongwei, Wang Jianchao</i>	57
Petrogenesis of Early Paleozoic I-type granitoids in the Wuyi–Yunkai orogen, South China	
<i>Tang Yuan-Lan, Shi Yu, Hu Xiu-Mian, Liu Xi-Jun, Wang Yong-Qiang, Sun Yi-Rong</i>	58
Microfractures study on the metamorphic rock buried hill reservoirs in Bozhong Sag, Bohai Bay Basin	
<i>Tao Wei, Guo Lingli, Li Sanzhong, Liu Yongjiang, Wang Guangzeng, Chen Xin, Lv Chunxiao</i>	60
Zircon U-Pb ages of paragneisses in the Grove Mountains, East Antarctica: evidence for poly-metamorphic events and tectonic implications for supercontinent assembly	
<i>Tong Laixi, Liu Xiaohan, Li Chao, Liu Zhao</i>	61
Early Paleozoic low pressure-high temperature metamorphism and tectonic implications: insights from garnet-amphibolite and meta-sediments in the northern Yili Block (NW China)	
<i>Wang Bo, Deng Ju</i>	62
Response characteristics of basins on both sides of the Yangjiang-Yitong'ansha Fault Zone to the Huizhou Movement and their genesis mechanism	
<i>Wang Guangzeng, Li Sanzhong, Liu Xinying, Yang Yue, Zhan Huawang, Yu Haiyang, Ma Xiaoqian, Cheng Haohao</i>	63
3D Geological Model for Active Tectonics: from North China Area to Japan Subduction Zone	
<i>Wang Jianchao, Tan Yuyang, Jin Zongwei, Pang Shuo, Xing Huilin</i>	64
Weak linkage between subduction initiation and plateau collision at the Ontong-Java Plateau and the Solomon Island Arc	
<i>Wang Liangliang, Dai Liming, Gong Wei, Li Sanzhong, Jiang Xiaodian, Foulger Gillian, Dong Hao, Li Zhonghai</i>	65
Structural, kinematic analysis in the northern margin of the South China Sea	
<i>Wang Pengcheng, Li Sanzhong, Suo Yanhui, Guo Lingli, Wang Guangzeng, Zhou Jie, Jiang Suhua, Liu Ze</i>	67
Zircon geochronology and Hf isotopes of dacite from Hezhou, northeastern Guangxi and its geological significance	
<i>Wang Yong-Qiang, Shi Yu, Hu Xiu-Mian, Liu Xi-Jun, Tang Yuan-Lan, Sun Yi-Rong</i>	68
Tectonic coupling between the Dabie Orogen and the Hefei Basin	
<i>Wang Yongsheng, Bai Qiao, Jiang Cong, Yang Juanhao</i>	70
Eocene thickening without extra heat in a collisional orogenic belt: A record from the Eocene metamorphism in mafic dike swarms within the Tethyan Himalaya, southern Tibet	
<i>Wang Yuhua</i>	72
Linking ~1.4-0.8 Ga volcanic-sedimentary records in eastern Central Asian Orogenic Belt with southern Laurentia in supercontinent cycles	
<i>Wang Zhiwei, Peng Jia, Wang Zhihui, Zhang Yanjie, Xu Bei, Tian Yingjie</i>	73
Distribution of Mesozoic-Cenozoic magmatic arc in East Asian Continental Margin and their response to the Paleo-Pacific Plate subduction evidence from gravity and magnetic anomalies	
<i>Wei Dong, Jiang Suhua, Li Sanzhong, Zhang Jianli, Guan Xueting, Suo Yanhui</i>	74
Environmental controllings on coral reefs in the Yongxing Island, Xuande Atoll, Xisha, South China Sea—the evidence from rare earth elements	
<i>Wei Haotian, Zhao Yanyan, Yang Jun, Long Haiyan, Li Sanzhong, Bi Naishuang</i>	75
Nature and evolution of the northern margin of the Tarim Craton and its adjacent block in NW China during the Neoproterozoic: A review and new perspective	
<i>Wu Hongxiang, Zhang Fengqi, Wang Caiyun, Dilek Yildirim, Zhu Kongyang, Lin Xiubin, Cheng Xiaogan, Chen Hanlin</i>	76
Complex strata architectures of the Luzon forearc basin constrained by arc–continent collision process	
<i>Xu Shumei, Shu Pengcheng, Li Sanzhong</i>	78
Genesis of the compositional diversity in composite batholith: a case study in the Laiyuan granitoid complex, central NCC	
<i>Xue Fei, Santosh M., Xie H.J., Wu G., Zhu M.T., Zhong W., Mei M., Liu J.</i>	79

Multiple enrichment of subcontinental lithospheric mantle with Archean to Mesozoic components: Evidence from the Chicheng ultramafic complex, North China Craton	
<i>Yang Fan</i>	80
Controlling mechanisms of sea surface salinity in the Central South China Sea over the last 12.6ka	
<i>Yang Jun, Zhao Yanyan, Wei Haotian, Long Haiyan, Li Sanzhong, Bi Naishuang</i>	81
Student Himalayan Exercise Program 9 years	
<i>Yoshida Masaru and Student Himalayan Exercise Project</i>	82
Multistage anatexis during tectonic evolution from oceanic subduction to continental collision: A review of the North Qaidam UHP Belt, NW China	
<i>Yu Shengyao, Li Sanzhong, Liu Yongjiang, Zhang Jianxin, Peng Yinbiao</i>	84
Mafic-ultramafic rocks in the Buqingshan Complex of the East Kunlun Orogen, northern Tibetan Plateau: Remnants of the Paleo-Tethys Ocean	
<i>Yue Yuangang, Dong Yunpeng, Sun Shengsi, He Dengfeng, Hui Bo, Ren Xiang, Zhang Bin, He Weidong</i>	86
Petrological and geochemical constrains for carbon bearing fluid evolutions and its implications for geological CO2 capture in sandstone aquifers, Yinggehai Basin, South China Sea	
<i>Yu Lei, Li Sanzhong, Wu Keqiang, Zhao Yanyan, Liu Li, Liu Na, Pang Kun</i>	87
Formation of the wide rift system at the northern South China Sea: insight from architecture and nature of basement	
<i>Zhang Cuimei, Sun Zhen, Zhao Minghui, Pang Xiong, Manatschal Gianreto</i>	89
The northern boundary of the Proto-Tethys Ocean: Constraints from early Paleozoic deformation and detrital zircon geochronology of the North Qinling Terrane and Qinling-Qilian connection zone	
<i>Zhao Shujuan, Li Sanzhong, Cao Huahua, Li Xiyao</i>	90
Petrogenesis and geodynamic implications of collisional granitoid from the northern Qinghai-Tibet Plateau	
<i>Zhong Shihua, Li Sanzhong, Qu Hongying, He Shuyue, Liu Guoyan, Lai Zhiqing</i>	92
Does U-Pb signatures of river sediment represent the age distributions in the catchments? A study of variegated catchments along the eastern border of the Songliao Basin, NE China	
<i>Zhou Jianping, Dunkl István, Liu Yongjiang, Li Sanzhong, Li Weimin, Eynatten Hilmar von</i>	94
The strike-slip structural model and dynamics concerning middle section of Pearl River Mouth Basin in north margin of South China Sea	
<i>Zhou Jie, Li Sanzhong, Suo Yanhui</i>	95
Characteristics and Environmental Significance of Late Carboniferous Brachiopods within the Qijiagou Area, Southern Margin of the Junggar Basin	
<i>Zhou Xiaohu, You Jiyuan</i>	96
Global large-magnitude oceanic intraplate seismicity: Implications for lithosphere evolution	
<i>Zhu Junjiang, Li Sanzhong, Xing Huilin, Jia Zhongjia, Ou Xiaolin, Zhang Shaoyu,</i> <i>Chen Ruixue, Cao Xianzhi</i>	98
Study on the characteristics of horizontal zoning of fluorite orebody: A case of Wushan fluorite deposit in Zhejiang	
<i>Zou Hao, Li Min, Yu Liming, Xiao Bin, Yu Huidong</i>	99

Carboniferous–Triassic subduction in East Qinling

Thomas Bader^{1*}, Leander Franz², Lifei Zhang¹, Joseph Mullis², Xiaowei Li³

¹ Key Laboratory of Orogenic Belts and Crustal Evolution, MOE, School of Earth and Space Science, Peking University, Beijing 100871, P. R. China,

² Department of Environmental Sciences, Mineralogy and Petrography, University of Basel, 4056 Basel, Swiss Confederation

³ State Key Laboratory of Geological Processes and Mineral Resources and School of Earth Sciences and Resources, China University of Geosciences, Beijing 100083, P. R. China

*Email: thomas.bader@pku.edu.cn

Ancient orogens are pivotal parts in the line of evidence paleogeographic reconstructions base on. The Qinling–Tongbai–Hong’an–Dabie–Sulu Orogen helps to understand how the North China (NCC) and Yangtze–Cathaysia (YC) cratons evolved from Rodinia to Gondwana and Eurasia. Subduction–accretion–collision processes formed the North Qinling orogenic collage at the southern margin of NCC from Cambrian to Lower Devonian times, and subduction underneath North Qinling led to the Triassic–Early Jurassic collision of NCC and YC. The limited knowledge of the intervening period causes controversy about the relation of both cratons with Gondwana: they could have been islands detached from, or constituents of, Gondwana, and even a joint NCC–YC island continent could have existed. Conclusive evidence for orogenic processes such as metamorphism during burial and exhumation at Lower Devonian–Triassic times would imply prolonged plate convergence and therefore rule out several paleogeographic configurations.

This contribution utilizes phase equilibrium modeling and conventional thermobarometry to determine new pressure–temperature (P–T) paths for a section from North Qinling into YC at about 111° eastern longitude. Here, we highlight the characteristics of the documented tectonometamorphic units from north to south. The Qinling Complex features a lower crustal mélangé containing (U)HP and (U)HT metamorphic rocks. The peak metamorphism happened episodically at c. 520–420 Ma, exhumation to mid-crustal levels proceeded till 389 Ma, and the reactivation of faults, reheating, and fluid percolation occurred till c. 315 Ma (Bader et al., 2013; Dong et al., 2018). The Wuguan Complex is an imbrication of nappes and comprises siliciclastic sediments and scarce tuffites. Garnet grew discontinuously during two stages of amphibolite facies

metamorphism. The first stage (560–710 °C, 0.5–0.7 GPa) was diverse, pointing to a different origin of the nappes, one being the Qinling Complex. The second at c. 590 °C, 0.9 GPa overprinted the entire Wuguan Complex equally, wherefore the juxtaposition of the nappes ended at or before the second metamorphic stage. Geochronology dates both stages at c. 305 Ma and 252 Ma, respectively (Chen et al., 2020). The Proterozoic basement of the Douling Complex and Wudang Shan shows upper amphibolite to granulite facies metamorphism at 565–745 °C, 0.80–0.95 GPa and 760–825 °C, 0.7–0.9 GPa, respectively. Triassic low-grade metamorphism regionally extends across both units, created stilpnomelane in metapelites and magnesioriebeckite in mafic schists, and widely obscured basement features. We estimated c. 300 °C, 0.5–0.8 GPa and 270–330 °C, 0.5–0.9 GPa, respectively. Mafic schists from Wudang Shan locally contain blueschist facies tension gashes with a mineralization of epidote, magnesioriebeckite–winchite, and albite. Primary, pseudo-secondary, and secondary fluid inclusions in epidote and albite contain a low-saline hydrous fluid, and isochores concur with the metamorphic P–T estimates. Medium-grade metamorphism at 490–550 °C, c. 1.2 GPa characterizes the central section of Wudang Shan to the southwest of the Liangyong Fault. It predates the regional low-grade metamorphism but both regimes belong to one and the same orogenic cycle, and the low-grade metamorphism reflects the juxtaposition of medium- and low-grade nappes during exhumation. After the pressure peak of the low-grade metamorphism, the Wudang Shan evolved into a metamorphic core complex. A Triassic age is revealed by 40Ar/39Ar and (U-Th)/He ages of c. 235 Ma and 230–220 Ma while apatite fission track modeling proves subsequent cooling to 130–150 °C at 240–200 Ma (Dong et al.,

2018 and therein; Hu et al., 2006).

An along-strike correlation across the orogen identifies the Guishan Complex of Tongbai–Hong’an as extension of the Wuguan Complex. The low-grade metamorphism ties the Douling Complex and Wudang Shan to the Susong–Zhangbaling blueschist–greenschist belt extending south of Tongbai–Hong’an–Dabie–Sulu. However, the exhumation of material buried along a geotherm of about 12 °C/km in a metamorphic core complex is unique. Our field work and laboratory analysis did not reveal a counterpart of the Huwan Mélange, a mechanical mixture of oceanic and continental material—likely with blocks from the Qinling Complex—northerly abutting the Triassic HP–UHP units of Hong’an. The Huwan Mélange shows quartz eclogite facies metamorphism at c. 310 Ma, protracted and prolonged garnet growth (c. 400–255 Ma; (Cheng et al., 2018) as well as multiple broad peaks in a continuum (457–223 Ma) of metamorphic zircons (Zhou et al., 2015 and therein).

The reactivation of the Qinling Complex, the two-phase metamorphism at lower crustal levels with mechanical mixture of material in the Wuguan Complex, and the episodic evolution of the Huwan Mélange are snapshots of Lower Devonian–Permian orogenic processes, consistent with prolonged subduction beneath North Qinling with stress coupling between hanging- and foot-wall plate. The paucity of contemporaneous arc magmatic rocks may be a challenge to this deduction, but broad gaps in arc magmatism also occur in the history of the Alps and the Himalayas. Possible reasons for such gaps can be a flat slab subduction zone, specific plate geometries, and stalling of the subduction of hydrated oceanic lithosphere (Yang et al., 2020). A prolonged orogenic history is inconsistent with the amalgamation of NCC to Gondwana and supports paleogeographic reconstructions with NCC as Devonian–Permian island continent. While Carboniferous–Permian subduction at the northern margin of NCC led to its accretion to paleo-Asia (Eizenhöfer and Zhao, 2018),

subduction on its southern margin commenced the subsequent welding with YC.

References

- Bader, T., Franz, L., Ratschbacher, L., Capitani, C. de, Webb, A.A.G., Yang, Z., Pfänder, J.A., Hofmann, M., Linnemann, U., 2013. The Heart of China revisited: II Early Paleozoic (ultra)high-pressure and (ultra)high-temperature metamorphic Qinling orogenic collage. *Tectonics* 32, 922–947.
- Chen, L., Liu, X., Qu, W., Hu, J., 2020. Metamorphic evolution and ⁴⁰Ar/³⁹Ar geochronology of the Wuguan complex, eastern Qinling area, China: Implications for the late Paleozoic tectonic evolution of the Qinling orogen. *Lithos* 358–359, 105415.
- Cheng, H., Vervoort, J.D., Dragovic, B., Wilford, D., Zhang, L., 2018. Coupled Lu–Hf and Sm–Nd geochronology on a single eclogitic garnet from the Huwan shear zone, China. *Chemical Geology* 476, 208–222.
- Dong, Y., Neubauer, F., Genser, J., Sun, S., Yang, Z., Zhang, F., Cheng, B., Liu, X., Zhang, G., 2018. Timing of Orogenic Exhumation Processes of the Qinling Orogen: Evidence From ⁴⁰Ar/³⁹Ar Dating. *Tectonics* 37, 4037–4067.
- Eizenhöfer, P.R., Zhao, G., 2018. Solonker Suture in East Asia and its bearing on the final closure of the eastern segment of the Palaeo-Asian Ocean. *Earth-Science Reviews* 186, 153–172.
- Hu, S., Raza, A., Min, K., Kohn, B.P., Reiners, P.W., Ketcham, R.A., Wang, J., Gleadow, A.J.W., 2006. Late Mesozoic and Cenozoic thermotectonic evolution along a transect from the north China craton through the Qinling orogen into the Yangtze craton, central China. *Tectonics* 25, TC6009.
- Yang, J., Lu, G., Liu, T., Li, Y., Wang, K., Wang, X., Sun, B., Faccenda, M., Zhao, L., 2020. Amagmatic Subduction Produced by Mantle Serpentinization and Oceanic Crust Delamination. *Geophys. Res. Lett.* 47.
- Zhou, L.-G., Xia, Q.-X., Zheng, Y.-F., Chen, R.-X., Hu, Z., Yang, Y., 2015. Tectonic evolution from oceanic subduction to continental collision during the closure of Paleotethyan ocean: Geochronological and geochemical constraints from metamorphic rocks in the Hong’an orogen. *Gondwana Research* 28, 348–370.

Island-arc crustal growth rates along the Izu-Bonin-Mariana subduction system

Yongliang Bai*, Diya Zhang

China University of Petroleum, Qingdao 266580, China
*Email: ylbai@upc.edu.cn

1 Introduction

The temperature field of the subduction zone combined with the melt migration path has been confirmed to be the first order control on the arc position (Grove et al., 2009) and the mantle wedge thermal structure is the primary control on arc magma composition (Turner et al., 2016). In addition to the arc position and composition, the arc crustal growth rate is a key parameter for understanding island-arc magmatism in subduction zones. However, whether the temperature structure of the subduction zone is still a main control on the island-arc crustal growth rate remains unknown. The gravity inversion will be used to map the island-arc crustal growth rate along the Izu-Bonin-Mariana (IBM) arc strike, and the potential controlling factors on the island arc magmatism will be discussed.

2 Methodology

The cross sectional area of the magma added to the island-arc crust along an arc-orthogonal profile can be estimated by integrating the growth in the crustal thickness. The arc crustal growth thickness is the result after removing the initial basement thickness from the present arc crustal thickness, and the later one can be derived based on the Moho depth, sediment thickness and seawater depth. The Moho geometries can be derived based on the free-air anomaly (Bai et al., 2019). To assess the connection between the remnant KPR and the active IBM arc, plate motion flow lines are obtained based on a plate rotation model via GPlates (<https://www.gplates.org/>) (the thin red lines in Fig. 1b), since GPlates is widely used in plate reconstructions. The detailed methodology and references can be found in the GPlates tutorials (<https://www.gplates.org/docs.html>). Finally, the crustal growth rate can be estimated according to cross-sectional area

of accreted arc crust along each flow line and the lifespan (52 Myr) of magmatic activity (Arculus et al., 2015).

3 Results

The first overview of the variations in the island-arc crustal growth rates for the entire IBM subduction system is derived (the thick black curve in Fig. 1a), which illustrates the variations in the crustal growth rate along the arc length. Thus, our study provides time-averaged island-arc crustal growth rates along the IBM subduction system, which is one of the inputs for estimating their potential relation to subduction zone temperatures.

According to crustal growth rate variations and geologic settings, we divide the IBM arc system into five sections from north to south: Izu, Bonin, Northern Mariana, Central Mariana and Southern Mariana (Fig. 1). No obvious variation trend is identified for the crustal growth rates of the Izu and Bonin sections. However, clear rate trends from north to south for the other three sections are shown in Fig. 1a: in the Northern Mariana section, the rate mainly decreases; in the Central Mariana section, the rate at the northern end increases, and the rate in the main part decreases; and in the Southern Mariana section, the rate increases overall.

4 Discussion

The correlation between the island-arc crustal growth rates and the melt amounts along three different cross sections (Fig. 1) in the Central Mariana section reaches 95% when the subduction zone temperatures are modelled based on the present subduction-zone parameters via the abovementioned methods. Therefore, the subduction zone temperature is the first order control on the island-arc crustal growth rate.

5 Conclusions

We use a combination of gravity inversion modelling, seismic interpretations, plate reconstruction, arc crustal growth thickness integration and magmatism lifespan to compute the first arc crustal growth rate overview of the entire IBM subduction system. There is a high correlation between the island-arc crustal growth rates and the present mantle melt amounts in the wedge along different cross sections in the Central Mariana section, which indicates that the subduction zone temperature is a potential main factor controlling the island-arc crustal growth rate.

References

- Arculus, R.J., Ishizuka, O., Bogus, K.A., Gurnis, M., Hickey-Vargas, R., Aljahdali, M.H., Bandini-Maeder, A.N., Barth, A.P., Brandl, P.A., Drab, L., do Monte Guerra, R., Hamada, M., Jiang, F., Kanayama, K., Kender, S., Kusano, Y., Li, H., Loudin, L.C., Maffione, M., Marsaglia, K.M., McCarthy, A., Meffre, S., Morris, A., Neuhaus, M., Savov, I.P., Sena, C., Tepley Iii, F.J., van der Land, C., Yogodzinski, G.M., Zhang, Z., 2015. A record of spontaneous subduction initiation in the Izu-Bonin-Mariana arc. *Nature Geosci* 8, 728-733. doi: 10.1038/ngeo2515.
- Bai, Y., Gui, Z., Li, M., Dong, D., Wu, S., Wang, Z., 2019. Crustal thickness over the NW Pacific and its tectonic implications. *Journal of Asian Earth Sciences* 185, 104050. doi: 10.1016/j.jseas.2019.104050.
- Grove, T.L., Till, C.B., Lev, E., Chatterjee, N., Médard, E., 2009. Kinematic variables and water transport control the formation and location of arc volcanoes. *Nature* 459, 694-697. doi: 10.1038/nature08044.
- Turner, S.J., Langmuir, C.H., Katz, R.F., Dungan, M.A., Escrig, S., 2016. Parental arc magma compositions dominantly controlled by mantle-wedge thermal structure. *Nature Geoscience* 9, 772. doi: 10.1038/ngeo2788.

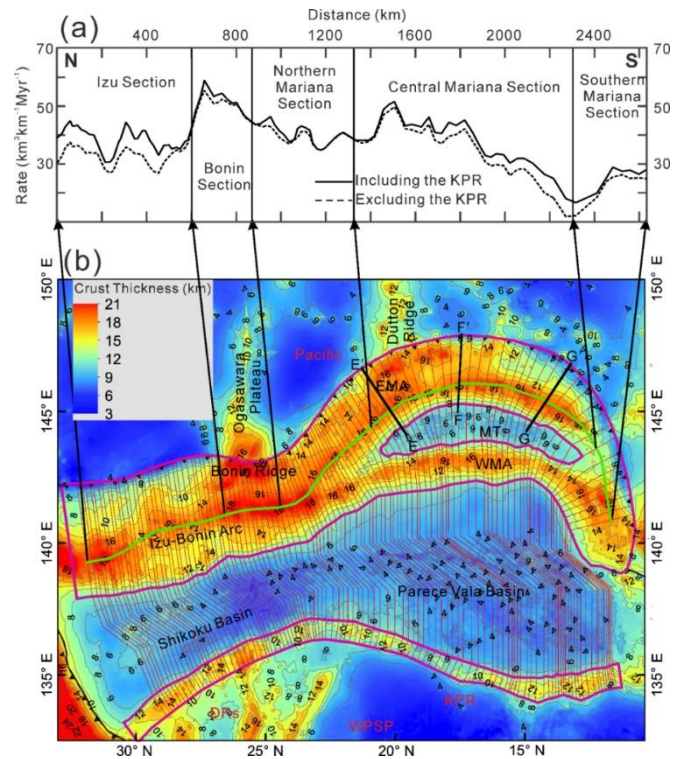


Figure 1 Overview map of the island-arc crustal growth rate variations in the Izu-Bonin-Mariana subduction system. (a) The solid black line represents the crustal growth rate when including the Kyushu-Palau Ridge (KPR), and the dashed black line represents the rate when excluding the KPR. (b) A crustal thickness map. The three thick black lines EE', FF' and GG' represent the locations of the temperature modelling sections.

Generation of andesite through partial melting of basaltic metasomatites in the mantle wedge: insight from quantitative study of Andean andesites

Long Chen^{1,2*}, Yong-Fei Zheng², Zheng Xu^{2,3}, Zi-Fu Zhao²

¹ Frontiers Science Center for Deep Ocean Multispheres and Earth System, Key Lab of Submarine Geosciences and Prospecting Techniques, Ministry of Education and College of Marine Geosciences, Ocean University of China, Qingdao 266100, China

² CAS Key Laboratory of Crust-Mantle Materials and Environments, School of Earth and Space Sciences, University of Science and Technology of China, Hefei 230026, China

³ State Key Laboratory of Isotope Geochemistry, Guangzhou Institute of Geochemistry, Chinese Academy of Sciences, Guangzhou 510640, China

*E-mail: chenlong@ouc.edu.cn

Continental crust in average exhibits a similar composition in both major and trace elements to andesites along active continental margins. For this reason, andesitic magmatism above oceanic subduction zones is considered to have played a key role in the generation of continental crust along convergent plate boundaries. With respect to the origin of andesites themselves, however, there is still a hot debate on how they have acquired their geochemical compositions. The debate is mainly centralized on the relative contributions of magma differentiation, including fractional crystallization, crustal contamination and magma mixing, and source mixing, which reaches an impasse in the past decades. The essential reason for this kind of debates is that both of these mechanisms can account for some of the geochemical observations for andesites, leading to insufficient discrimination among them. Nevertheless, the geochemical features of andesites are primarily controlled from early to late by the composition of their source rocks in addition to partial melting and magma differentiation processes. If source mixing and partial melting processes in the early stage of andesite magmatism can account for the first-order geochemical features of andesites, there is no need to invoke the late processes of magma differentiation for andesite petrogenesis. This is illustrated by quantitative forward modeling of the geochemical data for Quaternary andesites from the Andean arc in South America based on an integrated

interpretation of these data. The modeling has run with four steps from early to late: (1) dehydration of the subducting oceanic crust at forearc depths; (2) partial melting of the subducting terrigenous sediment and altered oceanic basalt at subarc depths to produce hydrous felsic melts; (3) the generation of basaltic metasomatites (e.g., Si-excess pyroxenite) in the mantle wedge through reaction of the mantle wedge peridotite with large amounts of the hydrous felsic melts; (4) the production of andesitic melts by partial melting of the basaltic metasomatites. The results not only testify the hypothesis that the trace element and radiogenic isotope compositions of andesites can be directly produced by the source mixing and mantle melting but also demonstrate that partial melting of the basaltic metasomatites can reproduce the lithochemical composition of andesites. The compositional variations of Andean andesites within a single volcanic zone and among different volcanic zones can be explained by incorporating different amounts of heterogeneous hydrous felsic melts into their mantle sources, followed by different degree of partial melting under different pressures and temperatures. Therefore, the source mixing and partial melting processes at subarc depths can account for the first-order geochemical features of Andean andesites. In this regard, it may be not necessary for andesite petrogenesis to invoke the significant contributions from the processes of magma differentiation.

Geochemical and Seismic Tomography Constraints of Two-Layer Magma Chambers beneath the Bimodal Volcanism: A Case Study of Late Cenozoic volcanic rocks from Ulleung Island and Mt. Changbai (Paektu)

Shuang-Shuang Chen^{1, 2}, Seung-Gu Lee³, Saulè Simutè⁴, Andreas Fichtner⁴, Tae Jong Lee³, Youn-Soo Lee³, Jia-Qi Liu⁵, Rui Gao^{1, 2*}

¹ School of Earth Sciences and Engineering, Sun Yat-sen University, Guangzhou 510275, China

² Southern Marine Science and Engineering Guangdong Laboratory (Zhuhai), Zhuhai 519080, China

³ Geological Research Division, Korea Institute of Geoscience and Mineral Resources, 124 Gwahak-ro Yuseong-gu, Daejeon 34132, South Korea

⁴ Department of Earth Sciences, ETH Zurich, Zurich, Switzerland

⁵ Key Laboratory of Cenozoic Geology and Environment, Institute of Geology and Geophysics, Chinese Academy of Sciences, Beijing 100029, China

We take two typical Northeast Asia bimodal volcanoes as examples to explain the general features of Cenozoic bimodal ocean island basalt (OIB)-type volcanism in Northeast Asia. We present mineralogical, petrological, geochemical, isotopic, and full-waveform seismic tomographic evidence for the existence of two-layer magma chambers of Late Cenozoic volcanic activity beneath Ulleung Island and Mt. Changbai (Paektu). Ulleung Island volcanic rocks, which are composed of alkaline basalt, phonotephrite, trachyte, and phonolite, belong to the alkaline magma series and display enrichment of light rare earth elements (LREEs) and large ion lithophile elements (LILEs), slight depletion of heavy rare earth elements (HREEs), enriched $^{87}\text{Sr}/^{86}\text{Sr}$ and $^{143}\text{Nd}/^{144}\text{Nd}$ isotopic values, and enriched $^{207}\text{Pb}/^{204}\text{Pb}$ and $^{208}\text{Pb}/^{204}\text{Pb}$ values, similar to the geochemistry of OIB. Ulleung Island felsic volcanic rocks are characterized by significant negative Ba, Sr, P, Eu, and Ti anomalies and positive Pb anomalies, slightly higher $^{87}\text{Sr}/^{86}\text{Sr}$ isotopic ratios relative to those of mafic volcanic rocks, although the mafic and felsic samples have similar Sr, Nd, and Pb isotope compositions without significant differences. Ulleung Island and Mt. Changbai volcanic activities are likely related to the involvement of subduction-related compositions, but parts of the Mt. Changbai samples have been contaminated by crustal components to a certain extent. Mafic volcanic rocks of Ulleung

Island are segregated from a deeper mantle source within a pressure range of 10.1–21.2 kbar compared with felsic volcanic rocks, which exhibit fractional crystallization of clinopyroxene, spinel, plagioclase, and olivine. To explain this, a two-layer magma chamber beneath Ulleung Island with depths of 30–40 and 60–80 km is proposed (Figure 1), which is supported by mineral crystallization pressure and a three-dimensional full-waveform seismic tomography model. We also suggest that similar magma eruption processes and a two-layer magma chamber with depths of ~10 and 40–60 km also exist beneath Mt. Changbai (Fig. 1). Taking the typical Cenozoic bimodal samples from Ulleung Island and Mt. Changbai as examples, we argue that two-layer magma chambers exist beneath Cenozoic bimodal OIB-type volcanic activities in Northeast Asia (Fig. 1).

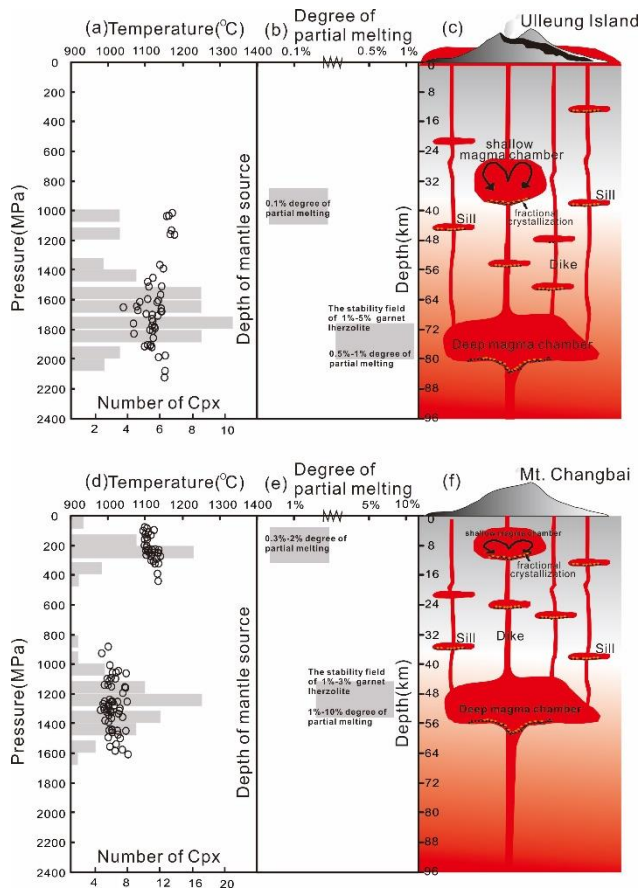


Figure 1 Ulleung Island clinopyroxene equilibration pressures and temperatures calculated by clinopyroxene-liquid thermobarometer (a); the depth of mantle source and the degree

of partial melting (b) and a schematic two-layer magma chamber model beneath the Ulleung Island (c). Mt. Changbai clinopyroxene equilibration pressures and temperatures calculated by clinopyroxene-liquid thermobarometer (d); the depth of mantle source and the degree of partial melting (e) and a schematic two-layer magma chamber model beneath the Mt. Changbai (f). The formation of the bimodal volcanic rocks might be facilitated by the existence of a two-layer magma chamber beneath Ulleung Island with different temperature and pressure environments. This conjecture is supported by the three-dimensional full-waveform seismic tomography, which shows two strong negative velocity anomalies beneath Ulleung Island. The shallow anomaly at a depth of ~30 km can be associated with the shallow magma chamber, whereas the strongest anomaly centered at a depth of ~80 km can be associated with the deeper magma chamber.

Origin and accumulation process of crude oil in the Dongsha uplift far from the source rocks in Pearl River Mouth Basin, South China Sea

Wei Duan^{1, 2}, Jin-Qiang Tian³, San-Zhong Li^{1, 2}, Zulie Long⁴

¹ Frontiers Science Center for Deep Ocean Multispheres and Earth System, Key Lab of Submarine Geosciences and Prospecting Techniques, MOE and College of Marine Geosciences, Ocean University of China, Qingdao 266100, China

² Laboratory for Marine Mineral Resources, Qingdao National Laboratory for Marine Science and Technology, Qingdao 266100, China

³ School of Geosciences, China University of Petroleum (East China), Qingdao 266580, China

⁴ Shenzhen Branch of CNOOC China Limited, Shenzhen 518000, China

Hydrocarbon reservoirs can be divided into a near-source type and a far-source type according to the distance from source rocks (Tao et al., 2017). The lateral displacement of the far-source reservoirs is obviously larger, and the longitudinal cross-layer distribution are relatively far (Pan et al., 2019). Although there are many exploration examples of far-source reservoirs worldwide outside the source at domestic and abroad, their connotation and characteristics are rarely described (Higley et al., 2009; Ma et al., 2017). Six large and medium-sized oil and gas fields have been discovered in Dongsha Uplift in Pearl River Mouth Basin, South China Sea (Hu et al., 2015). These fields are far from the center of hydrocarbon-generating depression and are beadlike distributed along the structural ridge (Fig. 1) (Bao et al., 2017). The far-source uplift belt of Dongsha Uplift is about 100 km away from the nearest source rock strata (Bao et al., 2017). What are the source rocks to form the oil and gas in the reservoir? What is the formation mechanism of hydrocarbons? How did oil migrate from the hydrocarbon-generating depression other than the Dongsha Uplift? In this article, based on the spatial distribution of oil and gas, nitrogen compounds, biomarker compounds and carbon isotope characteristics of source rocks and crude oil samples, and systematic analysis of fluid inclusions in the reservoirs of the Dongsha Uplift and its adjacent hydrocarbon-rich depression, we discussed the genetic types and sources of oil and gas in the far-source reservoirs. Combined with the analysis of fault-sand body-unconformity migration channels and barrier conditions, Pathway software was used to simulate and analyze three-dimensional hydrocarbon migration pathways. In addition,

we tried to jump out of the static model and analyze the hydrocarbon accumulation process from a dynamic point of view, to illustrate the formation mechanism of far-source reservoirs in the South China Sea.

The crude oil in the Dongsha uplift far from the source rocks mainly originates from the source rocks of the Wenchang Formation in the Huizhou depression. The biomarkers of the crude oil are mainly characterized by low C19/C23 Tricyclic terpene ratio (< 0.7), low C20/C23 Tricyclic terpene ratio (< 0.8), high C27 rearranged sterane/C27 regular sterane ratio (> 0.25), low ETR value (< 0.4), high 4-methylsterane /C29 sterane ratio (> 0.4) and low bisginate T/C30 hopane ratio (< 1). Two episodes of charging occurred in the L11-1 oilfield in the far-source uplift belt. The early charged fluid was characterized by high wax and methane contents, while the later charged fluid was characterized by higher hydrogen sulfide and inner naphthenic hydrocarbon contents. The 3-D hydrocarbon migration pathway simulation results showed that after generation in the H26 sag of Huizhou depression, under the control of the Hui-Liu tectonic ridge, oil and gas migrated to the Dongsha Uplift along the dominant migration path, and accumulated in the L11-1 oilfield in the far-source uplift belt at the top of structural ridge (Fig. 2). Along the same dominant migration path, the biomarker and carbon isotope characteristics of the crude oil samples from the far-source uplift belt are very similar to those from other oilfields, while the total nitrogen content decreases rapidly and the 1,8-DMCA/2,4-DMCA ratio increases gradually.

The study on the migration system of the Dongsha Uplift and

its surrounding areas shows that, the Tongyuan fault of the composite fracture zone in the southern Huizhou Depression was relatively quiet during the deposition of the Zhujiang-Hanjiang formations, and became strongly active at the end of the deposition of the Hanjiang Formation. The L11-1 trap was formed at the end of deposition of the Zhujiang Formation and a uniform large anticline was formed at the end of deposition of the Hanjiang Formation.

According to the 2-D source-rock generation simulation of the Huizhou Depression and the measured Ro data of drilled cores, the maturity of the Wenchang Formation source rocks in the Huizhou Depression has the following characteristics: At the end of the deposition of the Zhujiang Formation (16.5Ma), the Wenchang Formation source rocks in the H26 sag mainly entered the threshold of oil generation; At the end of the deposition of the Hanjiang Formation (10.2Ma), most of the source rocks of the Wenchang Formation in H26 sag were in the stage of oil generation; At the end of the deposition of the Yuehai Formation (5.3Ma), the deep sag center of source rock of Wenchang Formation in H26 sag also entered the stage of condensate generation. At present, active source rocks of the Wenchang Formation (Ro value is between 0.7 and 1.3%) are widely distributed, and thus the previously assumed spatial range of the Wenchang Formation source rocks which has reached the gas generation stage can be further expanded.

Therefore, we concluded that the crude oil in the far-source uplift belt of the Dongsha Uplift mainly comes from the middle and deep lacustrine source rocks of the Wenchang Formation in the H26 sag of Huizhou Depression. The deep lacustrine source rocks of the Wenchang Formation in the H26 sag of Huizhou Depression reached the stage of peak oil generation during the deposition of the late Hanjiang Formation. Affected by the strong fault activity of late Hanjiang Depression, oil and gas migrated along the Tongyuan fault from the deep to a regional carrier bed in the lower part of Zhuhai-Zhujiang Formation, and migrated towards the Dongsha Uplift along the preferential migration path in a big set of regional widely-distributed marine

sandstone carrier bed, formed oil reservoir via H33-1 and H26-1-1 traps, and eventually formed the large oil reservoir in the L11-1 trap in the far-source uplift belt of the Dongsha Uplift. During the formation of the reservoir in the far-source uplift belt of the Dongsha Uplift, two episodes of hydrocarbon charging occurred during the deposition of the upper Hanjiang and Yuehai formation, respectively.

Key words: Pearl River Mouth Basin; Dongsha Uplift; Far-source uplift belt; Biomarker compounds characteristics; Origin of oil and gas; Migration patterns

References:

- Bao, X., Ji, Y., Hu, Y., et al. Geochemical characteristics, origins, and model of lacustrine source rocks in the Zhu 1 depression, eastern Pearl River Mouth Basin, South China Sea[J]. AAPG Bulletin, 2017, 101(9): 1543-1564.
- Higley, D. K., Lewan, M. D., Roberts, L. N., 2009. Timing and petroleum sources for the Lower Cretaceous Mannville Group oil sands of northern Alberta based on 4D modeling[J]. AAPG Bulletin, 93(2): 203-230.
- Hu, Y., Hao, F., Zhu, J. Z., et al. Origin and occurrence of crude oils in the Zhu1 sub-basin, Pearl River Mouth Basin, China[J]. Journal of Asian Earth Sciences, 2015, 97: 24-37.
- Ma, X., Zhu, C., Lin, Y., Shu, Y., 2017. Evolution of the temperature – pressure system and far-source hydrocarbon accumulation in Junggar Basin. Petroleum Geology & Experiment, 39(4): 467-476.
- Pan, J., Huang, L., Wang, G., Guo, J., Ma, Y., Luo, Z., 2019. The connotation and characteristics of reservoir far away from hydrocarbon source: Case study of Well Pen-1 west hydrocarbon-enriched sag, Junggar Basin. Natural Gas Geoscience, 30(3): 312-321 (in Chinese with English abstract).
- Tao, S., Li, J., Liu, S., Bai, B., Zheng, M., Wei, Y., Cao, Z., Han, W., Ma, W., Liu, H., Yang, F., Liu, W., Gu, Z., Wu, Y., Tao, X., 2017. Formation condition, distribution law and exploration potential of far-source secondary oil and gas reservoirs. Journal of China University of Mining & Technology, 46(4): 699-714 (in Chinese with English abstract).

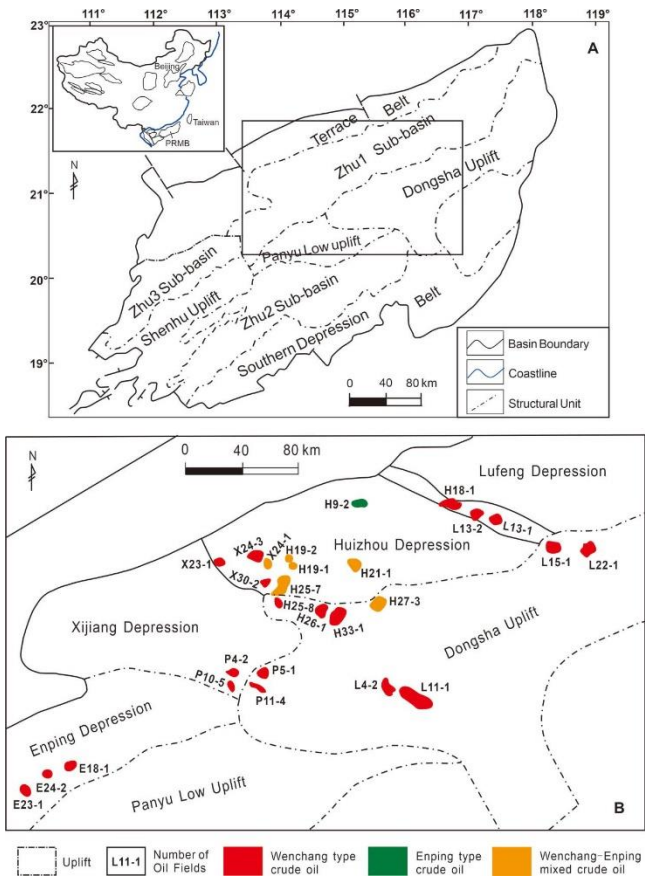


Figure 1 Geographic distribution of different types of crude oil in Dongsha Uplift and its surrounding areas in Pearl River Mouth Basin, South China Sea

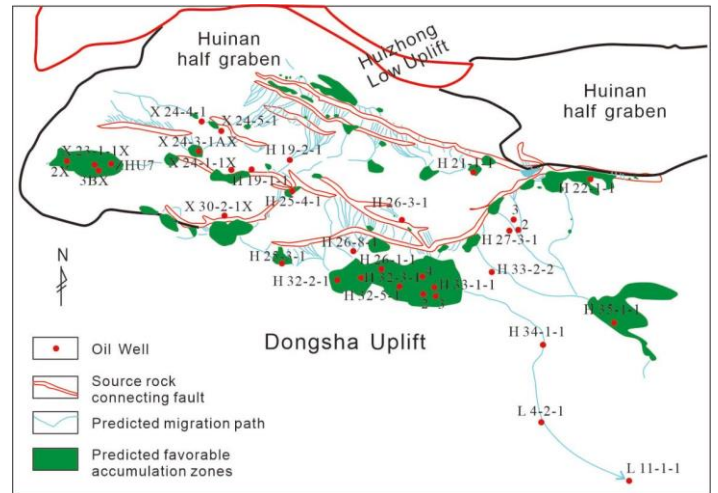


Figure 2 3-D hydrocarbon migration pathway simulation diagram of Dongsha Uplift and its surrounding areas in Pearl River Mouth Basin, South China Sea

Maihantewula ophiolitic mélangé from the Great Xing'an Range, NE China: Geochronology, geochemistry and tectonic implications for the geodynamic setting

Zhiqiang Feng¹, Yongjiang Liu^{2,3}, Weimin Li⁴, Xiaoyu Li⁵, Liwei Jiang²

¹ Department of Earth Science and Engineering, Taiyuan University of Technology, Taiyuan 030024, Shanxi, China

² MOE Key Lab of Submarine Geosciences and Prospecting Techniques, Institute for Advanced Ocean Study, College of Marine Geosciences, Ocean University of China, Qingdao 266100, China

³ Laboratory for Marine Mineral Resources, Qingdao National Laboratory for Marine Science and Technology, Qingdao 266237, China

⁴ College of Earth Sciences, Jilin University, Changchun 130061, China

⁵ Heilongjiang Geological Science Institute, Heilongjiang Haerbin 150080, China

The Great Xing'an Range, located in the eastern section of the Central Asian Orogenic Belt (CAOB), is a key region for understanding the subduction-accretionary evolution of the CAOB and finally closure history of Paleo-Asian Ocean. It is debatable issue that whether the Late Permian to Early Triassic Ocean in the CAOB is a slice of Paleo-Asian Ocean or a new limited intra-continental ocean basin. In order to better understand these geological problems, geological, geochemical and geochronological investigations were conducted on a new ophiolitic mélangé that we named the Maihantewu ophiolitic mélangé in the north-central Great Xing'an Range. The tectonic blocks in the Maihantewu ophiolitic mélangé are mainly composed of serpentinized peridotite, metagabbros, pillow basalts, variolitic basalt, Reddish radiolarian cherts and a small amount of limestone, with a matrix consisting of highly deformed siltstone. Laser ablation ICP-MS (LA-ICP-MS) U-Pb zircon ages of 248 ± 2 Ma, 280 ± 4 Ma and 257 ± 9 Ma were

obtained for the basalts, while a U-Pb zircon age of 250 ± 4 Ma were determined for the gabbro. Those pillow basalt and gabbro samples display enrichment of light rare earth element (REE) relative to heavy REEs, and moderate depletion of Ta and Th, and the pillow basalt exhibit mantle-type Sr [$^{87}\text{Sr}/^{86}\text{Sr}$ (i) = 0.704904-0.705241], Nd=[$\epsilon_{\text{Nd}}(t) = +4.60 - +5.44$] isotopic compositions. Referring to the most zircons of continental crust in the pillow basalt and metagabbros, we speculate that the Maihantewula ophiolitic mélangé were likely formed in the extensional tectonics resulting from the delamination of the lithosphere after the closure of the Paleo-Asian Ocean, and related to the representing a tectonic setting of limited intra-continental ocean basin.

Keywords: Great Xing'an Range, Maihantewula ophiolitic mélangé, Paleo-Asian Ocean, Zircon, LA-ICP-MS

A curious case of continental breakup across an orogenic front

Gillian R. Foulger (姬玲)

Institute of Marine Geodynamics, College of Marine Geosciences, Ocean University of China, Qingdao 266100, China
E-mail: gillianrosefoulger@ouc.edu.cn

It is well known that continents break up in different styles. The best-known of these are magmatic and amagmatic styles. In recent years there has been growing questioning of this bimodal division and it is becoming increasingly clear that there is variation in the amount of magmatism that accompanies breakup and is stored in passive margins. Likely, there is a wide spectrum of degrees of magmatism. It has also become clear that there is a spectrum of mechanical styles of breakup. Continents do not necessarily break "cleanly", to form a sharp transition between continental- and oceanic crust. Breakup may occur over a long period of time, with axes of extension migrating laterally multiple times before settling on a final location. Depth-dependent extension may occur and the lower parts of the crust may stretch and accommodate the upward-migrating melt instead of passing it directly from the asthenosphere to the surface. Stretched, thinned, magma-inflated crust subsides and may become inundated and part of the new ocean. Capping lavas are the "seaward-dipping reflectors" detected by seismic surveys.

If the "clean break" type of margin is one end-member of a spectrum, then the other end-member is the ultra-stretched margin. Perhaps the most extreme example of this has recently been reported for the Iceland region in the NE Atlantic ocean. There, it is postulated that embryonic seafloor spreading axes failed to propagate across the front of the ~ 400-Ma Caledonian

suture. In this model, whereas extension matured into classical seafloor spreading to the north and south, at the latitude of the orogenic front, distributed extension persisted along multiple parallel axes. Even at the present day, ~ 52 Myr after the onset of adjacent seafloor spreading, residual continental crust continues to extend at depth and crustal extension occurs along multiple, frequently migrating axes. Today, these axes can be seen onland in Iceland, which comprises the last remaining subaerial part of what was formerly a continuous landbridge spanning the ocean. This model implies that a swathe of continental crust, on which Iceland sits, still connects Greenland to Europe. This continental crust is topped with several kilometers of basalt intrusions and lava flows, the equivalent of the basalt production that forms the oceanic crust along the adjacent marine spreading ridges to the north and south.

In my presentation I shall briefly describe the sequence of events when Pangea breakup formed the NE Atlantic. I shall present the observations that gave rise to the theory that the Greenland-Iceland-Faroe region is lava-topped, hyper-extended continental crust, and describe future experimental work that may be done to test this hypothesis. It would furthermore be interesting to explore whether any older analogous structures are preserved in continental regions where breakup-related rocks are to be found.

New Paleomagnetic Results from the South Shetland Islands: Implications for the Cretaceous Tectonic Framework of the Antarctic Peninsula

Liang Gao^{1,2,*}, Junling Pei^{2,3,*}, Yue Zhao^{1,2,3}, Zhenyu Yang⁴, Teal R. Riley⁵, Xiaochun Liu^{2,3},
Shuan-Hong Zhang^{2,3}, Jian-Min Liu^{2,3}

¹ School of Ocean Sciences, China University of Geosciences, Beijing 100083, China.

² Key Laboratory of Paleomagnetism and Tectonic Reconstruction of Ministry of Land and Resources, Beijing 100081, China.

³ Institute of Geomechanics, Chinese Academy of Geological Sciences, Beijing 100081, China.

⁴ College of Resources, Environment and Tourism, Capital Normal University, Beijing 100048, China.

⁵ British Antarctic Survey, High Cross, Madingley Road, Cambridge CB3 0ET, UK.

E-mail address: peijunling@gmail.com (Junling Pei); lgao@live.cn (Liang Gao)

There is a continuing debate on the tectonic framework of the Antarctic Peninsula and its paleoposition in the Gondwana supercontinent during Cretaceous global plate reorganization (Jordan et al., 2020). The following models have been proposed for the Antarctic Peninsula: an autochthonous continental subduction model (Suárez, 1976; Burton-Johnson and Riley, 2015); an allochthonous terrane accretion model (Vaughan and Storey, 2000); and a para-autochthonous geophysical model in which part of the arc was formed in situ but part of it may have been exotic, even if not from a distant location (Ferraccioli et al., 2006). In this study, we applied paleomagnetic constraints on the autochthonous continental subduction model and allochthonous terrane accretion model in explanation of tectonic framework of the Antarctic Peninsula. We present a new reliable paleopole (58.1°S, 354.3°E, $A_{95}=6.3^\circ$) from Livingston Island in the South Shetland Islands at ~102 Ma, which provide valuable paleoposition constraints on the Western domain of the Antarctic Peninsula. Plate reconstruction models from the Early Cretaceous attach the South Shetland Islands to the Pacific margin of southern Patagonia-Fuegian Andes at ~140 Ma. The South Shetland Islands then experienced southward translation to its current position to the northwest of the Antarctic Peninsula following counterclockwise rotation during ~100-90 Ma. Similar counterclockwise rotation has also been identified from southern Patagonia-Fuegian Andes but is absent in the Antarctic Peninsula, suggesting direct affinity between the South

Shetland Islands and southern Patagonia-Fuegian Andes. However, the consistent, almost northward Cretaceous paleomagnetic declination in the Antarctic Peninsula, and the near-synchronous tectonic-magmatic history between the Antarctic Peninsula and the southern Patagonia-Fuegian Andes support an autochthonous continental subduction model for most of the Antarctic Peninsula.

Acknowledgments

This research was funded by the National Key R&D Program of China (2018YFC1406904), the Natural Science Foundation of China (NSFC) (41930218, 41706222, 42076223), and the open foundation project (KLPTR-03) of the Key Laboratory of Paleomagnetism and Tectonic Reconstruction, Ministry of Land and Resources.

References

- Burton-Johnson, A., Riley, T. R., 2015. Autochthonous v. accreted terrane development of continental margins: a revised in situ tectonic history of the Antarctic Peninsula. *Journal of the Geological Society*, v. 172(6), p. 822-835. <https://doi.org/10.1144/jgs2014-110>
- Ferraccioli, F., Jones, P. C., Vaughan, A. P. M., Leat, P. T., 2006. New aerogeophysical view of the Antarctic Peninsula: More pieces, less puzzle. *Geophysical Research Letters*, v. 33(5).

<https://doi.org/10.1029/2005GL024636>

Jordan, T. A., Riley, T. R., Siddoway, C. S., 2020. The geological history and evolution of West Antarctica. *Nature Reviews Earth & Environment*, p. 1-17. <https://doi.org/10.1038/s43017-019-0013-6>

Suárez, M., Pettigrew, T. H., 1976. An Upper Mesozoic island–arc–back–arc system in the southern Andes and South Georgia. *Geological Magazine*, v. 113, p. 305–328.

<https://doi.org/10.1017/S0016756800047592>

Vaughan, A. P. M., Storey, B. C., 2000. The eastern Palmer Land shear zone: a new terrane accretion model for the Mesozoic development of the Antarctic Peninsula. *Journal of the Geological Society*, v. 157(6), p. 1243-1256. <https://doi.org/10.1144/jgs.157.6.1243>

Ocean Plate Stratigraphy of a long-lived Precambrian subduction-accretion system: The Wutai Complex, North China Craton

Pin Gao¹, M. Santosh^{1,2*}, Sanghoon Kwon³, Sung Won Kim⁴

¹ School of Earth Sciences and Resources, China University of Geosciences Beijing, 29 Xueyuan Road, Beijing 100083, P. R. China

² Department of Earth Sciences, University of Adelaide, Adelaide SA 5005, Australia

³ Department of Earth Sciences, Yonsei University, Seoul 03772, Republic of Korea

⁴ Geological Research Division, Korea Institute of Geoscience and Mineral Resources, Daejeon 305-350, Republic of Korea

*E-mail: santosh@cugb.edu.cn

Ocean Plate Stratigraphy (OPS) is the travelogue of the oceanic lithosphere from its birth at the Mid Ocean Ridge to its demise at the subduction zone in convergent plate margins. We present an OPS succession preserved onland in the Wutai Complex of the North China Craton (NCC), representing a prolonged subduction-accretion-collision system and continental growth during the Neoproterozoic-Paleoproterozoic. The OPS succession in Wutai includes metabasalts and banded iron formations (BIFs) representing the pelagic sequences together with intercalated metacarbonates, phyllite, greenschist, and mica schist representing the hemipelagic sequence. Quartzite and conglomerate corresponding to the turbidite sequence, with a progressive southward accretion with a magmatic arc to the north. The trace elements including the rare-earth elements (REEs) data of the metabasalt show transitional features from normal mid-ocean ridge basalt (N-MORB) to enriched mid-ocean ridge basalt (E-MORB). The REY (lanthanide elements and Y) data of the BIFs, greenschists, and phyllites suggest the interaction of high-temperature hydrothermal fluids and seawater. Magmatic zircon grains from the quartzite show $^{206}\text{Pb}/^{207}\text{Pb}$ upper intercept age of 2443 ± 21

Ma, were as zircon grains in the phyllite show upper intercept age of 2494 ± 32 Ma, with minor xenocrysts with older ages of 2726 ± 46 Ma and 2672 ± 48 Ma. The metaconglomerate shows upper intercept age of 2569 ± 32 Ma. The zircon grains from the siliceous and intercalated bands in the BIF yield upper intercept ages of 2583 ± 34 Ma and 2524 ± 49 Ma. The zircon Lu-Hf data on zircon grains from the BIF, phyllite, quartzite, and metaconglomerate all show positive $\epsilon_{\text{Hf}}(t)$ values (+1.3 to +7.4) in the range of depleted mantle to new crust, suggesting Neoproterozoic intra oceanic arc processes. Four tectonic evolution stages identified of the Wutai Complex: ~ 2800 Ma subduction initiation, ~ 2750 - 2300 Ma arc-accretionary complex, ~ 2300 - 2100 Ma back-arc rifting, and ~ 1900 - 1750 Ma arc-continent collision. The metavolcanics and part of the metasedimentary rock assemblages in the Wutai complex represent a deformed and dismembered OPS sequence generated through northward subduction and closure of the Wutai Ocean.

Keywords: North China Craton; Wutai complex; Ocean Plate Stratigraphy; Neoproterozoic to Paleoproterozoic; Zircon U-Pb-Hf isotopes.

Reconstructing seepage activities over the past 20000 yrs in the Okinawa Trough: Evidences from methane index and trace metals

Hongxiang Guan^{1*}, Lei Liu¹, Yu Hu^{2,3*}, Zhilei Sun⁴, Nengyou Wu⁴

¹ Frontiers Science Center for Deep Ocean Multispheres and Earth System, Key Lab of Submarine Geosciences and Prospecting Techniques, MOE and College of Marine Geosciences, Ocean University of China, Qingdao 266100, China

² Shanghai Engineering Research Center of Hadal Science and Technology, College of Marine Sciences, Shanghai Ocean University, Shanghai 201306, China

³ Southern Marine Science and Engineering Guangdong Laboratory (Guangzhou), Guangzhou 511458, China

⁴ Key Laboratory of Gas Hydrate, Ministry of Natural Resources, Qingdao Institute of Marine Geology, Qingdao, 266071, China

* E-mail address: guan hongxiang@ouc.edu.cn (H. Guan)

The amounts of methane released from the seabed to the ocean is largely controlled by sulfate-driven anaerobic oxidation of methane (SD-AOM). Authigenic precipitations within anoxic sediments are widely used as indicators of current and fossil seepage events. However, uncertainties are present in identifying fossil seepage activities and reconstruct the dynamic histories since information may have been lost during diagenesis. Here, carbon, oxygen, lipid biomarkers, major and trace element geochemistry of seep-related sediments from the Okinawa Trough, East China Sea, were analyzed to distinguish factors controlling methane seepage events, methane consumptions and the time methane seepages has (had) been last. The extremely low $\delta^{13}\text{C}$ values of bulk sediments and organic matters, increased methane index, as well as Molybdenum (Mo) and Uranium (U) enrichments in depths 225-255 cm and 75-142.5 cm below the seafloor, along with the pore water sulfate and methane concentrations, a current and a fossil sulfate-methane transition zones (SMTZ) were identified. The low Sr/Ca and the relatively high Mg/Ca in both the current

and fossil SMTs indicated the formation of high-Mg calcite, which was in good accordance with the dominance of high-Mg calcite testified from pore waters of the sediments. The estimated $\delta^{18}\text{O}$ values for authigenic carbonates are higher than the theoretical equilibrium $\delta^{18}\text{O}$ value of high-Mg calcite at the fossil SMT, whereas it is not the case for the current SMT, suggesting that only authigenic carbonates formed at the fossil SMT was influenced by the fluids from the dissociation of gas hydrates. Based on the calcium and magnesium carbonate precipitation fluxes, the time required for the accumulation of the authigenic carbon in the current and fossil SMTs are around 1.4 and 3.8ka, respectively. The combination of geochemistry and estimation is a promising approach, allowing to better understand the dynamic histories of seepage activities.

Keywords: anaerobic oxidation of methane (AOM); sulfate-methane transition zones (SMTZ); authigenic precipitations; Okinawa Trough; East China Sea

Opening of the West Paleo-Tethys Ocean: Constraints from zircon U-Pb-Hf isotopic and geochemical characteristics of the earliest Devonian meta-mafic rocks in Saualpe basement, Eastern Alps

Qingbin Guan^{1,2*}, Yongjiang Liu^{1,2}, Franz Neubauer³

¹ Frontiers Science Center for Deep Ocean Multispheres and Earth System, Key Lab of Submarine Geoscience and Prospecting Techniques, MOE and College of Marine Geosciences, Ocean University of China, Qingdao 266100, China

² Laboratory for Marine Mineral Resources, Qingdao National Laboratory for Marine Science and Technology, Qingdao 266237, China

³ Department Geography and Geology, Paris-Lodron-University Salzburg, Hellbrunner Str. 34, 5020 Salzburg, Austria
E-mail: guanqingbin@ouc.edu.cn

The timing of the opening of the West Paleo-Tethys Ocean in Eastern Alps remains unclear. To constrain this event, we present new zircon U-Pb ages, Hf isotopic compositions, and whole-rock major- and trace-element data for the meta-mafic rocks (amphibolites) in the southern and western Saualpe crystalline basement, Eastern Alps. Zircon U-Pb dating of three samples yield crystallization ages of 418 ± 6 Ma, 417 ± 3 Ma and 415 ± 3 Ma, indicating that they formed during the earliest Devonian. Geochemically, these meta-mafic rocks have relatively low SiO₂ and MgO contents and high TiO₂ contents. They are enriched in light rare earth elements (LREE), particularly in Nb and Ta, and show relatively flat heavy rare-earth elements (HREE) patterns, suggesting that they have affinities with the alkaline oceanic island basalts (OIB). The geochemical characteristics, together with the positive $\epsilon_{\text{Hf}}(t)$ values of 0.7–11.1, imply that the OIB-like meta-mafic rocks

originated from partial melting of a lherzolite source including spinel and garnet. The primary magma shows complex sources involving asthenospheric, lithospheric mantle and subducted slab components, which was subsequently modified by crustal contamination. This reveals that the magma formed in a slab window environment associated with mid-ocean ridge subduction. The contemporaneous OIB-like alkaline amphibolites were also found in the Central Austroalpine basement and in Northwestern Turkey. We suggest that the Late Silurian–earliest Devonian OIB-like magmatism is related to a back-arc extension setting along the northern margin of Gondwana leading to the separation of the European Hunic terranes and hence placing age constraints on the opening of the West Paleo-Tethys Ocean.

Keywords: Earliest Devonian; West Paleo-Tethys Ocean; Meta-mafic rocks; Eastern Alps; Saualpe crystalline basement

Gravity and Magnetic Characteristics of Micro-blocks in the Subduction System of Southeast Asia

Xueting Guan^{1,2}, Suhua Jiang^{1,2}, Sanzhong Li^{1,2}, Dong Wei^{1,2}, Jie Liu^{1,2}, Yanhui Suo^{1,2}, Jianli Zhang^{1,2}

¹ Frontiers Science Center for Deep Ocean Multispheres and Earth System, Key Lab of Submarine Geosciences and Prospecting Techniques, MOE, College of Marine Geosciences, Ocean University of China, Qingdao 266100, China

² Laboratory for Marine Mineral Resources, Qingdao National Laboratory for Marine Science and Technology, Qingdao 266237, China

Southeast Asia is located in the convergence zone of the Eurasian, Indo-Australian and Philippine sea plates, with a wide range of modern and ancient convergence areas, and the arc-continent collision plays an important role. The tectonic setting is complex, mainly developed with rifting micro-blocks, residual micro-blocks and accreting micro-blocks. However, the interior and boundary characteristics of these micro-blocks are not well studied, especially the lack of geophysical evidence. To this end, the latest gravity and magnetic processing methods, such as wavelet multi-scale analysis, upward continuation, directional derivative and residual gravity anomaly, are used to study the interior and boundary characteristics of the block in this region. The results show that the free-air gravity anomaly in the subduction system is closely related to the topographic relief and is proportional to the elevation. In addition, the subduction zone, mid-ocean ridge and other regional tectonic characteristics have a clear response to the free-air gravity anomaly, which is a negative anomaly zone. The isostatic gravity anomalies of the subduction system often show positive and negative opposite anomalies on both sides of the plate boundary, and the outliers are inversely proportional to the elevation on land and positively proportional to the elevation in the ocean. For example, the magnetic anomaly continuation results of the Mariana oceanic micro-block reveal that the

magnetic anomaly in the micro-block has fewer high-frequency components, but retains the linear characteristics of the microplate interior. Since the boundary of micro-block is often represented as gradient zone in the magnetic anomaly field, thus it will be represented as an extreme value in the horizontal first derivative field. Therefore, the directional derivative is very effective in identifying the boundary of micro-block. In the interior of the micro-block, generally within the same tectonic unit, the directional derivative outliers change little and strike the same direction. In addition, the wavelet multi-scale decomposition of the Bouguer gravity anomaly of the subduction system reveals that the low-order approximation field inherits the original Bouguer gravity anomaly, and the low-order detail field reflects the small-scale geological structure and local anomaly characteristics, such as the southern Bismarck microplate. The results show that gravity and magnetic processing results can better identify the characteristics of microplate interior and boundary in the subduction system of Southeast Asia, which make a difference for improving the microplate theory and studying the evolution of microplates in the South China Sea.

Keywords: Southeast Asia; Subduction system; Micro plate; Gravity and magnetic method; The Marianas

A rare earth element and Nd isotopic investigation of Neoproterozoic iron formations: Constraints on Neoproterozoic seawater compositions

Jun Hu^{1,2*} He Wang³

Institute of Geology and Mineralogy RAS, Koptyuga 3, Novosibirsk, 630090, Russia

¹ Frontiers Science Center for Deep Ocean Multispheres and Earth System, Key Lab of Submarine Geosciences and Prospecting Techniques, MOE and College of Marine Geosciences, Ocean University of China, Qingdao 266100, China

² Laboratory for Marine Mineral Resources, Qingdao National Laboratory for Marine Science and Technology, Qingdao 266237, China

³ Key Laboratory of Mineralogy and Metallogeny, Guangzhou Institute of Geochemistry, Chinese Academy of Sciences, Guangzhou 510640, China

*E-mail address: hujun@ouc.edu.cn

1. Introduction

The Neoproterozoic is one of the most important times in earth's history, because substantial changes of environmental conditions occurred during this epoch (Stern et al., 2013; Viehmann et al., 2016). One of the hallmark indicators is Neoproterozoic iron formations (hereafter referred to as NIFs), which present a unique opportunity into Late Precambrian atmosphere-hydrosphere conditions, and their trace element and isotopic features have been used with great success as proxies for understanding the chemical compositions of seawater from which they precipitated (e.g., Lottermoser and Ashley, 2000; Klein and Ladeira, 2004; Basta et al., 2011; Halverson et al., 2011; Stern et al., 2013; Viehmann et al., 2016; Busigny et al., 2018). The rare earth element and yttrium (REY), especially PAAS-normalised light-to-middle-to-heavy rare earth element ratios, Y/Ho values, Eu and Ce anomalies, coupled with Nd isotope systematics, are particularly useful for such studies due to their coherent behaviour in geochemical systems, and can be used as a proxy not only for constraining the relative magnitude of continental and hydrothermal fluxes to the oceans, but also as a means to estimate the bulk compositions and redox-structure of ancient seawater (Haugaard et al., 2016; Viehmann et al., 2016; Busigny et al., 2018; Hu et al., 2020).

2. Method summary

We compiled REY and Nd isotopic data of representative

NIFs worldwide, particularly those with well constrained in age, including Shilu NIF (~ 0.83 Ga, South China; Xu et al., 2014; Sun et al., 2018), Wadi Karim and Um Anab NIFs (~ 0.75 Ga, East Egypt; Basta et al., 2011), Sawawin NIF (~ 0.75 Ga, NW Saudi Arabia; Stern et al., 2013), Jucurutu NIF (~ 0.75 Ga, NE Brazil; Sial et al., 2015), Braemar NIF (~ 0.75 Ga, South Australia; Lottermoser and Ashley, 2000), Fulu NIF (~ 0.72 Ga, South China; Busigny et al., 2018), Rapitan NIF (~ 0.716 Ga, North Canada; Halverson et al., 2011), Xinyu NIF (~ 0.648 Ga, South China; Li et al., 2014), Urucum NIF (~ 0.635 Ga, West Brazil; Viehmann et al., 2016), Dahongliutan NIF (0.593 ~ 0.532 Ga, NW China; Hu et al., 2017; Hu et al., 2020), as well as Zankan, Taaxi and Jierteike NIFs (~ 0.52 Ga, NW China; Li et al., 2018).

We carried out the strict screening procedure to minimize the potential impact of syn-depositional clastic contamination and post-depositional diagenesis, before interpreting the distinctive geochemical tracers in term of depositional processes, and therefore, may more really reflect the geochemical compositions of Neoproterozoic seawater where the NIFs precipitated.

3. Conclusions

Taking reported REY and Nd data of Neoproterozoic NIFs together, the geochemical compositions and evolution of the coeval Precambrian seawater are obtained, as follows: (1) Some NIFs typically show positive Eu anomalies, indicating REY

input from high-T hydrothermal fluids into the Neoproterozoic seawater; (2) The large range of Ce anomalies, both positive and negative Ce anomalies, in the NIFs imply the Neoproterozoic marine inhomogeneous redox magnitude; (3) Negative ϵ_{Nd} (t) values, mostly falling in -10 and 0, in most NIFs suggest that the great majority of Nd in bulk Neoproterozoic seawater originated from sedimentary continental source materials transported by river water; (4) The Neoproterozoic seawater in which the NIFs formed strongly affected by continentally derived freshwaters (> 10%) and limited (< 5%) high-T hydrothermal fluids as indicated by Sm/Yb and Eu/Sm ratios.

CRediT authorship contribution statement

Jun Hu: Investigation, Formal analysis, Software, Writing-original draft, Writing-review & editing. **He Wang:** Investigation, Project administration, Supervision.

Declaration of Competing Interest

The authors declare that they have no known competing financial interests or personal relationships that could have appeared to influence the work reported in this paper.

Acknowledgements

This study is financially supported by the National Natural Science Foundation of China (41602063) and the State Technology Support Program (2015BAB05B03). We appreciate Hongwei Han and Yong Wei from the Xinjiang Xindi Geological Exploration Company for their logistic supports during the field work.

References

Basta, F.F., Maurice A.E., Fontbote, L., Avarger, P.Y., 2011. Petrology and geochemistry of the banded iron formation (BIF) of Wadi Karim and Um Anab, Eastern Desert, Egypt: implications for the origin of Neoproterozoic BIF. *Precambrian Research* 187 (3–4), 277–292.

Busigny, V., Planavsky, N.J., Goldbaum, E., Lechte, M.A., Feng, L.J., Lyons T.W., 2018. Origin of the Neoproterozoic Fulu iron formation, South China: Insights from iron isotopes and rare earth element patterns. *Geochimica et Cosmochimica Acta* 242, 123–142.

Halverson, G.P., Poitrasson, F., Hoffman, P.F., Nédélec, A., Montel, J.M., Kirby, J., 2011. Fe isotope and trace element geochemistry of the Neoproterozoic syn-glacial Rapitan iron formation. *Earth and Planetary Science Letters* 309 (1), 100–112.

Haugaard, R., Ootes, L., Creaser, R.A., Konhauser, K.O., 2016. The nature of Mesoarchean seawater and continental weathering in 2.85Ga banded iron formation, Slave craton, NW Canada. *Geochimica et Cosmochimica Acta* 194, 34–56.

Hu, J., Wang, H., Wang, M., 2017. Geochemistry and origin of the Neoproterozoic Dahongliutan banded iron formation (BIF) in

the Western Kunlun orogenic belt, Xinjiang (NW China). *Ore Geology Reviews* 89, 836–857.

Hu, J., Wang, H., Zhang, L.G., 2020. A rare earth element and Nd isotopic investigation into the provenance and deposition of the Dahongliutan banded iron formation and associated carbonates, NW China: Implications on Neoproterozoic seawater compositions. *Precambrian Research* 342, 105685.

Klein, C., Ladeira, E.A., 2004. Geochemistry and mineralogy of Neoproterozoic banded iron-formations and some selected, siliceous manganese formations from the Urucum district, Mato Grosso do Sul, Brazil. *Economic Geology* 99, 1233–1244.

Li, Z.H., Zhu, X.K., Sun, J., 2014. Geochemical characters of Banded Iron Formations from Xinyu and North China. *Acta Petrologica Sinica* 30(5), 1279–1291 (in Chinese with English abstract).

Li, Z.Q., Zhang, L.C., Xue, C.J., Zhu, M.T., Zheng, M.T., Robbins, L.J., Konhauser, K.O., 2018. Earth's youngest banded iron formation implies ferruginous conditions in the Early Cambrian ocean. *Scientific Reports* 8 (1), 9970.

Lottermoser, B.G., Ashley, P.M., 2000. Geochemistry, petrology and origin of Neoproterozoic ironstones in the eastern part of the Adelaide Geosyncline, South Australia. *Precambrian Research* 101, 49–67.

Sial, A.N., Campos, M.S., Gaucher, C., Frei, R., Ferreira, V.P., Rielva, C., Nascimento, R.C., Pimentel, M.M., Pereira, N.S., Rodler, A., 2015. Algoma-type Neoproterozoic BIFs and related marbles in the Serido Belt (NE Brazil): REE, C, O, Cr and Sr isotope evidence. *Journal of South American Earth Sciences* 61, 33–52.

Stern, R.J., Mukherjee, S.K., Nathan, R.M., Kamal, A., Peter, R.J., 2013. 750Ma banded iron formation from the Arabian-Nubian Shield – Implications for understanding Neoproterozoic tectonics, volcanism, and climate change. *Precambrian Research* 239, 79–94.

Sun, J., Zhu, X.K., Li, Z.H., 2018. Confirmation and global significance of a large-scale early Neoproterozoic banded iron formation on Hainan Island, China. *Precambrian Research* 307, 82–92.

Viehmann, S., Bau, M., Bühn, B., Dantas, E.L., Andrade, F.R.D., Walde, D.H.G., 2016. Geochemical characterisation of Neoproterozoic marine habitats: Evidence from trace elements and Nd isotopes in the Urucum iron and manganese formations, Brazil. *Precambrian Research* 282, 74–96.

Xu, D.R., Wang, Z.L., Chen, H.Y., Hollings, P., Jansen, N.H., Zhang, Z.C., Wu, C.J., 2014. Petrography and geochemistry of the Shilu Fe–Co–Cu ore district, South China: Implications for the origin of a Neoproterozoic BIF system. *Ore Geology Reviews* 57, 322–350.

The influence of the magnetic structure complexity of the oceanic crust on the marine magnetic anomalies

Yuewei Hu¹, Jianli Zhang^{1,2*}, Zhaoxia Jiang^{1,2*}, Sanzhong Li^{1,2}

¹Frontiers Science Center for Deep Ocean Multispheres and Earth System/Key Lab of Submarine Geosciences and Prospecting Techniques, MOE, College of Marine Geosciences, Ocean University of China, Qingdao 266100, P.R. China

²Laboratory for Marine Mineral Resources, Qingdao National Oceanography Laboratory for Marine Science and Technology, Qingdao 266237, P.R. China

*Email: zhangjianli@ouc.edu.cn; jiangzhaoxia@ouc.edu.cn

Marine magnetic anomaly strips play important roles in the research of plate tectonics and movement, and promote the development of geoscience revolution. However, previous researches often ignored the complexity of the magnetic structure of the oceanic crust. The complex oceanic crusts with multiple magnetic source layers, including lava layer, dike layer and gabbro layer, and various polarity boundary tilt angles were considered as a simple oceanic crust magnetic structure with a single magnetic source layer and vertical polarity boundary. At present, there are still lack of systematic understandings on how the dike layer and gabbro layer affect the whole magnetic anomalies, how the lava layers with different inclinations affect the intensity and polarity boundary of the magnetic anomaly. In order to dissolve these problems, this paper uses the forward modeling method through setting different magnetic layer characteristics, to systematically simulate and analyze the whole magnetic anomaly characteristics, and determine the impact of the complexity of the magnetic structure of the ocean crust on the magnetic anomaly.

Firstly, based on the previous rock magnetic analysis on different magnetic source layers, the thickness, depth and magnetization of each magnetic source layer in models are adjusted uniformly on the premise that the polarity boundary shape remains vertical. The magnetization is set as 5 ~ 10 A/m for lava layer and 1 A/m for dike layer and gabbro layer. The thickness is set 1 km for both lava layer and dike layer, and 3 km for gabbro layer. The single magnetic source layer model (lava layer) is compared with the multiple magnetic source layers' model including lava layer, dike layer and gabbro layer. Results show that the dominant contributed magnetic layer for marine magnetic anomalies is lava layer, but the contribution of dike layer and gabbro layer cannot be ignored.

Secondly, due to the different formation modes of each magnetic source layer, there are different polarity boundary shapes. The polarity boundary shape of the lava layer is the most complex. Affected by the lava flow properties and the plate stretch movement toward both sides, the polarity boundary of the lava layer tilts towards the mid ocean ridge, and presents simple tilt, complex tilt or other shapes. The polarity boundary shape of dike layer and gabbro layer is relatively simple, both of which are simple tilt. Among them, the polarity boundary of dike layer is controlled by the intrusion mode of dike, while the polarity boundary of gabbro layer is controlled by isotherm, both of which are inclined back to the mid ocean ridge. According to this series of tilt methods, the thickness, depth and magnetization of these magnetic layers are fixed, only the shapes and tilt angles of the polarity boundary are changed to observe the variation of the magnetic anomalies boundary. It can be found that these tilt modes will stretch the magnetic anomaly curve to the extension direction of the magnetic layer, and the polarity conversion region will also move to the extension direction.

The peak and valley values representing the positive and negative polarity junction will become smaller with the decrease of the tilt angle, while the magnetic anomaly values representing the stable magnetic region will not change significantly. Although the tilt directions of both dike and gabbro layer are opposite to that of lava layer, the simulation results are roughly equivalent to that of lava layer. However, the difference is that the magnetization of the dike layer is relatively weak and the tilt angle is slightly larger, so that its influence on the whole magnetic anomaly is weaker than that of the lava layer. Although the thickness of gabbro layer is much larger, the change of polarity boundary shape has a great impact on the

magnetic anomaly of this layer, but plays a less influence on the whole magnetic anomaly due to its weak magnetization and deeper position.

Finally, a new ocean crust model is produced by integrating the lava layer, dike layer and gabbro layer after adjusting the polarity boundary shape. The corresponding magnetic anomaly modeling results are the same as those layers, but the decrease of anomalies intensity, the shift of polarity conversion area and the stretching trend of the whole shape of magnetic anomaly are

remarkable.

In conclusion, the influence of the complex magnetic structure of the ocean crust on the whole magnetic anomaly is systematically investigated through the forward modeling of the ocean crust magnetic structure, which provides a theoretical basis for the inversion and structural analysis of the ocean crust structure using the ocean magnetic anomaly data.

Permian-Triassic A-type and I-type granites in the Schladming Complex, Austroalpine Unit: Constraints on subduction of Paleo-Tethys Ocean in the Eastern Alps

Qianwen Huang^{1,2,3}, Yongjiang Liu^{1,2}, Johann Genser³, Franz Neubauer³, Ruihong Chang³, Sihua Yuan⁴, Qingbin Guan^{1,2}, Shengyao Yu^{1,2}

¹ Frontiers Science Center for Deep Ocean Multispheres and Earth System; Key Lab of Submarine Geosciences and Prospecting Techniques, MOE and College of Marine Geosciences, Ocean University of China, Qingdao 266100, China. liuyongjiang@ouc.edu.cn; yushengyao@ouc.edu.cn; guanqingbin@ouc.edu.cn; HuangQW_31@163.com

² Laboratory for Marine Mineral Resources, Qingdao National Laboratory for Marine Science and Technology, Qingdao 266237, China.

³ Paris-Lodron-University of Salzburg, Department of Geography and Geology, Geology Division, Hellbrunnerstraße 34, 5020 Salzburg. franz.neubauer@sbg.ac.at; johann.genser@sbg.ac.at; sihua.yuan@sbg.ac.at; ruihong.chang@stud.sbg.ac.at

⁴ College of Earth Science, Institute of Disaster Prevention, Sanhe, 065201, Hebei Province, China; yuansihua@126.com

⁵ College of Earth Sciences, Jilin University, Jianshe Str. 2199, Changchun 130061, China. jinwei@jlu.edu.cn

The orocline shaped Alpine-Carpathian-Himalaya orogeny belt is a continent collision orogeny, which known for their typical strong deformation and polyphase metamorphism. In addition to notable Permian-Triassic magmatism in the Eastern Alps and the surrounding areas, Permian to Triassic granitic magma activities is found in the Tweng basement and Schladming Complex. In order to understand the tectonic setting of these granitic rocks, we presented their zircon geochronology and whole-rock geochemistry in this study.

Tweng basement as part of Radstadt Complex overlain by the Schladming Complex, locally formed as mylonitic crystalline rocks thin layers or individual nappes (Liu et al., 2001). Granitic orthogneisses and subordinate paragneiss, muscovite-schist and amphibolite are the main rocks of the Tweng basement, they are generally deformed and metamorphosed together. The granites of Schladming Complex are mainly exposed in the north and southeast area. According to Schermaier et al. (1997), the I-type granites are common in the northern area, while the A-type granite dominant in the southeast part.

Zircon U-Pb data show that the Tweng granitic gneisses and leucogranites formed at 262 Ma and 244 Ma, respectively. In the Schladming Complex, we found, for the first time, Triassic granitic gneisses with zircon ages of 244-241 Ma. Their positive $\epsilon_{\text{Hf}}(t)$ values (0.2 ~ +5.6), with one grain outlier at -0.9, indicate

they mainly derived from the lower crust but involved minor upper crust or old continent materials. Geochemically, the granitic rocks from the Tweng basement and Schladming Complex have the common features with subduction-related features and show A2-types granite affinity, they have high crystalline temperature with 784-835°C and 781-818°C, respectively. While the Tweng leucogranites exhibit I-type granite features and low crystalline temperature of 720-724°C. The Tweng granitic gneisses and leucogranites display similar characteristic with continental arc andesite (CAA). The Tweng granitic gneisses originated from the lower crust, and the Tweng leucogranites were sourced by melted their host rock (Tweng granitic gneiss) and mixed with continent melts.

Therefore, we propose a model that the subduction of the Paleo-Tethys Ocean formed the Permian continent arc related granite (Fig. 1a), a rift developed in the back-arc domain during Late Permian to Middle Triassic times, inducing A-type granite magma intrusions (Fig. 1b). In the Tweng basement, persistent magma and high temperature produced the continent arc andesite-related granite melts, the continents-related magma mixed with the melts in the fracture of Tweng granitic gneisses and formed the Tweng leucogranite.

Reference

Liu, Y., Genser, J., Handler, R., Friedl, G., Neubauer, F., 2001. $^{40}\text{Ar}/^{39}\text{Ar}$ muscovite ages from the Penninic-Austroalpine plate boundary, Eastern Alps. *Tectonics* 20, 526-547.

Schermaier, A., Haunschmid, B., Fringer, F., 1997. Distribution of Variscan I- and S-type granites in the Eastern Alps: a possible clue to unravel pre-Alpine basement structures. *Tectonophysics* 272, 315-333.

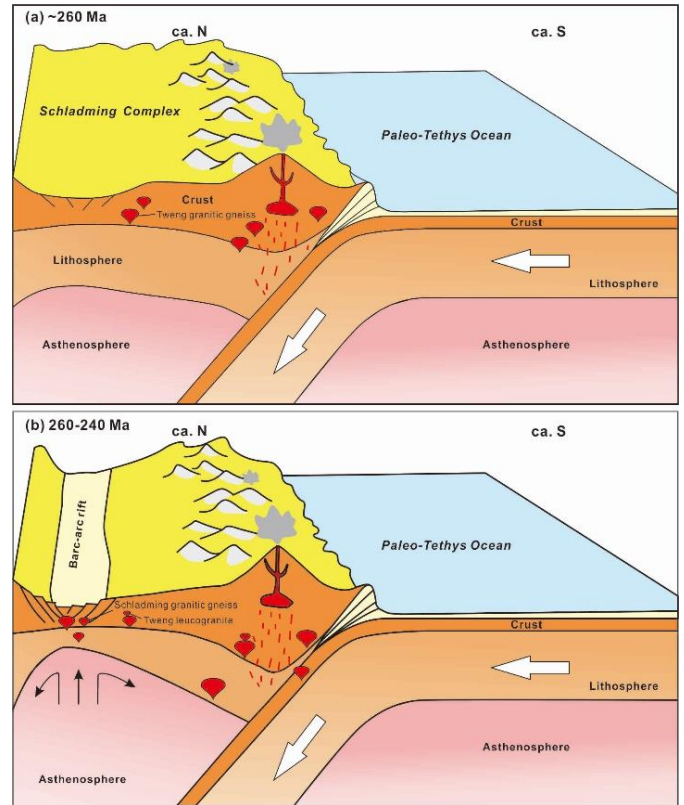


Figure 1 Permian to Triassic tectonic evolution model for the Tweng basement and Schladming Complex

Tsunami origin from focal mechanism solutions of global Tsunami earthquakes

Zhongjia Jia^{1,2}, Junjiang Zhu^{1,2*}, Xiaolin Ou^{1,2}, Shengsheng Zhang^{1,2}, Ruixue Chen^{1,2}, Shaoyu Zhang^{1,2}

¹ Frontiers Science Center for Deep Ocean Multispheres and Earth System, Key Lab of Submarine Geosciences and Prospecting Techniques, MOE and College of Marine Geosciences, Ocean University of China, Qingdao 266100, China

² Laboratory for Marine Mineral Resources, Qingdao National Laboratory for Marine Science and Technology, Qingdao 266100, China

Tsunami is one of the five major marine natural disasters and it seriously threatens the safety of human life and property. Most of earthquake and Tsunami study are mainly focused on the numerical simulation of the generation, propagation, climbing and inundation of tsunamis, as well as on the paleo-tsunami sediments. However, there is still a lack of research on the focal mechanisms of Tsunami earthquakes, especially the Tsunami earthquake with magnitude less than 6.5. In view of the research status of earthquake and Tsunami in China, it is emphasized that the problem of Tsunami caused by earthquakes with magnitude less than 6.5 cannot be ignored. In this paper, 766 global earthquake and Tsunami events have been summarized and sorted out. Based on Frohlich's basic principle of the triangulation of focal mechanism solutions, focal mechanism solutions of Tsunami earthquakes and focal depth have been analyzed. The 341 events occurred after the year of 1976 and the 633 events were analyzed by statistical methods.

Singular mechanism of fault types cause to tsunamis. The Tsunami caused by the thrust type accounts for the largest

proportion. Tsunami earthquakes with magnitude less than 6.5 have a wave height up to 10 meters, which can also produce huge destruction. The thrust type, normal fault type and odd-type earthquakes directly cause the vertical variation of the submarine topography, which cause the Tsunami. While strike-slip type earthquakes may cause Tsunami with the action by the submarine landslide. According to the analysis of focal depth, more than 97% of Tsunami earthquakes are shallow earthquakes within 30 km depth, but there are also medium-deep earthquakes and tsunamis.

Based on the geographical location of China coast and the occurrence of tsunamis in the past, we consider that the earthquakes and tsunamis threatening the coastal areas of China are mainly concentrated in the Manila trench and the Taiwan strait. These locations need to be paid more attention for the tsunami early warning in future, so as to it can reduce the loss by establishing and improving the tsunami early warning system.

The Trials and Tribulations of the Hawaii hot spot model

Zhaoxia Jiang^{1,2*}, Sanzhong Li^{1,2}, Qingsong Liu^{3,4}, Jianli Zhang⁵, Zaizheng Zhou⁶,
Yuzhen Zhang¹

¹Frontiers Science Center for Deep Ocean Multispheres and Earth System/Key Lab of Submarine Geosciences and Prospecting Techniques, MOE, College of Marine Geosciences, Ocean University of China, Qingdao 266100, P.R. China

²Laboratory for Marine Mineral Resources, Qingdao National Oceanography Laboratory for Marine Science and Technology, Qingdao 266237, P.R. China

³ Centre for Marine Magnetism (CM²), Department of Ocean Science and Engineering, Southern University of Science and Technology, Shenzhen 518055, P.R. China

⁴Laboratory for Marine Geology, Qingdao National Oceanography Laboratory for Marine Science and Technology, Qingdao 266237, P.R. China

⁵Frontiers Science Center for Deep Ocean Multispheres and Earth System/ Institute for Advanced Ocean Study, Ocean University of China, Qingdao 266100, P.R. China

⁶College of Earth Science and Engineering, Shandong University of Science and Technology, Qingdao 266590, China

The Hawaiian-Emperor volcanic chain (H-E chain) is located in the middle of the North Pacific Ocean. It extends from northwest to southeast, including two segments, the older Emperor chain and the younger Hawaiian chain between which is a 60° change in strike, here termed the H-E bend. The H-E chain is the clearest and most intensively researched hot spot track in terms of plate motion, mantle plumes, tectonics, geochemical evolution, and lithospheric studies. However, debates on the formation of the H-E chain, in particular the H-E bend, concerning its origin in hot spot drift and/or Pacific plate motion change, have been ongoing for several decades. In this paper, we review current understanding and ideas concerning this debate and suggest ways forward. So far, neither hot spot southerly drift nor Pacific plate motion change can perfectly account for the geometry and progression of the H-E chain. In this review, we put forward a joint model where these two competing processes together can reasonably explain the evolution of the H-E chain and the H-E bend. In addition, we proposed three stages for formation of the H-E chain, including: 1) A ridge-plume interaction stage: Meiji~Detroit seamounts and a possible subducted section; 2) A combination of hot spot-Pacific plate motion: South of Detroit seamount ~ H-E bend; and 3) Pacific plate motion with a fixed hot spot: Hawaiian volcanic chain. In addition, any plate movement at the surface must be balanced by motion deeper in the mantle. Therefore, we consider that the surface Pacific plate motion and the state of

deep mantle plume at 47-55 Ma are not totally separated but co-evolved. Furthermore, reconstructions of the Pacific plate and its boundaries should be considered if Hawaiian hot spot motion makes great contributions to the formation of the H-E chain. Nevertheless, establishing the causal links between these events and their underlying dynamic triggers requires further, more comprehensive work.

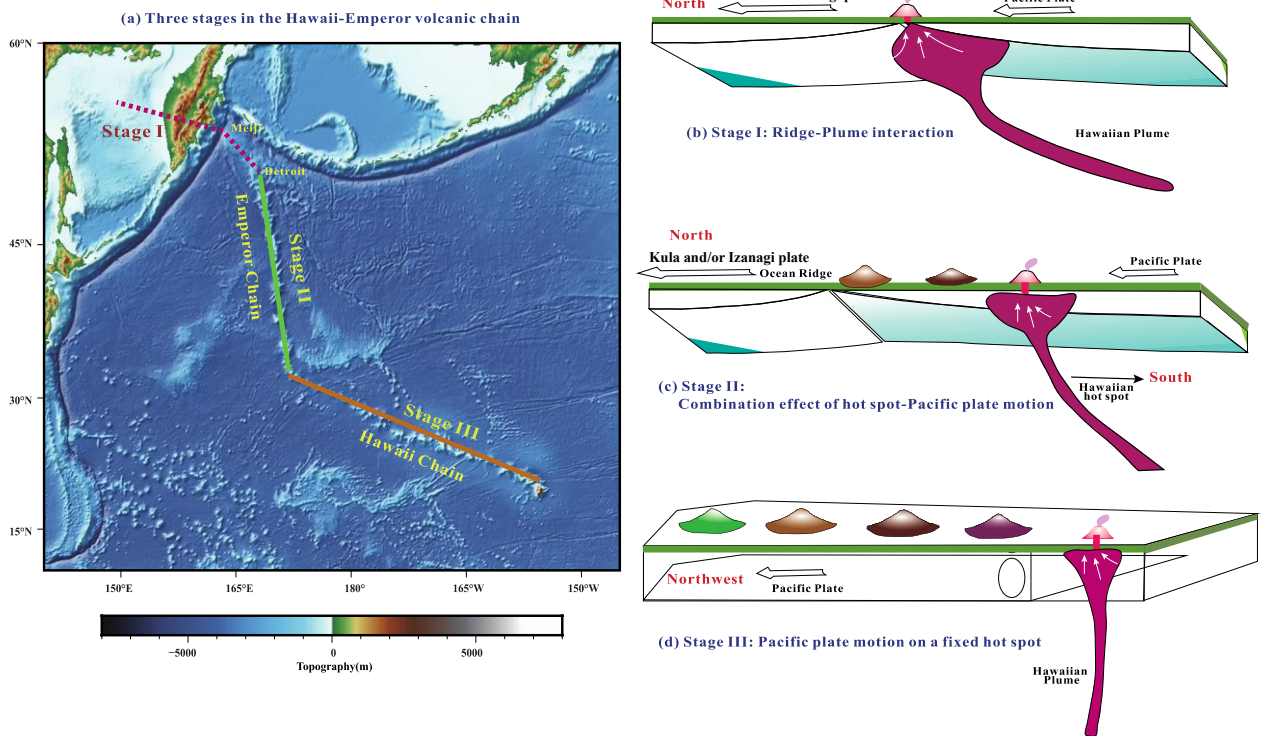


Figure 1 Sketch map for the three stages of formation of the Hawaii-Emperor seamount chain. (a) Three stages range in the geological setting of the Hawaiian-Emperor seamount chain. (b) sketch map for stage I ridge-plume interaction, where the ocean ridge is the Izanagi-Pacific or Kula-Pacific ridge. Here, the mantle plume is close to, and fed by, the ocean ridge and the corresponding ocean crust is young and thin. Materials from ocean ridge and mantle plume contribute to the formation of Meiji and Detroit. In addition, as the Izanagi, Kula and Pacific plate as well as the ridges inbetween all moved northward, the drag from the plates results in tilting of the plume tail. (c) sketch map for stage II combination effect of the hot spot and Pacific plate motion. As the ridge moved the tilted plume tail breaks away from the ridge and gradually returns to its original position, which leads to latitude shift of the hot spot. Meanwhile, the Pacific plate moved northward. Motion of the plate and hot spot resulted in formation of the Emperor chain. (d) Sketch map for stage III Pacific plate motion on a fixed hot spot. At around 47 Ma, Hawaiian hot spot movement stopped. At the same time, Pacific plate motion changed from northward to northwestward due to the trigger of subduction initiation. Then the Pacific plate moved on a fixed hot spot, leading to formation of the Hawaiian volcano chain.

Mg isotopic fractionation involving magmatic-hydrothermal transition recorded in the Himalayan granites

Dong-Yong Li^{1,2,3*} Fang-Zhen Teng², Yilin Xiao³

¹ Ocean University of China, Qingdao, China

² University of Washington, Seattle, WA, USA

³ University of Science and Technology of China, Hefei, China

*Email: lidongyong@ouc.edu.cn

Fluids can not only make a substantial contribution to pegmatite deposits but also play an important role in the magmatic differentiation of granitic melts. Whether or not stable isotopes fractionate during the evolution of granitic magma involving fluid- melt interaction remains unclear. Mg isotopic compositions of Himalayan leucogranites, including two-mica leucogranites and muscovite leucogranites, were carried out in this study, and the results display that muscovite leucogranites have lower $\delta^{26}\text{Mg}$ values than two-mica leucogranites. The positive or negative relations are observed between $\delta^{26}\text{Mg}$ values and other geochemical makers for magmatic-hydrothermal transition, indicating Mg isotopes

fractionate during the magmatic evolution involving fluids. Our modellings of Rayleigh fractionation equation demonstrate that the Mg isotopic variations of Himalayan granites in this study is the consequence of magmatic-hydrothermal transition. Thus we speculate that muscovite leucogranites are formed from more evolved felsic than two-mica leucogranites, excluding the possibility of heterogeneous rocks or different melting reactions. Furthermore, the ubiquitous fluids during late stage of evolution of granites imply that the Himalayan leucogranites have significant potential for pegmatite deposits, especially the LCT-family pegmatite deposits.

Numerical modeling of the coupling between tectonism and sedimentation: A case from the Yangjiang sag of Northern South China Sea

Li Fakun, Dai Liming

College of Marine Geosciences, Ocean University of China, Qingdao 266100, P.R. China

As one of the western Pacific marginal seas, the South China Sea had experienced multiple tectonic movements and sedimentary process, and it's very suitable for the study of the coupling between tectonism and sedimentation. As a secondary sag of the Northern South China Sea, the Yangjiang sag had experienced all the tectonic evolution events and sedimentary processes of the South China Sea. Therefore, the analysis of tectonic-sedimentary for the Yangjiang sag will reveal the tectonic evolution history and the "source-sink" process of the whole basin of the Northern South China Sea. This paper applied the 3D Move balance recovery method and Badlands numerical modeling method to study the tectonic-sedimentary evolution of the Yangjiang sag. We discussed the evolution processes of the coupling between tectonism and sedimentation, and proposes a more intuitive and effective way to investigate sedimentary response to the tectonism. It was of great significant to further understand the "source-sink" process in the northern South China Sea Basin.

The Yangjiang sag in Northern South China Sea was taken as an example to modeling the coupling process between tectonism and sedimentation. Through comprehensive geological and geophysical data, this paper got the ancient landform of the Yangjiang sag based on the accurate 3D seismic data. Then, Badlands numerical modeling software was used to study the paleogeomorphology and "source-sink" process. Based on the research results, we believed that the coupling characteristics of the tectonism and sedimentation of the Yangjiang sag can be summarized into the following four points: (1) Tectonism controlled the basement subsidence process. (2) Basement subsidence controlled the migration of the sedimentary center. (3) Basement subsidence and deposition rate jointly controlled the evolution of paleogeomorphology of the basin. (4) The evolution of paleogeomorphology and the "source-sink" process controlled the changes of sedimentary system.

Geochemical and lead isotope compositions of olivine-hosted melt inclusions from Okinawa Trough: Implications for petrogenesis and slab subduction

Xiaohui Li

Key Lab of Submarine Geoscience and Prospecting Techniques, Ocean University of China, Qingdao 266100, China

Olivine-hosted melt inclusions provide crucial information about their parental magma composition and evolution and represent ideal targets for determining the nature of the poorly understood and still-debated magma sources in the Okinawa Trough, a back-arc basin in the western Pacific. We present the first analyses of the lead (Pb) isotope compositions of olivine-hosted melt inclusions to evaluate the mantle properties and petrogenesis of middle and southern Okinawa Trough volcanic rocks. Melt inclusions have widely variable element and Pb isotope compositions, while erupted host whole-rock compositions are homogeneous.

Two groups of melt inclusions can be distinguished by their trace elements and Pb isotopes in both middle and southern Okinawa Trough. Group 1 melt inclusions have geochemical compositions similar to those of their host whole rocks, which have low $^{207}\text{Pb}/^{206}\text{Pb}$ ratios (<0.850), and may be attributed to the mixing of Pacific Ocean-type mantle (MORB), an EMI-like component from recycled lower continental crust and EMII-like material from subducted sediments. Group 2 melt inclusions

have higher $^{207}\text{Pb}/^{206}\text{Pb}$ ratios (>0.850) and Rb, and U contents and lower Cu, and Pb contents than their host whole rocks. High Rb and U contents may be induced by specific melts generated by possible breakdown reactions of some accessory minerals, such as phengite and cordierite, while low Cu and Pb contents are attributed to sulfide precipitation, metal flushing and/or metallic element fractionation during magma evolution. In addition, the Pb isotopes of the group 2 melt inclusions are similar to those of the Kuanhsi-Chutung basalts, which are correlated with some intraplate volcanism in the Fujian-Taiwan region. We infer that the group 2 melts were preexisting small volumes of magma that were emplaced in the middle-lower continental crust (~ 11 km), experienced extensive magma evolution and were entrained by upwelling magma. Our melt inclusion data suggest that pervasive magma mixing may have occurred in the magma source prior to eruption in the Okinawa Trough because of Philippine Sea Plate subduction and preexisting intraplate magmatism.

High-silica rhyolites in the latest stage of massive Cretaceous volcanism in the SE China: insights into modified crustal sources and low-pressure magma chamber

Xi-Yao Li^{1,2}, Sanzhong Li^{1,2}, Yanhui Suo^{1,2}, Pengcheng Wang¹, Jie Zhou¹

¹ Frontiers Science Center for Deep Ocean Multispheres and Earth System, Key Lab of Submarine Geosciences and Prospecting Techniques, MOE and College of Marine Geosciences, Ocean University of China, Qingdao 266100, China

² Laboratory for Marine Mineral Resources, Qingdao National Laboratory for Marine Science and Technology, Qingdao 266237, China

High-silica rhyolites (i.e., SiO₂ > 75%, anhydrous basis) are important components in the continental crust, although their origin, evolution and eruption conditions are controversial. Late Cretaceous felsic volcanism erupted as calderas in the latest stage of the massive Cretaceous volcanism in the SE China. Our recent work on the high-silica rhyolites from the Shiniushan and Xiaoxiong calderas in eastern Fujian–Zhejiang provinces, SE China. Zircon U–Pb dating constrains these rhyolites eruptions to 94–92 Ma and 93–89 Ma in the sites of the two calderas. All the high-silica rhyolite samples possess high-silica contents with peraluminous characteristics and are enriched in light rare earth elements, Rb and Th–U, and depleted in Ba, Nb–Ta, Sr and Eu. These samples have high whole-rock F but low Cl

contents. Apatite minerals separated from the high-silica rhyolites are classified as fluorapatite and show F-rich, Cl-poor, low (La/Sm)_N and high (Gd/Yb)_N ratios. The samples yield negative whole-rock $\epsilon_{Nd}(t)$ (–3.3 to –6.3), negative apatite $\epsilon_{Nd}(t)$ (–5.2 to –6.6) and negative zircon $\epsilon_{Hf}(t)$ values (–0.1 to –9.6). Our work suggest that their primary magma was derived from modified crustal sources that could contain a mixture of ancient and juvenile components, and it then evolved, was injected into a low-pressure magma chamber. And finally erupted with the release of volatiles at the magma chamber roof. We infer that the SE China was mainly under lithospheric extension setting during early Late Cretaceous because of slab roll-back and steepening of the subducted Paleo-Pacific Plate.

Disintegration and deformation characteristics of the Keluo Complex in Nenjiang, Heilongjiang Province: Evidence for multistage evolution of Da Hinggan Mountains

Chenyue Liang^{1,2}, Zhiwei Song¹, Yongjiang Liu^{3,4}, Changqing Zheng^{1,2}, Franz Neubauer⁵, Long Chen¹, Xiaojing Liu¹

¹ College of Earth Sciences, Jilin University, Changchun, Jilin, 130061, China

² Key laboratory of Mineral Resources Evaluation in Northeast Asia, Ministry of Natural Resources, Jilin University, Changchun, Jilin, 130061, China

³ Key Lab of Submarine Geosciences and Prospecting Techniques, Ministry of Education, College of Marine Geosciences, Ocean University of China, Qingdao, Shandong, China

⁴ Laboratory for Marine Mineral Resources, Qingdao National Laboratory for Marine Science and Technology, Qingdao, Shandong, China

⁵ Department of Geography and Geology, University of Salzburg, Salzburg, Austria

*Email: chenyueliang@jlu.edu.cn (C. Y. Liang)

The Da Hinggan Mountains (DHM) is the typical mark of the morphology in NE China, which evolution history and uplift mechanism have remained controversial up to now. We present comprehensive research of micro-macro-structures, kinematics, rheology, quartz EBSD fabric, geochemistry and geochronology data of the Keluo Complex (KC) exposed in the northern DHM. The KC is not the Precambrian basement rock of the Xing'an massif. However, it is dominated by the deformed Late Paleozoic rocks (294.9 ~ 327.3 Ma), and also was intruded by the Early Mesozoic multistage granitic rocks (219.8 ~ 175.5 Ma), and finally suffered the magmatism and metamorphic deformation of the Late Jurassic (152.0 ~ 157.7 Ma) and late Early Cretaceous (118.3 Ma). The Late Paleozoic rocks are dominantly granitic mylonite and deformed rhyolite formed in a post-collisional extensional environment that might closely relate to the collision and amalgamation of the Xing'an and Songnen massifs.

The Early Mesozoic granitic gneiss was derived from magma generated by partial melting of the lower continental crust within an active continental margin setting related to the southward subduction of the Mongolia-Okhotsk Ocean. In addition, two deformation events (D_1 and D_2) were recognized in the KC, which occurred in the Late Jurassic and late Early Cretaceous, respectively. The D_1 is dominated by the top-to-the-SW sinistral strike-slip, which is a mid-high temperature

deformation with temperature between 500 and 600 °C developed at a deep ductile regime resulted from NW-SE compression, and the deformation process has a high strain rate ($4.48 \times 10^{-12} \sim 8.74 \times 10^{-15} \text{ s}^{-1}$), which is characterized by both simple-shear and pure-shear dominated general shearing with SL and S tectonites. The D_2 was a bi-directional extensional and detachment deformation corresponding to a low temperature (300 ~ 400 °C) deformation corresponded to a greenschist metamorphic facies conditions. The deformation developed at a shallow ductile regime resulted from NW-SE extension, characterized by pure-shear dominated general shearing with L = S tectonites.

Different tectonic regimes may control the D_1 and D_2 . The former was influenced by the subduction and closure of the Mongolia-Okhotsk Ocean, while the latter may be caused by the superposition of the extension after the closure of the Mongolia-Okhotsk Ocean and the rollback of the Paleo-Pacific Plate.

Keywords: Keluo Complex; Zircon U-Pb age; EBSD; Rheological parameters; Da Hinggan Mountains

***This project was financially co-supported by the National Natural Science Foundation of China (No. 42130305 and 41972215) and the National Key R&D Program of China (Grant No. 2017YFC0601401).

Microplate identification of mid-ocean ridge system in South America and the eastern Pacific Ocean based on potential field data processing and analysis

Jie Liu^{1,2}, Sanzhong Li^{1,2*}, Suhua Jiang^{1,2}, Yanhui Suo^{1,2}

State Key Laboratory of Lithospheric Evolution, Institute of Geology and Geophysics, Chinese Academy of Sciences, Beijing 100029, China

¹ Frontiers Science Center for Deep Ocean Multispheres and Earth System, Key Lab of Submarine Geosciences and Prospecting Techniques, MOE, College of Marine Geosciences, Ocean University of China, Qingdao 266100, China

² Laboratory for Marine Mineral Resources, Qingdao National Laboratory for Marine Science and Technology, Qingdao 266237, China

*E-mail: sanzong@ouc.edu.cn

Geophysical potential field data provides information on the rock properties and is a powerful tool for tectonic interpretation at regional and local scales (Jiang et al., 2018). The edge detection technique has been widely applied to identify the boundaries of local target bodies in the subsurface (e.g., ore bodies, veins, mineralized zones, etc.). In addition, this technique is also applied in the study of large-scale tectonic framework, which can provide geophysical basis for regional and even global plate classification and boundary identification.

With the continuous improvement of plate tectonics theory, more and more scholars have paid attention to microplates (Matthews et al., 2016; Li et al., 2018). The area of microplate is smaller than that of major and medium plates, about the order of 100,000 square kilometers, and its interior is a relatively uniform rigid block. The boundary of microplate can be composed of various tectonic structures such as mid-ocean ridges, subduction zones, transform faults, fracture zones and pseudo-faults, etc. These structures often show distinct and unique response characteristics on the gravity and magnetic data, which provides a basis for processing and identifying oceanic micro-block boundaries using the potential field data.

Here, we focus on the mid-ocean ridge system in South America and the eastern Pacific Ocean. The data of free-air gravity anomaly, Bouguer gravity anomaly and magnetic anomaly are collected and analyzed. Combined with anomaly separation, edge detection methods (such as horizontal derivative, vertical derivative, total horizontal derivative, tilt angle, analytic signal amplitude and Theta map) are used and

compared. The following results were obtained:

(1) The vertical derivatives of the free-air gravity anomaly and the magnetic anomaly after polarization have good correspondence with the large-scale tectonics, which can clearly identify the regional tectonic boundaries such as mid-ocean ridges, subduction zones and transform faults;

(2) Three methods including total horizontal derivative, tilt angle and total horizontal derivative of tilt angle have good effects on the identification of shallow oceanic micro-block boundaries, and can identify the fracture zones and the fractures cutting the lithosphere;

(3) Vertical gravity gradients have higher horizontal resolution, and the identified conjugate pseudo-faults and rotated abyssal hill fabric are revealing to the evolutionary patterns of microplates;

(4) The opposite polarity of crustal residual gravity anomalies can be observed on both sides of the microplate boundary, such as the Easter microplate and the Juan Fernandez microplate, which suggests that the boundary of the microplate may be a transition zone between high and low gravity;

(5) From the deep source gravity field after anomaly separation, the mid-ocean ridge shows relatively low gravity values, and the interior of microplates show relatively high gravity values, according to which the Cocos, Nazca and Bauer microplates can be clearly identified;

(6) The Bouguer gravity field and deep source gravity field show that both the northwestern and eastern parts of the Caribbean plate exhibit relatively low gravity relative to the

central part, suggesting that several microplates exist in the Caribbean plate. Thus, the Caribbean plate may have undergone a more complex tectonic movement history than other plates.

The above study shows that the potential field data processing and analysis can play an important role in microplate identification and boundary detection, and its potential can be exploited by means of potential field inversion and cross-validation of multiple types of data, so as to be a powerful geophysical tool to support the development of microplates theory.

Acknowledgements

This work is supported by National Natural Science Foundation of China (grants 91958214 and 41976054).

References

- Li, S., Y. Suo, X. Li, B. Liu, L. Dai, G. Wang, J. Zhou, Y. Li, Y. Liu, X. Cao, I. Somerville, D. Mu, S. Zhao, J. Liu, F. Meng, L. Zhen, L. Zhao, J. Zhu, S. Yu, Y. Liu and G. Zhang, 2018. Microplate tectonics: New insights from micro-blocks in the global oceans, continental margins and deep mantle. *Earth-Science Reviews*, 185, 1029-1064.
- Matthews, K.J., R. Dietmar Müller and D.T. Sandwell, 2016. Oceanic microplate formation records the onset of India–Eurasia collision. *Earth and Planetary Science Letters*, 433, 204-214.
- Jiang, S., W. Cao, S. Li, G. Wang, I. Somerville, W. Zhang, F. Zhao and H. Chen, 2018. Tectonic units of the Early Precambrian basement within the North China Craton: Constraints from gravitational and magnetic anomalies. *Precambrian Research*, 318, 122-132.

Dynamics of Closure of the Proto-Tethys Ocean: the Southeast Asian Tethys realm

Junlai Liu^{1*}, Xiaoyu Chen¹, Wenkui Fan¹, Hongshuai Shan¹, Jiaxin Yan¹, Xu Ding¹, Tianyu Zhao¹, Xinqi Yu¹, Zhenghong Liu², Zhongyuan Xu²

¹ State Key Laboratory of Geological Processes and Mineral Resources, China University of Geosciences, Beijing 100083, China

² Faculty of Earth Sciences, Jilin University, Changchun 130061, China

*E-mail: jliu@cugb.edu.cn

The Proto-Tethys evolution exemplifies a scenario of drifting of continental plates during closure of the Proto-Tethys Ocean. The Pan-Cathaysian blocks in the Southeast Asian tectonic realm (SATR) derived from break-up of the Rodinia supercontinent witnessed the process of the Proto-Tethys evolution. The blocks and suture zones between them offer information on the dynamics of continental drifting linked to shallow mantle convection and deep mantle flow.

Early Proto-Tethys break-up tectonics is evidenced by volcano-sedimentary records and their source affinities in the SATR. Gondwana-centered convergence of the blocks initiated when the Rodinia supercontinent broke-up in the Neoproterozoic. The Proto-Tethys convergent tectonics in the SATR was formed from the subduction of the Proto-Tethys Changning-Menglian (CM) Ocean beneath the northern margin of the Gondwana and of a subsidiary basin, i.e., the Tam Ky-Phuoc Son-Po Ko (TPP) Ocean. Occurrence of tectonic mélanges (e.g., the Lancang mélange) and extensive arc (continental or intra-oceanic) magmatic rocks attests the switch from passive to active plate margins, forming advancing subduction zones (Andean-type) along both distal and proximal margins of the CM Ocean, and within and along the proximal margin of the TPP Ocean. Rifting (Jinshajiang-Ailao Shan-Song Ma, or JAS) and back-arc rifting (Dapingzhang) occurred

during or subsequent to the transition from advancing subduction to retreating subduction along the southern margin of the Indochina block. Suturing and collision of the blocks in the SATR occurred in the late early Paleozoic, which is evidenced by, e.g., existence of high-pressure rocks along the CM suture and post-collisional magmatic rocks along the Tam Ky-Phuoc Son suture.

The Proto-Tethys evolution narrates a scenario of supercontinent break-up and assembly. Progressive Gondwana-centered convergent drifting of the Pan-Cathaysian blocks induced progressive closure of the Proto-Tethys main and subsidiary oceans, and rifting and closing of the rift basin or back-arc basin. Advancing subduction-ridge spreading-retreating subduction systems (ARRs) or subduction-spreading-subduction systems (SSSs) were formed and transported toward the Gondwana during the convergent drifting of the continental blocks. It is suggested that coupled shallow- and deep mantle flow (i.e., stratified mantle convection) is the major driving mechanism of the Gondwana-centered convergence of the Pan-Cathaysian blocks. In the model, the shallow-mantle convections directly affected the subduction geometries and plate kinematics, while the deep-mantle convection is responsible for the drifting of the continental blocks, formation of ARR and migration of the SSSs.

The impact of dust on the Neoproterozoic climate

Peng Liu

Frontiers Science Center for Deep Ocean Multispheres and Earth System, Key Lab of Submarine Geosciences and Prospecting Techniques, MOE, College of Marine Geosciences, Ocean University of China, Qingdao 266100, China

The land surface during the Neoproterozoic (1000 – 540 million years ago; Ma) should be more susceptible to dust emission than that of the present day since land plants have not evolved yet during that time. The impact of dust on the Neoproterozoic climate, however, to the best of our knowledge has not been studied. This impact could have important implication to the formation of snowball Earth events that occurred in the late Neoproterozoic. As an initial investigation, we use a fully coupled atmosphere-ocean general circulation model to study the sensitivity of the Neoproterozoic climate to different land surface erodibility. The model employed in this study is CESM1.2 developed by the National Center of Atmospheric Research's (NCAR), and is run at F19g16 horizontal resolution. The atmospheric component of the model is CAM4, in which dust is arranged into four size bins (0.1–1.0, 1.0–2.5, 2.5–5.0, and 5.0–10 μm diameter), and the volume fraction emitted into each bin is independent of wind speed, and distributed following brittle fragmentation theory. The emission, transportation, dry and wet deposition processes of dust, as well as its impact on the snow albedo, are all simulated by the model. Only the direct and semi-direct radiative effect of dust is considered in this version of the model. The solar luminosity is

assumed to be 94% of the present-day value. The concentration of CO_2 , CH_4 and N_2O are set to be 2000 ppmv, 805.6 ppbv and 276.7 ppbv, respectively. The super-continental configuration for the 720 Ma is employed. The land surface is characterized as desert, but the surface erodibility is set to 0, 0.0375, 0.07, 0.15, and 0.3 in four simulations, respectively. The global mean optical depth due to dust in the visible band obtained by model is 0, 0.312, 0.504, 0.764, and 1.36 in the four sensitivity runs, respectively. Therefore, even with mild surface erodibility, the optical depth due to dust alone is much greater than that (~ 0.15) due to all the aerosols on the present-day Earth. The global mean temperature decreases dramatically from 15°C when there is no dust to 3.3°C when the surface erodibility is set to 0.0375. It decreases further to 0.0°C and -2.5°C when the surface erodibility is increased to 0.07 and 0.15, respectively. The temperature even decreased to -5.4°C when erodibility is increased to 0.3. Such large effect means that previous estimates for the CO_2 threshold for the formation of snowball Earth events might need to be increased substantially. Moreover, it is found that the distribution of sea-ice thickness is significantly impacted by the presence of dust, and shows some strikingly different patterns than when there is no dust.

3D numerical simulation of deep-shallow coupling in pull-apart basins

Ze Liu^{1,2}, Sanzhong Li^{1,2*}, Guangzeng Wang^{1,2}, Xuesong Ding³, Pengcheng Wang^{1,2}, Liming Dai^{1,2}, Yanhui Suo^{1,2}, S. Wajid, Hanif Bukhari^{1,2}

¹ Frontiers Science Center for Deep Ocean Multispheres and Earth System, Key Lab of Submarine Geosciences and Prospecting Techniques, MOE, College of Marine Geosciences, Ocean University of China, Qingdao 266100, China

² Laboratory for Marine Mineral Resources, Qingdao National Laboratory for Marine Science and Technology, Qingdao 266237, China

³ Department of Earth, Planetary and Space Sciences, University of California, Los Angeles, CA 90095, USA

*Email: sanzong@ouc.edu.cn

Strike-slip faults in pull-apart basins commonly display complex 3D geometric structures, which makes it difficult to interpret the spatial and temporal evolution of those basins. Coupled thermo-mechanical and surface process models represent a powerful tool to investigate the structural development of pull-apart basins and the associated sedimentary architectures. We established three cases with representative endmember strike-slip fault patterns: 45° underlapping releasing stepover, 90° non-overlapping releasing stepover, and 135° overlapping releasing stepover. Our numerical simulation have successfully simulated the evolution of the pull-apart basins developed dextral strike-slip fault system in rigid basement. We associated the different input tectonic forcing with the sedimentary strata testing the effect under different deep processes. According to simulation results, the different types of master faults produced different basin geometries and fault system. Furthermore, we found that the

sedimentary distribution varied in each model at different stages of the basin's evolution. At the beginning, the sedimentary range was the largest in the 45° underlapping releasing stepover model, but at the end it was the smallest. However, 135° overlapping releasing stepover model showed the opposite result. The geometry of the basin usually depends on the underlying fault system. We observed that the activity of the inner extensional fault has been higher than the outside during the evolution process. Therefore, inner tensional faults are more dominant for the development of basin than external tensional faults, especially in the 135° overlapping releasing stepover model.

Keywords: Pull-apart basin; Strike-slip fault; Coupled thermo-mechanical and surface process modeling; Deep dynamic process; Earth's surface system

A step-like crustal growth pattern in response to the evolution of supercontinent cycles: Evidence from the eastern Central Asian Orogenic Belt

Xinyu Long¹, Jie Tang^{1*}, Wenliang Xu^{1,2}, Chenyang Sun¹, Jinpeng Luan¹

¹ College of Earth Sciences, Jilin University, Changchun 130061, China

² Key Laboratory of Mineral Resources Evaluation in Northeast Asia, Ministry of Natural Resources of China, Changchun 130061, China

*Email: 893335234@qq.com (J. Tang)

The formation of felsic and buoyant continental crust is particular to Earth in the solar system, and the study of the processes through and rates at which continental crust has grown through time is a fundamental focus of earth science research. The role of supercontinent cycles in controlling the generation and evolution of continental crust can be detected in the episodic geological record, but their role remains unclear in existing models for the growth of global continental crust. This is probably due to the choice of study subject and scale, i.e., previous researches mostly focused on geological records from cratons. However, a systematic and detailed study on crustal growth pattern of microcontinent in an accretionary orogen, is expected to bring about a different growth model, as well as a more complete account of the influence of the assembly, evolution, and breakup of supercontinents on regional crustal growth. Here we present *in situ* zircon U–Pb and Lu–Hf isotopic data for 64 granitoids from the Songnen Massif and the Duobaoshan arc terrane (a typical suture belt in the eastern Xing'an Massif) in the eastern Central Asian Orogenic Belt (CAOB). A total of 1225 magmatic zircon U–Pb dating analyses yield ages ranging from 1094 to 174 Ma, and 571 dated zircons were chosen for Hf isotope analysis, with $\epsilon_{\text{Hf}}(t)$ values and T_{DM2} ages ranging from -8.9 to $+15.6$ and 2295 to 234 Ma, respectively. The zircon $\epsilon_{\text{Hf}}(t)$ values for the granitoids appear to progressively decrease from the Zhangguangcai Range in the south to the Lesser Xing'an Range in the north, reflecting a northward increase in the proportion of ancient crustal material in the magma source regions. In contrast, granitoids selected from the Duobaoshan arc terrane exhibit quite distinct zircon Hf isotopic features. They are characterized by markedly high $\epsilon_{\text{Hf}}(t)$

values ($+7.4$ to $+16.5$) and young T_{DM2} ages (329 to 813 Ma). The spatiotemporal variations in zircon Hf isotopic compositions of granitoids from the Songnen Massif and the Duobaoshan arc terrane indicate not only a heterogeneous lower continental crust within individual microcontinent, but also markedly different crustal evolution processes between the microcontinents and suture belts in the eastern CAOB.

Based on zircon U–Pb ages and T_{DM2} ages of the granitoids, this study established the crustal growth curve of the Songnen Massif. Neoproterozoic–Mesozoic granitoids in the region show a step-like crustal growth pattern over time with three major periods of development: Paleoproterozoic crustal growth at 2.2–1.8 Ga, Mesoproterozoic growth at 1.6–1.0 Ga, and a third pulse of growth at 0.85–0.6 Ga, along with three short pauses at 1.8–1.6 Ga, 1.0–0.85 Ga, and ca. 420 Ma. The enhanced and degressive rates of crustal growth of microcontinents in the eastern CAOB are linked to the assembly, collision, and breakup phases of supercontinents through time. Crustal reworking of the Songnen Massif occurred during 1000–180 Ma, with two obvious fluctuations at 800–600 and ca. 420 Ma, which provided a major contribution to the heterogeneity of lower continental crust and was controlled by the evolution of supercontinents and plate tectonic processes. Combined with isotopic compositions of granitoids from the Duobaoshan arc terrane and other microcontinents in the eastern CAOB, we propose that most of the continental crust beneath the eastern CAOB accreted during the Precambrian, whereas a small amount of lateral crustal growth occurred in continental arc settings during orogenies and amalgamation of microcontinents during the Phanerozoic.

Pre-Alpine tectonic evolution of the Eastern Alps: From Prototethys to Paleotethys

Franz Neubauer^{1,*}, Yongjiang Liu^{2,3}, Yunpeng Dong⁴, Ruihong Chang¹, Johann Genser¹, Sihua Yuan⁵

¹ Department of Geography and Geology, Paris-Lodron-University of Salzburg, Austria.

² Frontiers Science Center for Deep Ocean Multispheres and Earth System, Key Lab of Submarine Geoscience and Prospecting Techniques, College of Marine Geosciences, Ocean University of China, Qingdao 266100, China

³ Laboratory for Marine Mineral Resources, Qingdao National Laboratory for Marine Science and Technology, Qingdao 266237, China

⁴ State Key Laboratory of Continental Dynamics, Department of Geology, Northwest University, Northern Taibai Str. 229, Xi'an 710069, China

⁵ College of Earth Science, Institute of Disaster Prevention, Sanhe 065201, Hebei, China

*Email: franz.neubauer@sbg.ac.at

In all reconstructions published during the last two decades, the Austroalpine and the correlative Southalpine basement units of the Eastern Alps were considered to represent a uniform continental block that split off from the northern Gondwana margin during Early Paleozoic times and collided with microcontinental blocks during the Variscan orogeny in the early Late Carboniferous. Afterwards, these units formed finally the outboard part of the European Variscides adjacent to the Paleotethys Ocean. The combined Austroalpine /Southalpine basement extends to the Western Carpathians, contains Ediacaran and Early Paleozoic ophiolites and magmatic arcs and Devonian passive margin successions and represents a key region for resolving the Late Neoproterozoic to Late Paleozoic tectonic evolution of the basement in the Alpine-Mediterranean mountain belts. The Austroalpine and Southalpine basement contains well-known fossil-rich Ordovician and Silurian rift and mainly Devonian passive margin successions summarized as the Noric and Carnic domains juxtaposed to amphibolite-grade metamorphic complexes during Early Carboniferous plate collision. In the metamorphic units the following main stages of two distinct Ediacaran to Cambrian arc systems were recognized, correlating with subduction of the Prototethys Ocean (Fig. 1): The continental Wechsel Arc was inactivated during Late Cambrian times, whereas the Silvretta-Gleinalpe Arc was reactivated at the Devonian/Carboniferous boundary during subduction of the Devonian Balkan-Carpathian Ocean.

Prototethyan oceanic crust is preserved in the ophiolitic Upper Neoproterozoic to Middle Ordovician Speik Complex, that was obducted onto the Silvretta-Gleinalpe Arc during Late Ordovician to Early Silurian times. On the other hand, the Noric domain was initially part of the northern Gondwana margin and includes a virtually continuous sedimentary section ranging from the Early Ordovician to earliest Pennsylvanian. It started with an Early to Late Ordovician rift succession with mafic and acidic volcanic rocks related to rifting of parts of the Noric domain from the northern Gondwana margin forming the Rheic Ocean in between. In both Noric and Carnic domains, Silurian strata were deposited during a quiet tectonic period followed by onset of a second rifting period during Late Silurian times, which resulted in deposition of thick Devonian carbonates heralding the opening of the Balkan-Carpathian Ocean and separation of the Paleo-Adria microcontinent from Gondwana. Late Devonian–Carboniferous plate convergence led to subduction of this oceanic rift followed by subduction of the Paleo-Adria margin underneath the accreted Variscan convergence belt followed by collision and Late Carboniferous intramontane molasse deposition. However, new data argues that a third ophiolitic belt, the Plankogel ophiolitic mélange, that formed as part of the Paleotethys Ocean during Devonian, and was reactivated as trench during initial consumption of the Paleotethys Ocean during Late Permian–Triassic times. The Middle-Late Triassic plutonic and volcanic rocks of the

Southern Alps are considered, in this preliminary model, to represent the magmatic arc associated with Paleotethys subduction.

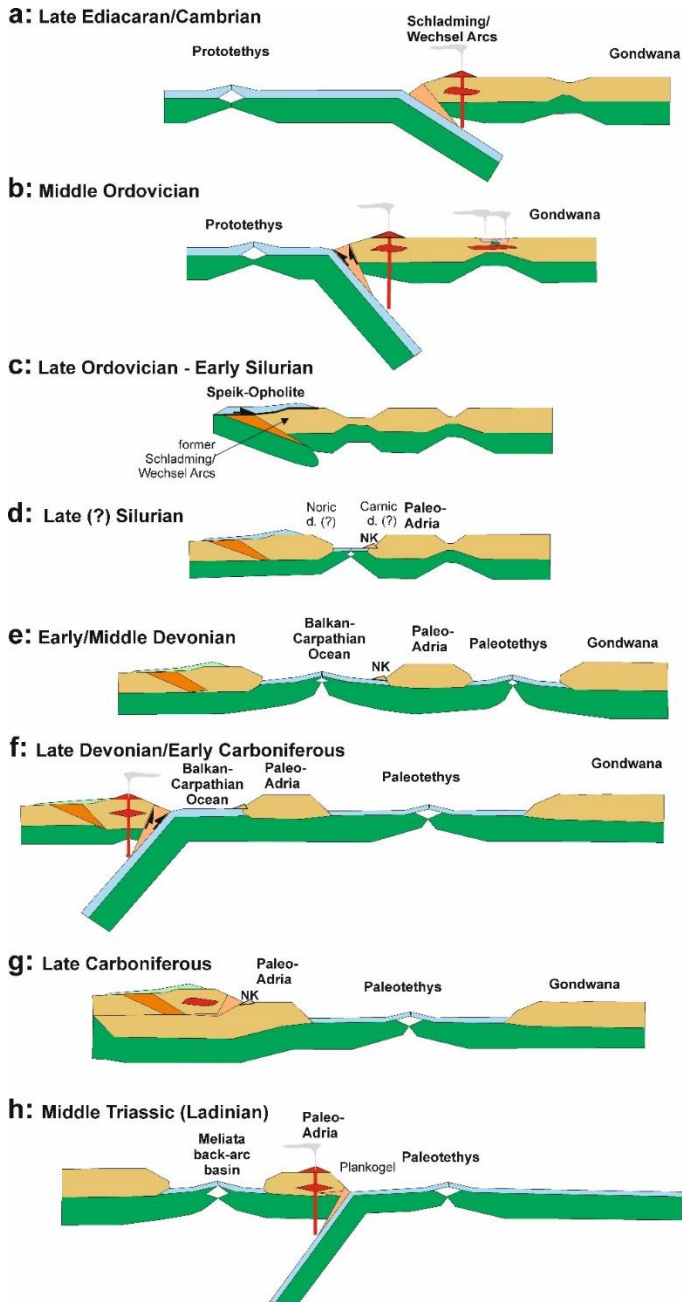


Figure 1. Cross-sectional view of a new plate tectonic reconstruction. NK: Nötsch-Kaintaleck-Klatov tectonic belt. For explanation, see text.

Frequency-dependent anisotropy in partially saturated porous rock with multiple sets of meso-scale fractures

Shuo Pang^{1,2,3}, Huilin Xing^{1,2,3,*}, Alexey Stovas⁴

¹ Frontiers Science Center for Deep Ocean Multispheres and Earth System, Key Lab of Submarine Geosciences and Prospecting Techniques, MOE and College of Marine Geosciences, Ocean University of China, Qingdao, 266100, China.

² Laboratory for Marine Mineral Resources, Qingdao National Laboratory for Marine Science and Technology, Qingdao, 266237, China.

³ International Center for Submarine Geosciences and Geoengineering Computing (iGeoComp), Ocean University of China, Shandong Qingdao 266100, China

⁴ Department of Geoscience, Norwegian University of Science and Technology, Trondheim, 7491, Norway.

*Email: h.xing@ouc.edu.cn

Accurate modeling of the frequency-dependence of seismic wave velocity related to fracture system and fluid content is crucial to the quantitative interpretation of seismic data in fractured reservoirs. Both meso-scale fractures and patchy saturation effects can cause significant velocity dispersion and attenuation in the seismic frequency band due to wave-induced fluid flow (WIFF) mechanism. Considering the coupled impact of “meso-scale fractures” and “patchy saturation”, we derive expressions for the frequency-dependent anisotropy in partially saturated porous rock containing two fracture sets with different orientations, sizes and connectivities. Especially, we simplify the rock-physics model as an orthorhombic (ORT) media by assuming the meso-scale fractures to be orthogonal and give the explicit expressions for frequency-dependent elastic constants. Finally, we give the expressions for the frequency-dependent

phase velocity in patchy saturated and fractured ORT media and investigate the effect of patchy saturation on P-wave velocity at different polar and azimuth angles. In this paper, we investigate the effects of fluid saturation and fluid pressure on frequency-dependent velocities and Thomsen anisotropy parameters. Also, the effect of the relative permeability is very noticeable. The relaxation frequency can be lower in partially saturated fractured rocks compared with the fully saturated case, which makes the rock have a larger stiffness. The non-monotonic relationships between frequency-dependent anisotropy and fluid saturation add complexity to seismic forward modeling and inversion in reservoirs with complex fracture patterns.

Keywords: Elasticity and anelasticity; Permeability and porosity; Wave propagation

Detrital zircon U-Pb ages, Lu-Hf isotopes and whole-rock geochemical and isotope data from greywacke sandstones of eastern Kazakhstan

A. Perfilova^{1,2}, I. Safonova^{1,2}, S. Aoki³, T. Komiya⁴, B. Wang⁵, M. Sun⁶

¹ Sobolev Institute of Geology and Mineralogy SB RAS, Koptyuga ave. 3, Novosibirsk 630090, Russia

² Novosibirsk State University, Pirogova St. 1, Novosibirsk, 630090, Russia

³ Graduate School of International Resource Sciences, Akita University, 1-1 Tegatagakuen-machi, Akita 010-8502, Japan

⁴ Department of Earth Science and Astronomy, University of Tokyo, Tokyo, Meguro 153-8902, Japan

⁵ State Key Laboratory for Mineral Deposits Research, School of Earth Sciences and Engineering, Nanjing University, 210023 Nanjing, China

⁶ Department of Earth Sciences, the University of Hong Kong, Pokfulam, Road, Hong Kong, China

The Char and Zharma zones are located in the western Central Asian Orogenic Belt, in the eastern Kazakhstan (Fig. 1). The Char zone includes Devonian to Carboniferous igneous and sedimentary rocks of Ocean Plate Stratigraphy (OPS), arc-related igneous rocks and fore-arc and continental sediments (Safonova et al., 2012, 2018). The sandstones are associated with late Devonian and early Carboniferous volcanic rocks of supra-subduction (intra-oceanic arc) geochemical affinities. The Zharma zone is a part of the Zharma-Saur terrane located in Kazakhstan, and the Saur zone is located mostly in NW China. The samples under study are massive grey to dark-grey and greenish grey sandstones. They are fine- to medium-grained and medium to poorly sorted. Petrographically the sandstones represent greywackes, lithic arenite and litharenite and geochemically they are greywackes or Fe-shales.

The detrital zircon from sandstones are rounded or euhedral prismatic in shape, transparent or slight yellow. The values of Th/U for all analyzed zircons are higher than 0.04, but lower than 2.09 suggesting their igneous origin. The U-Pb age spectrum of sample Ch-01-17 is generally unimodal with the major peak at ca. 325 Ma (Serpuchovian). The U-Pb age spectra are also unimodal for samples Ch-27-16 and Ch-37-16 with the major peak at ca. 330 Ma (Visean-Serpuchovian boundary). Ch-03-16 and Ch-50-16 yielded unimodal distribution of U-Pb ages peaked at 340 and 345 Ma (Visean). Seventy-six grains were analyzed in the Zharma sample (Zh-01-13), of which 65 showed relatively good concordance. The U-Pb age spectrum is also

unimodal with the peak at 340 Ma. In general, the dominantly unimodal distributions of U-Pb detrital zircon ages from Char and Zharma sandstones have peaks at 345, 340, 330 and 325 Ma (Fig. 2).

The Char greywackes show lower Al₂O₃ (av. 17 wt.%), Fe₂O₃ (av. 5.75 wt.%), TiO₂ (av. 0.8 wt.%), K₂O (av. 2.03 wt.%) and MnO (av. 0.08 wt.%), but higher MgO (av. 2.5 wt.%), CaO (av. 2.82 wt.%) and Na₂O (av. 4.79 wt.%) compared to PAAS (Taylor and McLennan, 1985), implying a relatively mafic source. The Zharma sample has a composition different from most of the Char samples. Compared to PAAS it shows lower Fe₂O₃ (6.5 wt.%), MgO (2.2 wt.%) and MnO (0.11 wt.%), but similar in other oxides.

Both the Char and Zharma samples are generally less felsic than the average upper continental crust (UCC). The Char samples show negative SiO₂ vs. TiO₂, Al₂O₃, MgO and Fe₂O₃ correlations similar to those found out in the Char volcanic rocks (Safonova et al., 2018). In the classification diagram of Pettijohn et al. (1987), the Char and Zharma samples plot in the field of greywacke. In the diagram by Herron et al. (1988) the Char samples plot in the field of Fe-shales, whereas the Zharma sample plots in the field of shale. All samples have similar chondrite-normalized REE patterns showing enrichment in the light rare earths (La_N/Yb_N = 4.3-7.2, Gd_N/Yb_N = 1.4-1.6), small Eu troughs and flat HREE segments. The primitive mantle normalized multi-element spectra for all samples show clear Ta-Nb negative anomalies relative to La (Nb/La_{pm} = 0.29-0.4,

Ta/La_{pm} = 0.27-0.46) and Th (Nb/Th_{pm} = 0.16-0.24, Ta/Th_{pm} = 0.17-0.28).

The Char sandstones yielded positive εNd(t) values of 5.9, 6.5 and 7.6 and positive εHf(t) values ranging from 5.5 to 14.0. The Zharma sample peaked at 339 Ma also yielded highly positive εHf(t) values ranging from 7.2 to 13.5.

The U-Pb age distribution curves are dominantly unimodal suggesting intra-oceanic arc tectonic settings of deposition. Their major geochemical features in terms of both major oxides and trace elements are very close to those of supra-subduction igneous rocks, in general, and those of the Char zone, in particular. Both, the Hf-in-zircon and whole-rock Nd data suggests derivation of their igneous protoliths from juvenile mantle sources typical also of intra-oceanic arcs. The holistic analysis of all new data and previous results allows us to conclude that the Char and Zharma greywacke sandstones were deposited at a Pacific-type convergent margin associated with one or more intra-oceanic arcs.

Acknowledge:

The study was supported by the Russian Science Foundation (projects no. 20-77-10051, 21-77-20022), Russian Foundation for Basic Research (project no. 20-35-90091).

References

Herron, M.M., 1988. Geochemical classification of terrigenous sands and shales from core or log data. *Journal of Sedimentary Research* 58, 820-829.

Khromykh, S.V., Semenova, D.V., Kotler, P.D., Gurova, A.V., Mikheev, E.I., Perfilova, A.A., 2020. Orogenic volcanism in Eastern Kazakhstan: composition, age, and geodynamic position. *Geotectonics* 54, 510-528.

Safonova, I.Yu., Simonov, V.A., Obut, O.T., Kurganskaya, E.V., Romer, R., Seltmann, R., 2012. Late Paleozoic oceanic basalts hosted by the Char suture-shear zone, East Kazakhstan: geological position, geochemistry, petrogenesis and tectonic setting. *Journal of Asian Earth Sciences* 49, 20-39.

Safonova, I., Komiya, T., Romer, R., Simonov, V., Seltmann, R., Rudnev, S., Yamamoto, Sh., Sun, M., 2018. Supra-subduction igneous formations of the Char ophiolite belt, East Kazakhstan. *Gondwana Research* 59, 159-179.

Safonova, I., Perfilova, A., Obut, O., Kotler, P., Aoki, S.,

Komiya, T., Wang, B., Sun, M., 2021. Traces of intra-oceanic arcs recorded in sandstones of eastern Kazakhstan: implications from U-Pb detrital zircon ages, geochemistry, and Nd-Hf isotopes. *International Journal of Earth Sciences*.

Pettijohn, F.J., Potter, P.E., Siever, R., 1987. *Sand and sandstone*. 2nd edn, Springer, New York, 553 p.

Taylor, S.T., McLennan, S.M., 1985. *The continental crust: composition and evolution*. Blackwell, Oxford, 312 p.

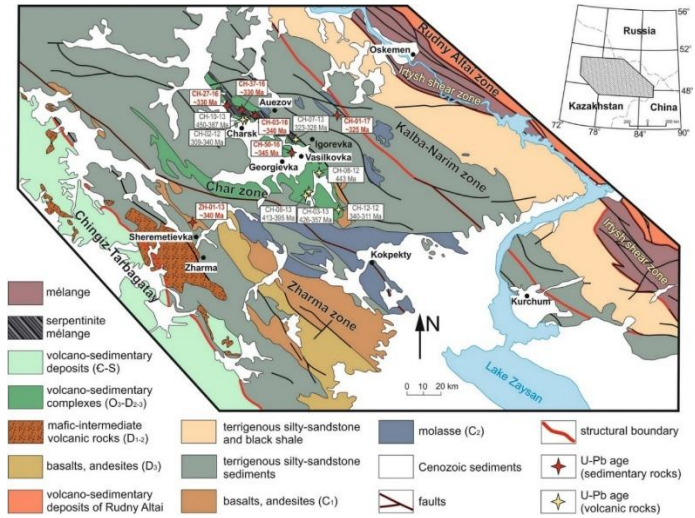


Figure 1. Geological scheme of eastern Kazakhstan (modified from Khromykh et al., 2020).

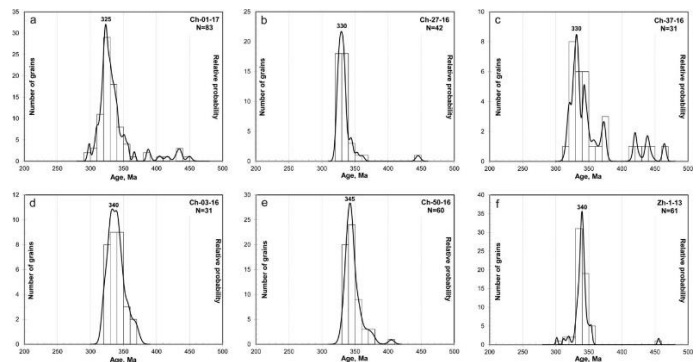


Figure 2. Histograms and probability curves of the U-Pb ages of detrital zircons separated from greywacke sandstones of the Char and Zharma zones of eastern Kazakhstan (concordant ages only) (Safonova et al., 2021).

Jurassic fold-thrust belts of overriding plate on the northeastern North China record Paleo-Pacific Plate subduction

Liang Qiu^{1*}, Dan-Ping Yan^{1**}, Ruoyan Kong¹, Hong-Xu Mu², Weihua Sun¹, Shouheng Sun¹, Xiaoyu Dong¹, Shahnawaz Ariser¹

Jilin University, College of Earth Sciences, Changchun, China

¹ State Key Laboratory of Geological Processes and Mineral Resources, School of Earth Sciences and Resources, China University of Geosciences, Beijing 100083, China

² Beijing Research Institute of Uranium Geology, Beijing 100029, China

*Email: qiul@cugb.edu.cn; yandp@cugb.edu.cn

The Paleo-Pacific subduction along the eastern Asian margin has been well studied including surface geology, geophysical investigations, and numerical modeling, but the timing of its onset and the tectonic processes involved, remain not well constrained. We have now reconstructed the sedimentation and structural evolution of the Shihuiyao–Gangzidian–Yuantai region of the Liaodong Peninsula on the overriding plate at the eastern North China, using field mapping, borehole datasets, structural analyse, and zircon geochronology. Integrating the new data from the three study areas allowed us to identify one angular unconformity and at least two phases of later Mesozoic deformation (D_1 and D_2). The pre- D_1 unconformity is marked by a foreland basin that was filled with Middle Jurassic clastic rocks and unconformably overlie the Pre-Cambrian basement. The D_1 deformation is defined by NE–SW-striking thrust faults that displaced Neoproterozoic or Cambrian strata onto the Middle Jurassic strata. The D_2 deformation is represented by kilometer-scale variable high-angle normal faults. Although samples from the Middle Jurassic clastic rocks did not yield ideal maximum deposition ages (MDAs; ca. 246 Ma), unreformed porphyry dikes and diabase sills that intruded the Yuantai thrust system yielded zircon U–Pb ages of ca. 124 and

117 Ma, respectively. In addition, detrital-zircon geochronology yielded a MDA of ca. 129 Ma for Cretaceous deposits in graben with hanging walls formed by D_2 normal faults. Therefore, the D_1 and D_2 deformations can be constrained to the Late Jurassic and Early Cretaceous, respectively (D_1 between ca. 174 and 124 Ma, and D_2 after ca. 129 Ma). The provenance of the detritus in the Middle Jurassic clastic rocks implies that the deposits in the foreland basin had a source in a thrust sheet of the Paleoproterozoic rocks, but the source of deposits in the mini-graben (D_2) was probably the nearby Neoproterozoic basement. Therefore, we construct the retroarc foreland basin and fold–thrust belt of the southern Liaodong Peninsula in terms of a subduction margin and constrain a Toarcian–Aptian (ca. 174 to 124 Ma) age for the onset of Paleo-Pacific Plate subduction. Combined with recent discovery of fold-thrust belts in Wulong area and Lushan–Dalian area that are comparable with this study, we interpret the foreland system and the subsequent synconvergent extension as the result of episodic subduction of the Paleo-Pacific Plate.

Key words: Paleo-Pacific subduction; structural analysis; geochronology; North China Craton; Liaodong Peninsula

S-type granites in the southern East Kunlun Belt, northern Tibetan Plateau: Petrogenesis and tectonic implications

Xiang Ren¹, Yunpeng Dong^{1,2*}, Dengfeng He¹, Shengsi Sun¹

¹ State Key Laboratory of Continental Dynamics, Department of Geology, Northwest University, Northern Taibai Str. 229, Xi'an 710069, China

² Department of Earth Science, Western University, Richmond Str. 1151, London, Ontario N6A 3K7, Canada

* Email: dongyp@nwu.edu.cn (Y. Dong)

S-type granite is a striking end-member of crustal reworking and greatly crucial to understand the tectonic evolution process of an accretionary orogen. Here, we present geochronological, geochemical, and isotopic data for the two-mica granites from the Muztagh area, southern East Kunlun Belt (S-EKB). Integrated zircon and monazite dating suggested two-mica granites to be crystallized in the Late Permian (260–257 Ma). In addition, most zircons of two-mica granites contain inherited cores with concentrated ages of 458–365 Ma, and these inherited zircons have a slightly high Th/U value generally > 0.1 (up to 0.72). They are characterized by the presence of aluminous mineral of muscovite and a slightly high aluminum saturation index (ASI = 1.04–1.13) showing S-type granite affinities. These two-mica granites display enrichment in light rare earth element (LREE; (La/Yb)_N = 7.48–68.8), weak negative to positive Eu anomalies (0.73–1.64), and a remarkably scattered heavy REE pattern. On the mantle-normalized diagram, they are generally similar to characteristics

of the upper crust such as enrichment in large-ion lithophile elements (LILEs; Pb, Ba, and Sr) and depletion in high field strength elements (HFSEs; Nb, Ta, Ti, and P). Slightly high CaO/Na₂O ratios (0.51–0.95), Sr (158–299 ppm) and Ba (345–1667 ppm) contents, and low Rb (96–176 ppm) content, together with experimental data of melts produced through dehydration and H₂O-fluxed melting of metagreywacke and metapelite over various temperature-pressure conditions suggest that two-mica granites were derived by H₂O-fluxed melting of biotite of metagreywackes. A wide ε_{Hf}(t) range varying from -11.49 to +0.95 indicates an isotopically heterogeneous source for the production of two-mica granites and the protolith of two-mica granites are probably turbidites. Therefore, along with the regional geology, observation of the Late Permian S-type granites in the S-EKB suggests crustal anatexis had occurred in the S-EKB which is more likely to be a forearc accretionary wedge related to the northward subduction of the Paleo-Tethys oceanic plate.

The Tekturmas ophiolite belt of central Kazakhstan: geology and ore potential

I.Yu. Safonova¹⁻³, R.M. Antonyuk^{4,5}, S.N. Lis⁵, A.A. Kasimov⁵, A.A. Perfilova^{1,2}, I.A. Savinskiy¹, Kotler P.^{1,2}

¹ Novosibirsk State University, Pirogova St. 1, Novosibirsk, 630090, Russia; e-mail: inna03-64@mail.ru

² Sobolev Institute of Geology and Mineralogy, SB RAS, Koptyuga ave. 3, Novosibirsk 630090, Russia

³ Zavaritskiy Institute of Geology and Geochemistry, UB RAS, Vonsovskogo ave. 15, Yekaterinburg, 620016, Russia

⁴ Centrkaznedra, Bukahrzhyrau ave. 47, Karaganda, Republic of Kazakhstan

⁵ IPCON Joint Venture, Ippodromnaya 5, 100019, Karaganda, Republic of Kazakhstan

Central Kazakhstan is a large metallogenic province with numerous deposits of copper and other non-ferrous metals, but also a promising for copper-nickel deposits associated with mafic and ultramafic igneous complexes. By now, we know about only two Cu-Ni deposits (Kamkor and Maksut) and a relatively small number of ore occurrences. Those deposits may form in various tectonic environments. However, not all mafic and ultramafic massifs carry sulfide ores accessible/visible on the surface. An inspiring example is the discovery of numerous ore-bearing intrusions in NW China (Kalatongke deposit), a part of which carry no visible mineralization on the surface or fully buried. Geologists suggest that those deposits can be formed in active intracontinental shearing or rifting settings.

The middle-late Paleozoic igneous complexes of Central Kazakhstan formed in Pacific-type active continental or oceanic margin settings and are perspective for the searching copper-bearing deposits in Central Kazakhstan. Those complexes include ophiolites, volcanic and plutonic rocks of suprasubduction and post-collision origin. They may host potential ore-bearing mafic-ultramafic intrusions formed in geodynamic settings of (1) mid-ocean ridges, (2) suprasubduction zones, (3) transtensional to extensional arc rifting, (4) intraplate magmatism. The Tekturmas Ophiolite Belt located in Central Kazakhstan is a highly promising area hosting rocks formed in various geodynamic settings. It is 3-13 km wide and extended from west to east for a distance of more than 200 km. The belt consists of several tectonic plates composed of Early Paleozoic igneous and sedimentary (oceanic and terrigenous) rocks, peridotite, gabbro, and basalt and their metamorphosed

analogues. The Tekturmas belt is a serpentinite melange formed by accretion and collision of tectonic blocks of oceanic and suprasubduction origins and related exhumation of serpentinite and high-pressure metamorphic rocks (Maruyama et al., 2011; Safonova et al., 2020; Khassen et al., 2020). The processes occurring at Pacific-type convergent margins and later during collision and even at a post-collisional extensional stage provide favorable conditions both for the appearance of ore-bearing intrusions in accretionary and suprasubduction complexes composed of igneous and sedimentary rocks and for the exhumation of blocks with ore-bearing intrusions. Another promising region is the Uspenka zone of undifferentiated Paleozoic volcanic rocks located east of the Tekturmas belt. At present, there are no clear ideas about the genesis of the volcanics, but the well-known Cu-Ni Kamkor deposit is also located in the eastern Uspenka zone, suggesting that more ore localities may occur there.

The Tekturmas belt of central Kazakhstan consists of three structural-formational zones: Tekturmas (center), Bazarbai (north) and Sarysui (south). The Tekturmas zone includes serpentinite mélangé and Karamurun (O₁₋₂), Tekturmas (O₂₋₃), and Sarytau (S₁) formations, which are dominated by basaltic lavas (often pillowed), deep-sea sediments and terrigenous clastic deposits, respectively. The Bazarbai zone consists of the Kuzek (O₂) and Bazarbai (O₂₋₃) formations, which are dominated by volcanic and sedimentary rocks, respectively. The rocks of all three zones match the succession of Ocean Plate Stratigraphy: basalt – pelagic chert – hemipelagic sediments – trench sediments. The total interval of the formation of

ophiolites and OPS rocks is from the late Cambrian to late Ordovician.

The igneous rocks are basalt/dolerite, andesibasalt, and andesite, both alkaline and subalkaline. The subalkaline rocks are mostly tholeiitic with a number of calc-alkaline varieties in the Bazarbai Fm. Based on major oxides three groups of rocks can be distinguished: high-Ti, mid-Ti and low-Ti. The high-Ti Karamurun volcanics and low-Ti Bazarbai are variably enriched in LREE ($La_N = 70$ and 12 in average, respectively) showing LREE enriched (high-Ti) and LREE flat (low-Ti) REE patterns. The high-Ti group shows enrichment in Nb, Th, Zr and Sm compared to the low-Ti group. The low-Ti group is special for the Nb troughs in primitive mantle normalized multi-element diagrams, which are typical of supra-subduction settings. Both groups yielded positive ϵNd values, although the averages are 4.6 and 7.5 for the high- and low-Ti rocks, respectively. The association of the Karamurun basalts, both high-Ti and mid-Ti, with deep-sea sediments (pelagic chert and hemipelagic siliceous mudstones and siltstone) and their geochemical features suggest formation in oceanic environments: mid-oceanic ridge and oceanic island/seamount. The Bazarbai volcanic rocks are dominated by low-Ti varieties suggesting their derivation in a supra-subduction setting, probably, at an intra-oceanic arc.

We consider the Tekturmas ophiolite belt and adjacent accretionary complex with *mélange* as a Pacific-type orogenic belt, which formed during the subduction of an Ordovician oceanic plate of the Paleo-Asian Ocean. Lithologically, geochronologically and tectonically the Tekturmas belt is similar to the Itmurundy belt in northern Balkhash area (Safonova et al., 2020). Both belts include accretionary complex, ophiolite belt, metamorphic belt and *mélange* including sedimentary and igneous rocks of all origins. The formation of both the Tekturmas and Itmurundy *mélanges* can explain the co-occurrence of volcanic rocks of diverse origins within these generally ophiolitic belts. We suggest that the Tekturmas *mélange* formed by the exhumation of previously subducted rocks into a tectonically weak zone, which is a characteristic

part of any Pacific-type orogenic belt. A typical supra-subduction ophiolite belt formed either at an intra-oceanic and continental arc must be several hundred kilometers long and 30-40 km thick, which is not observed either in the Tekturmas, or in the Itmurundy zone. Therefore, we suggest that, first, the volcanic arcs related to the Tekturmas and Itmurundy subductions were tectonically eroded.

The overall geological, structural and geochemical features of the Tekturmas ophiolite belt allowed us to consider it as consisting of ophiolitic belt (ultramafic rocks, gabbro, serpentinite *mélange*) and accretionary complex. The geological structure of the whole Tekturmas belt accord well with the tectonic emplacement/exhumation of ophiolites and HP-rocks and formation of accretionary complex at a Pacific-type convergent margin similar to those in the western Pacific. In terms of copper mineralization the most promising localities are Urtynjal, Uспенka, Bella and Ordybasy.

The study was supported by the Ministry of Science and Education of Kazakhstan (project # AR08855920), Russian Science Foundation (projects No. 20-77-10051, 21-77-20022) and Ministry of Education and Science of RF (project # AAAA-A19-119072990020-6).

References

- Khassen B. P., Safonova I.Yu., Yermolov P.V., Antonyuk R.M., Gurova A.V., Obut O.T., Perfilova A.A., Savinskiy I.A., Tsujimori T., 2020. The Tekturmas ophiolite belt of central Kazakhstan: Geology, magmatism, and tectonics. *Geological Journal* 55, 2363-2382.
- Maruyama, S., Omori, S., Sensu, H., Kawai, K., Windley, B. F., 2011. Pacific-type Orogens: New concepts and variations in space and time from present to past. *Journal of Geography*, 120, 115–223 (in Japanese with English abstract and captions).
- Safonova I. Yu., Savinsky I.A., Perfilova A.A., Gurova A.V., Maruyama S., Tsujimori T., 2020. Itmurundy accretionary complex (Northern Balkhash): geological structure, stratigraphy and tectonic origin. *Gondwana Research* 79, 49-69.

Tectonic erosion at Pacific-type convergent margins of the Paleo-Asian Ocean: new evidence from Central Asia

I.Yu Safonova¹⁻³, A.A. Perfilova^{1,2}, I.A. Savinskiy¹, A.V. Gurova^{1,2}

¹ Novosibirsk State University, Pirogova St. 1, Novosibirsk, 630090, Russia

² Sobolev Institute of Geology and Mineralogy SB RAS, Koptyuga ave. 3, Novosibirsk 630090, Russia

³ IPKON LLC, Ippondromskaya 5, Karaganda, Republic of Kazakhstan

Pacific-type convergent margins (PCM) or their related orogenic belts form over subduction zones, where oceanic lithosphere is submerged under intra-oceanic arcs or active continental margins. PCMs are very important geological entities because on one hand they are major sites of juvenile crust formation on the Earth, but on the other hand they are places of strong crust destruction through tectonic erosion. The mechanism of tectonic erosion includes destruction of oceanic slab, island arcs, accretionary prism and fore-arc by thrusting, oceanic floor relief (horst/graben), and (hydro)fracturing. The tectonic erosion of intra-oceanic arcs and continental margin hanging walls takes place along almost all PCMs (Clift, Vanucchi, 2004; Scholl and von Huene, 2007). The first evidence for the tectonic erosion at Pacific-type convergent margins came from seismic reflection profiles made across the Tonga and Nankai trenches. The subduction of the Pacific plate provides high-rate tectonic erosion of the hanging walls of the western Pacific margins, in particular along the Andes active margins and the Nankai trough. Evidence for this comes from the Costa Rica- Guatemala consuming boundary in South America and from the Cretaceous Shimanto accretionary complex of Shikoku Island in Japan. In the latter, the accretionary units are spatially adjacent to the coeval granitoids of the Ryoke belt, suggesting that older accretionary complexes have been eroded (Safonova et al., 2015). Moreover, zircons from sandstones of Silurian to Quaternary ages indicate disappearance of at least two arc systems: early Devonian and Triassic (Isozaki et al., 2010). In Guatemala, geologists found gaps of fore-arc sedimentation under ongoing subduction witnessing huge rates of sediment destruction and suggesting that periods of accretion alternated with periods of subduction-related sediment erosion (Vannucchi et al., 2016). Another importance consequence and therefore a tool for deciphering histories of fossil P-type orogens is serpentinite mélangé and its hosted fragments of both oceanic crust and arc roots. Tectonic

erosion seems to be the most preferred process to mix all those units together and to form serpentinite-dominated mélangé belts.

The present Western Pacific is a most probable analogue of the Phanerozoic Central Asian Orogenic Belt (CAOB). Therefore, the processes of tectonic erosion could have been also active at the Pacific-type active margins of the Paleo-Asian Ocean, which evolution and suturing were responsible for formation of the CAOB (Safonova, 2017). Evidence for this comes from the Tamdytau and Bukantau foldbelts in the Uzbek Tienshan, Chatkal-Atbashi arc in the middle Kyrgyz Tienshan, Itmurundy accretionary complex in central Kazakhstan, Ulaanbaatar accretionary complex in northern Mongolia and from the Zharma and Char zones in eastern Kazakhstan. The Chatkal-Atbashi complex includes coeval and spatially adjacent Early Devonian arc granitoids, ophiolites and accretionary units. At those fossil convergent margins, the continental crust was probably eroded and submerged to the deep mantle. The Tamdytau, Bukantau, Itmurundy, Ulaanbaatar and Zharma-Char zones host thick greywacke units of andesitic composition but very limited outcrops of arc rocks. In addition, the detrital zircons from those greywackes show unimodal U-Pb age curves and positive epsilon Hf suggesting that intra-oceanic arcs once existed in the Paleo-Asian Ocean, but later were almost fully eroded (Fig.1). In addition, the Itmurundy, Tekturmas and Char accretionary complexes of Kazakhstan are spatially associated with mélangé zones including large blocks and smaller fragments of arc-related granitoids and packages of ocean plate stratigraphy units (MORB and OIB basalt, chert, siliceous mudstone).

The study was supported by the Russian Science Foundation (projects No. 20-77-10051, 21-77-20022) and the Ministry of Science and Education of Kazakhstan (project # AR08855920).

References

Clift, P.D., Vannucchi, P., 2004. Controls on tectonic accretion versus erosion in subduction zones: implications for the origin and recycling of the continental crust. *Rev. Geophysics* 42, RG2001.

Isozaki, Y., Aoki, K., Nakama, T., Yanai, S., 2010. New insight into a subduction-related orogen: a reappraisal of the geotectonic framework and evolution of the Japanese Islands. *Gondwana Research* 18, 82–105.

Safonova, I., 2017. Juvenile versus recycled crust in the Central Asian Orogenic Belt: Implications from ocean plate

stratigraphy, blueschists and intra-oceanic arcs. *Gondwana Research* 47, 6-27.

Scholl, D.W., von Huene, R., 2007. Crustal recycling at modern subduction zones applied to the past - Issues of growth and preservation of continental basement crust, mantle geochemistry, and supercontinent reconstruction. *Geological Society of America Memoirs* 200, 9-32.

Vanucchi, P., Morgan, J.P., Balestrieri, M.L., 2016. Subduction erosion and the de-construction of continental crust: The Central America case and its global implications. *Gondwana Research* 40, 184-198.

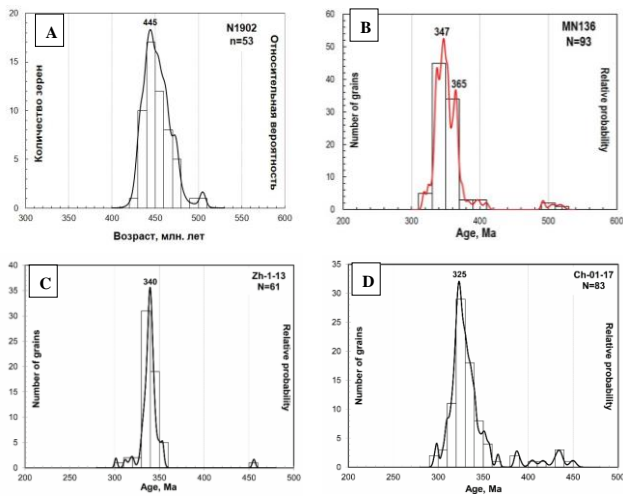


Figure 1 Unimodal U-Pb detrital zircon age patterns from accretionary complexes (FC) of the CAOB: A, Itmurundy AC (Ordovician-E/ Silurian); B, Ulaanbaatar AC, northern Mongolia; C, Zharma zone, eastern Kazakhstan (Visian); D, Char zone, eastern Kazakhstan (Serpuchovian). Note, that the occurrences of supra-subduction formation in these area are very limited in space and ranging in from medium (Zharma and Itmurundy), to small (Char) and negligible (Mongolia). Modified from (Safonova et al., 2021; Savinskiy et al., submitted).

Reconstruction ocean plate stratigraphy and thrust duplexes of Itmurundy accretionary complex, Northern Balkhash, Central Kazakhstan

I. Savinskiy¹, I.Yu. Safonova^{1,2}, S. Maruyama¹, A. Perfilova¹, A. Gurova¹

¹ Novosibirsk State University, Pirogova St. 2, Novosibirsk, 630090, Russia

² Sobolev Institute of Geology and Mineralogy, SB RAS, Koptyuga ave. 3, Novosibirsk 630090, Russia

Accretionary complexes form along the Pacific-type convergent margins, where the oceanic plate subducts under the island arc or continental margin. Most accretionary complexes consist of persistent lithological associations such as basalt-limestone-chert-siliceous mudstones-turbidites. Those rock associations are known as «ocean plate stratigraphy» (OPS; Isozaki et al., 1990). OPS is a major component of Archean to Paleozoic accretionary complexes worldwide (Kusky et al., 2013). OPS lithologies are formed on the oceanic plate and get detached from it during subduction and get incorporated into the accretionary wedge. During subduction, OPS undergo both ductile and brittle deformation, fragmentation and tectonic mixing. The detachment of OPS rocks from the subducting oceanic plate takes place along a sliding surface or décollement. OPS rocks get detached from the subducting plate and accreted to the pre-existing accretionary wedge by sequential cutting and mixing of OPS upper sedimentary rocks and underlying mafic rocks. It is observed in fault zones both the mixing inside the sedimentary packs of OPS and the consistent predominance of mafic OPS rocks among the sedimentary strata while the oceanic plate is submerged. The genesis of accreted mafic rock varieties depends on the position of the décollement (Safonova et al., 2016). When the décollement separates or cuts the seamount, the composition of basalt in the accreted OPS will be OIB-type. If the décollement is located deeper and cuts the lower part of the oceanic plate, then the mafic rocks can be represented by MORB-type.

We studied the Itmurundy zone of the northern Balkhash region of Central Kazakhstan for the reconstruction Ordovician-Early Silurian evolution of the Paleo-Asian Ocean. Reconstruction of the development history of the Paleo-Asian Ocean is the most important and topical issue for the geological history of Asia. Since its evolution the Central Asian Orogenic

Belt (CAOB) has been formed and it traces the Urals, the Tien Shan to the Far East (Sengör et al., 1993). Fragments of the oceanic crust and island systems were accreted to the active margins of the Paleo-Asiatic Ocean throughout the early and Middle Paleozoic. The CAOB includes accretionary complexes with OPS formations of Early-Middle Paleozoic that are identified in Chinese Dzungaria, Central Kazakhstan, Southern Tien Shan and Northern Mongolia (Kusky et al., 2013; Safonova et al., 2016).

The Itmurundy accretionary complex and ophiolite belt is in central Kazakhstan, northern Balkhash area. Structurally, the belt belongs to the Itmurundy-Kazyk folded zone, which, in turn, is a part of the north Balkhash anticlinorium in the central part of the Junggar-Balkhash folded system (Patalakha and Belyi, 1981). The Itmurundy accretionary complex includes rocks of three formations (bottom to top): Itmurundy, Kazyk, Tyuretai. The Itmurundy Fm. (O₁₋₂) consists of basalt, chert, siliceous mudstone, siltstone and shale. The Kazyk Fm. (O₂₋₃) is dominated by chert, siliceous mudstone, siltstone and shale. The Tyuretai Fm. (O₃-S₁) includes mainly sandstones, siliceous mudstones and siltstones plus subordinate basalt and chert.

The serpentinite mélangé of the Itmurundy accretionary complex hosts fragments of dunite-harzburgite, dunite-verlite-pyroxenite complexes, as well as layered and massive gabbro, fragments of OPS and deformed plagiogranites. In addition, it includes phengite eclogites, garnet-phengite-glaucophane shales, amphibole shales and metavolcanic rocks with glaucophane and metasomatic rocks, glaucophane-richterite albitites, serpentinites with veins of alkaline amphibole and jadeite. The eclogite and garnet-phengite-glaucophane metamorphism peaked at P=14–16 kbar and T=550–600 °C (Pilitsyna et al., 2019)

The Itmurundy zone possesses many structural and

lithological features typical of Pacific-type convergent margins accreted Ocean Plate Stratigraphy units (OPS): oceanic basalt, pelagic ribbon chert, hemipelagic siliceous mudstones and siltstone and trench sandstones and turbidites (Maruyama et al., 2010; Safonova et al., 2019). In Itmurundy zone the deformation, the relationship and the ratio of OPS rock changes from west to east, from ultramafic rocks to the most advantageous sedimentary strata of the Itmurundy Fm, the Kazyk Fm. and the Tyuretai Fm. finally.

In the Itmurundy Fm., basic effusive rocks represented by pillow lavas, in some places strongly sheared with multi-oriented slickenlines. In general, the deformations of the outcrops reflects the internal structure of the Itmurundy Fm. Siliceous rocks, clay rocks and turbidites are found as lenses and boudins. They have got sporadic outcrop throughout the Itmurundy Fm. Often, cherts retain their primary layering with the preservation of ribbons with the width from 5 to 10 cm. But they are highly deformed and recrystallized with the appearance of mullion structures, overturned folds and horse-structures with thrown kinematics. The intensity and nature of deformations of rocks show the numerous tectonic stages over a period of the accumulation of the Itmurundy Fm. that is also evidenced by the wide spread of breccia, gravels and gravel-breccia. The basalts of the Itmurundy Fm. are in close to the enriched type of OIB and E-MORB and to formation within oceanic islands or seamounts (Safonova et al., 2020).

The Kazyk Fm. is mainly composed of layered chert, siltstone, multi-grained polymictic sandstone and gravel. Breccia consists of angled fragments of chert, siliceous argillite, siltstone, sandstone, basic porphyrite with often acidic effusive that cements and siltstone-sandstone material. In some areas basic effusive horizons appear among the sedimentary rocks. Jet of basalts flow into the thickness of chert when they were weakly consoled. Among the basalts there are lenses and boudins of cherts. Chert are exposed along the ridges of hills mainly. Chert builds up overturned steeply falling folds with a western fall of hinges, flexures and box-shaped folds. Hemipelagic rocks represented by thick packs of multicolored siliceous argillites and siltstones (red and green) with layers of thick sandstones, cherts and lenses of basalts. In the Kazyk Fm. deformations can be represented on the late stages of accretion. The Tyuretai Fm is represented in the southeast of the Itmurundy accretion complex and is a so-called overturned duplex named after a similar structure of the Inuyama section of the Mino accretion complex on the island of Honshu in Japan - the standard of the world type of OPS (Isozaki et al., 1991). The composition of the Tyuretai formation includes mainly deposits of clastic rocks they build up large anticlinal structures in the east of the Itmurundy zone. Approximately the half of suite thickness is represented by gravel, breccia and sandstone. Fragments of breccia are represented by chert, basalt, siliceous siltstone. Structurally this suite is a large isoclinal fold with axial plane, and is paralleled to the main region faults. The core

of the fold consists of basic effusive while the flanks are siliceous mudstone, siltstone, gray sandstones with large lenses of basalts. The fold is locally disturbed by faults. All mentioned above is the evidence of duplexes when the folds were captured rocks from the central part by. Basalts of the Tyuretai Fm. are comparable to the vulcanite of the oceanic spreading centers N-MORB (Safonova et al., 2020).

The duplex deformation features of the Itmurundy accretionary complex are mostly spread strongly indicate the SE-NW direction of subduction and characterize the stage of deformation with the decollement position while oceanic plate is subducted (Safonova et al., 2019). So, the stage of deformation can be founded by U-Pb dating sandstone in the final sequence OPS (basalt-limestone-chert-siliceous mudstones-turbidites). The thrusts and thrusting related with deformations are identified in each of suite and can be easily founded by strongly sheared basalt, chert and siliceous mudstone as well as by the presence of large chert boudins within basalts and, vice versa, by the fragments of basalt submerged into cherty matrix. The later stage of deformations characterizes the northeastward compression, which resulted in the anticline folding of the eastern duplex (Tyuretai Fm.) and in the activation of the duplex thrusts. The ultramafic serpentized rocks possibly extruded at that compressional stage.

Conclusively, the Itmurundy zone structurally and lithologically represents a Pacific-type orogenic belt. The Itmurundy accretionary complex records successive detachment, fragmentation and "mixing" of OPS sediments and mafic and ultramafic rocks of the oceanic plate and the successive detachment of OPS rocks off the décollement and their emplacement into accretionary wedge.

The study was supported by Russian Science Foundation (№21-77-20022 and № 20-77-10051), Russian Foundation for Basic Research (№ 20-35-90091), Ministry of Education and Science of the Russian Federation (№ AAAA-A19-119072990020-6).

References

- Isozaki, Y., Maruyama, Sh., Fukuoka, F., 1990. Accreted oceanic materials in Japan Tectonophysics, 181, 179–205.
- Kusky, T., Windley, B., Safonova, I., Wakita, K., Wakabayashi, J., Pola, A., Santosh, M., 2013. Recognition of Ocean Plate Stratigraphy in accretionary orogens through Earth history: A record of 3.8 billion years of sea floor spreading, subduction, and accretion. Gondwana Research, 24, 501-547.
- Maruyama, S., Kawai, T., Windley, B.F., 2010. Ocean plate stratigraphy and its imbrication in an accretionary orogen: the Mona Complex, Anglesey-Lleyn, Wales, UK. In: Kusky, T.M., Zhai, M-G., Xiao, W. (Eds.) The Evolving Continents: Understanding Processes of Continental Growth.
- Patalakha, F.A., Belyi, V.A., 1981. Ophiolites of the Itmurundy-Kazyk zone. In: Abdulin, A.A., Patalakha, F.A. (Eds.), Ophiolites of Kazakhstan. Nauka, Alma-Ata, 7-102. [in Russian]

- Pilitsyna A.V., Degtyarev K.E., Tretyakov A.A., 2019. First find of phengite eclogites and garnet-glaucophane schists associated with jadeitites in the Kenterlau-Itmurundy serpentinite mélangé (North Balkhash ophiolite zone; Central Kazakhstan) Abstract Volume of the 13th International Eclogite Conference / Eds. C. Mattinson, D. Castelli, S.W. Faryad, J. Gilotti, G. Godard, A. Perchuk, D. Rubatto, H.-P. Schertl, T. Tsujimori, Y.-F. Zheng. Petrozavodsk: KRC RAS, P. 65.
- Safonova I, Maruyama S, Kojima S, Komiya T, Krivonogov S, Koshida K, 2016. Recognizing OIB and MORB in accretionary complexes: a new approach based on ocean plate stratigraphy, petrology, and geochemistry. *Gondwana Research*, 33, 92–114
- Safonova I., Savinskiy I., Perfilova A., Gurova A., Maruyama S., Tsujimori T., 2020. The Itmurundy Pacific-type orogenic belt in northern Balkhash, Central Kazakhstan: Revisited plus first U-Pb age, geochemical and Nd isotope data from igneous rocks. *Gondwana Research*, 79, 49–69.
- Safonova, I. Yu., Perfilova, A.A., Obut, O.T., Savinsky, I.A., Cherny, R. I., Petrenko, N.A., Gurova, A.V., Kotler, P.D., Khromykh, S.V., Krivonogov, S.K., Maruyama, S., 2019. Itmurundy accretionary complex (Northern Balkhash): geological structure, stratigraphy and tectonic origin. *Pacific Geology*, 38, 102–117.
- Sengör, A.M.C., Natal'in, B.A., Burtman, V.S., 1993. Evolution of the Altaid tectonic collage and Paleozoic crustal growth in Asia. *Nature*, 364, 299–307.

Discovery of Middle Jurassic lamprophyre in southeastern Guangxi Province and its tectonic implications

Yu Shi^{1,2,3*}, Yuan-Lan Tang^{1,2}, Xiu-Mian Hu³, Xi-Jun Liu^{1,2}, Yong-Qiang Wang^{1,2}, Yi-Rong Sun^{1,2}

¹ Guangxi Key Laboratory of Hidden Metal Mineral Exploration, Guilin University of Technology, Guilin 541004, China

² Collaborative Innovation Center for Exploration of Nonferrous Metal Deposits and Efficient Utilization of Resources, Guilin University of Technology, Guilin 541004, China

³ State Key Laboratory for Mineral Deposits Research, School of Earth Sciences and Engineering, Nanjing University, Nanjing 210093, China

*Email: shiyu_61@163.com (Y. Shi)

Previous studies on the tectonic property of the Mesozoic in the South China Block (SCB) have constrained mainly by granites and alkaline rocks, however, mafic rocks contain important geodynamic information for the tectonic properties, and thus, may help to understand the tectonic stress field of the SCB. Mafic rocks (e.g. lamprophyre dikes) hold the key to understanding the extensional characteristics of lithosphere, tectonic properties and mantle source information, which is of great significance to constrain the tectonic evolution (Shu, 2012; Wang et al., 2013; Zhou and Li, 2000). This study presents geochemical data and biotite ⁴⁰Ar/³⁹Ar age from the newly discovered lamprophyre in Southeastern Guangxi Province in order to constrain the tectonic regime in the Mesozoic in the SCB.

Lamprophyre samples of GX1501-1 and GX1501-2 were collected from Shoutang, west of Muge in Gangnan, Guigang in Southeastern Guangxi Province (49°22'56"N, 109°38'40"E) (Figs. 1a-1c). The lamprophyre presents negative terrain, showing as pipe (Fig. 1d). Major and trace element analyses were conducted at the State Key Laboratory of Isotope Geochemistry, Guangzhou institute of geochemistry, Chinese Academy of Sciences. The detailed analytical methods are documented by Shi et al. (2018). Biotite ⁴⁰Ar/³⁹Ar dating was performed by Argus- VI mass spectrometer at China University of Geosciences (Wuhan). The analytical details are performed by Bai et al. (2018).

Samples of GX1501-1 and GX1501-2 display lamprophyre structure, consisting of phenocryst and matrix. The phenocryst is mainly composed of olivine (15%-20%), biotite (15%-20%)

and K-feldspar (2%-7%) (Figs. 1h-1i), with olivine showing zoning structure and crack. The fine-grained matrix is composed of biotite, olivine, K-feldspar, magnetite and zoisite. The samples are ultra-mafic rocks with low SiO₂ contents of 40.68~41.04 wt.%, total alkali (ALK = Na₂O + K₂O) of 3.34~4.20 wt.%, high K₂O of 1.93~2.15 wt.% and high TiO₂ contents of 2.55~2.70 wt.%, very high MgO contents of 8.65~10.53 wt.% and Fe₂O₃^T contents of 14.56~15.57 wt.%, belonging to alkaline lamprophyre. The REE and trace elements of the lamprophyre samples are similar to OIB (Oceanic Island Basalt) (Figs. 1e-1f). It has high REE contents (\sum REE=227-301 ppm) and relatively high fractionation ((La/Yb)_n = 19.5-22.3) with little Eu anomaly (δ Eu = 0.97), showing no obvious fractional crystallization of plagioclase during the diagenesis. The primitive mantle normalized trace element patterns of the rocks do not show significant enrichment of large ion lithophile (LIL) elements.

New geochronological age data have been obtained by the ⁴⁰Ar/³⁹Ar method. Biotite was separated from the lamprophyre GX1501-1 and the results are given in Figs. 1g and 1j. Laser stepwise heating yielded an age plateau with around 55% of the cumulative ³⁹Ar released at 158.1 ± 1.5 Ma (MSWD = 0.3). The isotope correlation diagram yields an intercept age at 158.0 ± 1.5 Ma (MSWD = 0.3) and an initial ⁴⁰Ar/³⁶Ar ratio of 296.8 ± 9.2, which are consistent with the plateau age as well as the atmospheric value for the ⁴⁰Ar/³⁶Ar ratio.

This study demonstrates that the lamprophyres are alkaline olivine minettes with the geochemical characteristics similar to ocean island basalt (OIB). The lamprophyres formed in the

Middle Jurassic according to the biotite $^{40}\text{Ar}/^{39}\text{Ar}$ plateau age of 158.08 ± 1.53 Ma. The geochemical and $^{40}\text{Ar}/^{39}\text{Ar}$ dating characteristics of the lamprophyres indicate that it is still in an extensional tectonic setting in the Middle Jurassic in the Late Mesozoic in the SCB. The Middle Jurassic age of lamprophyre and extensional tectonic setting could also provide information for further studying the transition time from the Tethyan to the Pacific regime of the SCB.

Acknowledgements

This research was jointly supported by National Science Foundations of China (Grant Nos. 41862003, 41562005, 92055208); Guangxi Natural Science Foundations of China for Distinguished Yong Scholars (Grant Nos. 2019GXNSFFA245005 and 2018GXNSFFA281009).

References

Shu, L.L., 2012. An analysis of principal features of tectonic evolution in South China Block. *Geological Bulletin of China* 31, 1035-1053 (in Chinese with English abstract).

Wang, Y.J., Fan, W.M., Zhang, G.W., et al., 2013. Phanerozoic tectonics of the South China Block: Key observations and controversies. *Gondwana Research* 23, 1273-1305.

Zhou, X.M., Li, W.X., 2000. Origin of Late Mesozoic igneous rocks in southeastern China: Implications for lithosphere subduction and underplating of mafic magmas. *Tectonophysics* 326, 269-287.

Shi, Y., Huang, Q.W., Liu, X.J., et al., 2018. Provenance and tectonic setting of the supra-crustal succession of the Qinling Complex: Implications for the tectonic affinity of the North Qinling Belt, Central China. *Journal of Asian Earth Sciences* 158, 112-139.

Bai, X.J., Qiu, H.N., Liu, W.G., et al., 2018. Automatic $^{40}\text{Ar}/^{39}\text{Ar}$ dating techniques using multicollector argus vi noble gas mass

spectrometer with self-made peripheral apparatus. *Journal of Earth Science* 29, 408-415.

Sun, S.S., McDonough, W.F., 1989. Chemical and isotopic systematics of oceanic basalts: Implications for mantle composition and processed. *Magmatism in Ocean Basins*. In: Saunders, A.K., Norry, M.J. (Eds.), Geological Society of London Special Publication 42, 313-345.

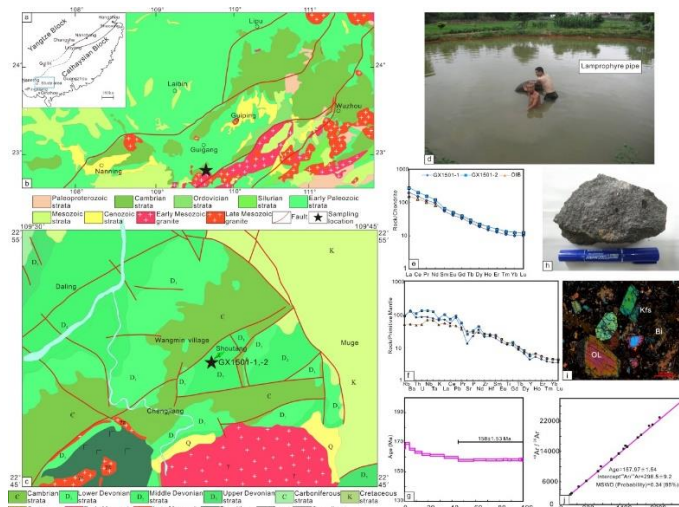


Fig. 1. Simplified geological map showing the distributions of units, igneous rocks and sampling location (a, b, c); Lamprophyre presenting as pipe in the field (d); REE patterns and spider diagram of trace element abundances of lamprophyres in Southeastern Guangxi (normalization values after Sun and McDonough, 1989) (e, f); Ar-Ar age spectra (g) and normal isochron diagram (j). Petrographic characteristics of lamprophyres in Southeastern Guangxi. Bi-biotite; Kfs-K-feldspar; OL-olivine (h, i).

Thermal state and evolving geodynamic regimes of the Meso- to Neoproterozoic North China Craton

Guozheng Sun^{1,2*}, Shuwen Liu², Peter A. Cawood³, Ming Tang², Jeroen van Hunen⁴,
Lei Gao², Yalu Hu², Fangyang Hu^{5,6,7}, Sanzhong Li¹

¹ Key Lab of Submarine Geosciences and Prospecting Techniques, MOE Ocean University of China, Qingdao 266100, China

² Key Laboratory of Orogenic Belts and Crustal Evolution, Ministry of Education, School of Earth and Space Sciences, Peking University, Beijing 100871, PR China

³ School of Earth, Atmosphere and Environment, Monash University, Melbourne, VIC 3800, Australia

⁴ Department of Earth Sciences, Durham University, Durham DH1 3LE, UK

⁵ Key Laboratory of Mineral Resources, Institute of Geology and Geophysics, Chinese Academy of Sciences, Beijing 100029, China

⁶ Innovation Academy for Earth Science, Chinese Academy of Sciences, Beijing 100029, China

⁷ Department of Geosciences, University of Arizona, Tucson, AZ 85721, USA

*E-mail: gzsun1994@pku.edu.cn

Constraining thickness and geothermal gradient of Archean continental crust are crucial to understanding geodynamic regimes of the early Earth. Archean crust-sourced tonalitic–trondhjemitic–granodioritic (TTG) gneisses are ideal lithologies for reconstructing the thermal state of early continental crust. Integrating experimental results with petrochemical data from the Eastern Block of the North China Craton allows us to establish temporal–spatial variations in thickness, geothermal gradient and basal heat flow across the

block, which we relate to cooling mantle potential temperature and resultant changing geodynamic regimes from vertical tectonics in the late Mesoproterozoic (~2.9 Ga) to plate tectonics with hot subduction in the early to late Neoproterozoic (~2.7–2.5 Ga). Here, we show the transition to a plate tectonic regime plays an important role in the rapid cooling of the mantle, and thickening and strengthening of the lithosphere, which in turn prompted stabilization of the cratonic lithosphere at the end of the Archean.

Large-scale asymmetry in thickness of crustal accretion at the Southeast Indian Ridge due to deep mantle anomalies

Yanhui Suo^{1,2*}, Sanzhong Li^{1,2*}, Xianzhi Cao^{1,3}

¹ Frontiers Science Center for Deep Ocean Multispheres and Earth System, Key Lab of Submarine Geosciences and Prospecting Techniques, MOE and College of Marine Geosciences, Ocean University of China, Qingdao 266100, China

² Laboratory for Marine Mineral Resources, Qingdao National Laboratory for Marine Science and Technology, Qingdao 266237, China

³ EarthByte Group, School of Geosciences, The University of Sydney, Sydney, New South Wales 2006, Australia

*Email: suoyh@ouc.edu.cn; sanzong@ouc.edu.cn

Abstract: Hot mantle plumes and ancient cold slabs have been observed beneath modern mid-ocean ridges, but their specific and detailed effects on mid-ocean ridge crustal accretion are poorly known. The oceanic lithosphere beneath the Southeast Indian Ocean (SEIO) displays unique morphological, geophysical and geochemical characteristics, which may reflect the influence of both mantle anomalies and upwelling plumes on seafloor spreading. In this study, we combined gravity-derived oceanic crustal thickness with plate tectonic reconstructions to investigate patterns of asymmetry in thickness of crust accreted at the Southeast Indian Ridge (SEIR) over the last 50 Myr. Our results reveal several distinct features: (1) Small-scale, short-lived asymmetries in the thickness of crustal accretion of up to 0.75 km are alternatively distributed on the southern and northern flanks of the 90°-120°E SEIR segment. These can be explained by variations in mantle depletion or mantle temperature. (2) Two large-scale, long-lived (duration of ~50 Myr) asymmetries in crustal accretion of >2.5

km are observed around the Kerguelen Plateau and Balleny Islands, which we attribute to excess crust from the off-axis Kerguelen and Balleny mantle plumes. (3) Two large-scale, long-lived (duration of ~50 Myr) asymmetries in crustal accretion of 0.75-2.5 km are observed on the northern flank of the westernmost (70°-80°E) SEIR and the southern flank of the eastern (120°-140°E) SEIR segment, respectively. We attribute these to asymmetry in mantle temperature of up to 20-53°C. We suggest these asymmetric temperatures across the SEIR are associated with the foundered lithospheric fragments of the Indian Craton triggered by the African Large Low-Shear-Velocity Province (LLSVP) during the breakup of Gondwanaland and an intraplate subducted slab of the Paleo-Tethys Ocean, respectively. The remnant craton fragments and subducted oceanic slab may have moved north in concert with the northward migrating SEIR since 50 Ma ago.

Keywords: Southeast Indian Ocean, asymmetric crustal accretion, mantle plumes, ancient subducted slabs

Three-dimensional velocity structure near the 2021 M7.3 earthquake sequence in Tohoku, Japan

Yuyang Tan^{1,2}, Huilin Xing^{1,2,3*}, Shuo Pang^{1,2}, Zongwei Jin¹, Jianchao Wang¹

¹ Key Laboratory of Submarine Geoscience and Prospecting Techniques MOE, Ocean University of China, Qingdao 266100, China

² Frontiers Science Center for Deep Ocean Multispheres and Earth System, Institute for Advanced Ocean Study, Ocean University of China, Qingdao 266100, China

³ Laboratory for Marine Mineral Resources, Qingdao National Laboratory for Marine Science and Technology, Qingdao 266237, Shandong, China

*Email: h.xing@ouc.edu.cn

A M7.3 earthquake struck the Pacific Coast of Tohoku, Japan on 13 February, 2021. To investigate the triggering mechanism behind this earthquake, we have utilized the seismic arrival time data compiled by Hinet and a newly developed seismic tomography method to image the velocity structure in the focal area of the earthquake sequence. The new method is derived from the double-difference (DD) seismic tomography. Compared to conventional DD tomography, the new method introduces a new Vp/Vs model consistency constraint, which can better determine the Vp/Vs model. The reliability of the tomographical results are verified by checkerboard resolution test. The Vs and Vp/Vs images, which are more sensitive to fluid distribution, show that the oceanic crust is characterized by low velocity anomaly due to hydration reaction while the oceanic mantle is associated with high velocity anomaly. The mainshock of the M7.3 earthquake sequence is located at the boundary between the high and low velocity anomalies. This

observation is consistent with the inland earthquakes, indicating that this earthquake is related to the variation of the physical properties of rocks. The aftershocks are mainly distributed in the low Vs, high Vp/Vs areas. This may be due to the brittleness of oceanic crust is higher than the mantle, and the rupture is more easily propagated in the fragile oceanic crust. The distribution of relocated earthquake hypocenters is mostly within the subducting Pacific plate and the inferred fault plane is about 60° obliquely to the slab interface. This observation implies that this fault is likely generated by the bending of slab before subduction. The association of the earthquake sequence with low velocity anomaly suggests that this earthquake is probably triggered by dehydration which increases the pore-pressure on the fault plane.

Keywords: seismic tomography, subduction, velocity anomaly, dehydration

Petrogenesis of Early Paleozoic I-type granitoids in the Wuyi–Yunkai orogen, South China

Yuan-Lan Tang^{1,2}, Yu Shi^{1,2,3*}, Xiu-Mian Hu³, Xi-Jun Liu^{1,2}, Yong-Qiang Wang^{1,2}, Yi-Rong Sun^{1,2}

¹ Guangxi Key Laboratory of Hidden Metal Mineral Exploration, Guilin University of Technology, Guilin 541004, China

² Collaborative Innovation Center for Exploration of Nonferrous Metal Deposits and Efficient Utilization of Resources, Guilin University of Technology, Guilin 541004, China

³ State Key Laboratory for Mineral Deposits Research, School of Earth Sciences and Engineering, Nanjing University, Nanjing 210093, China

Email address: shiyu_61@163.com (Y. Shi)

The Early Paleozoic Wuyi–Yunkai orogen in the South China Block (SCB), characterized by high-grade metamorphism, intensive deformation and extensive magmatism, is different from many other orogenic belts (Raimondo et al., 2010). It has attracted much attention over the last few decades, and provides an opportunity to constrain the magmatic–tectonic evolution of the SCB (Shu et al., 2015). Despite numerous studies are available, the Early Paleozoic magmatism and its geodynamic settings of the SCB remain controversial. On the one hand, the tectonic setting of the Early Paleozoic granites in SCB was related to intracontinental orogenic process (Shu et al., 2015) or oceanic subduction (Peng et al., 2016; Qin et al., 2017) remains enigmatic. On the other hand, the role of mantle in the formation of granites in the region also remains unclear.

The Wuyi–Yunkai orogen in the southwestern part of the junction zone of the Yangtze and Cathaysia (Fig. 1a) is characterized by the large-scale development of granite (Fig. 1b), which makes it a key area for studying the Early Paleozoic magmatism, tectonic evolution, and geodynamic driving forces of the SCB. However, previous study mostly focused on S-type granitoids (Zhang et al., 2012; Song et al., 2015), and relatively little attention has been paid to the Early Paleozoic I-type granitoids of the SCB. It is known that the study of I-type granite can provide more useful information on crust–mantle interactions of the orogen, therefore, I-type granites are powerful means of elucidating mantle source regions and the deep dynamic setting. In this paper, we present analyses of trace elements, U–Pb age, and Hf isotopes in zircons from the Early

Paleozoic granites of the Daning–Guiling area in the southwestern part of the Wuyi–Yunkai orogen. We use these data to constrain the petrogenesis of the granites and to offer new perspectives on the thermal–chemical conditions and tectonic setting of the Early Paleozoic magmatic activity in the SCB.

The I-type granitoids from Daning–Guiling contain zircon with U–Pb age of 422–418 Ma, taken as the age of emplacement. They have a wide range of $\varepsilon_{\text{HF}}(t)$ values (ranging from -9.62 to -0.14), and relatively old $T_{\text{DM}2}$ ages of 1.4–1.99 Ga. Our samples are rich in LREEs and moderately depleted in Eu ($\delta\text{Eu} = 0.49$ – 0.64), with negative Ba, Sr, Nb, and Ti anomalies, and positive in Rb, Th, U, and Pb anomalies. Those rocks are characterized by relatively high $\text{Mg}^\#$ values (44.2–67.1) and Rb/Sr ratios (0.96–4.76), and on a plot of molar Al_2O_3 ($\text{MgO} + \text{FeO}^\text{T}$) versus molar $\text{CaO}/\text{MgO} + \text{FeO}^\text{T}$, they plot along a mixing field between the metaigneous and metasedimentary rocks. Together with abundant enclaves observed in field work, those geochemical characteristics of the granites indicate that they formed via complicated petrogenetic processes, including the partial melting of a mixed source of metasedimentary rocks and metabasalts in the lower crust, magma mingling and mixing between two diverse magmas, and fractional crystallization.

Taking into account all the other geological evidence from the Wuyi–Yunkai region, we can further draw the following conclusions: (1) Mantle-derived magma played an important role in the formation of these Early Paleozoic granites by providing both heat and material, among which the material was

mainly ancient mantle-derived material, and its contribution was limited and uneven; (2) the tectono-magmatic events of the Early Paleozoic took place during intraplate orogenesis rather than oceanic subduction and collision, and that these events were triggered by a far-field tectonic response to the assembly of northern East Gondwana.

Acknowledgements

This research was jointly supported by National Science Foundations of China (Grant Nos. 41862003, 41562005, 92055208); Guangxi Natural Science Foundations of China for Distinguished Yong Scholars (Grant Nos. 2019GXNSFFA245005 and 2018GXNSFFA281009).

References

Peng, S.B., Liu, S.F., Lin, M.S., Wu, C.F., Han, Q.S., 2016. Early Paleozoic subduction in Cathaysia (I): new evidence from Nuodong ophiolite. *Earth Science* 41(05), 765–778 (in Chinese with English abstract).

Qin, X.F., Wang, Z.Q., Gong, J.H., Zhao, G.Y., Shi, H., Zhan, J.Y., Wang, Z., 2017. The confirmation of Caledonian intermediate-mafic volcanic rocks in northern margin of Yunkai block: Evidence for Early Paleozoic paleo-ocean basin in southwestern segment of Qinzhou–Hangzhou joint belt. *Acta Petrologica Sinica* 33(03), 791–809 (in Chinese with English abstract).

Raimondo, T., Collins, A.S., Hand, M., Walker–Hallam, A., Smithies, R.H., Evins, P.M., Howard, H.M., 2010. The anatomy of a deep intracontinental orogen. *Tectonics* 29, 1–31.

Shu, L.S., Wang, B., Cawood, P.A., Santosh, M., Xu, Z.Q., 2015.

Early Paleozoic and Early Mesozoic intraplate tectonic and magmatic events in the Cathaysia Block, South China. *Tectonics* 34, 1600–1621.

Song, M.J., Shu, L.S., Santosh, M., Li, J.Y., Li, J.Y., 2015. Late Early Paleozoic and Early Mesozoic intracontinental orogeny in the South China Craton: Geochronological and geochemical evidence. *Lithos* 232, 360–374.

Zhang, F.F., Wang, Y.J., Zhang, A.M., Fan, W.M., Zhang, Y.Z., Zi, J.W., 2012. Geochronological and geochemical constraints on the petrogenesis of Middle Paleozoic (Kwanghsian) massive granites in the eastern South China Block. *Lithos* 150, 188–208.

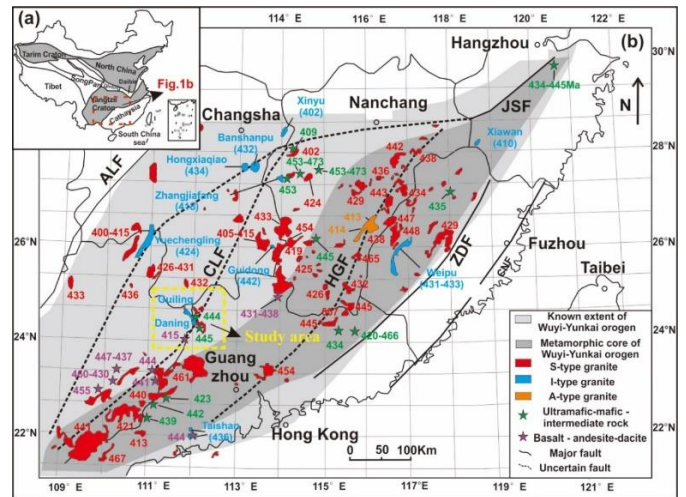


Fig. 1. Distribution of Early Paleozoic granites in the SCB. (a) The tectonic framework of China. (b) The distribution of the Early Paleozoic magmatic rocks in the South China Block.

Microfractures study on the metamorphic rock buried hill reservoirs in Bozhong Sag, Bohai Bay Basin

Tao Wei^{1,2}, Guo Lingli^{1,2*}, Li Sanzhong^{1,2}, Liu Yongjiang^{1,2}, Wang guangzeng^{1,2}, Chen Xin^{1,2}, Lv Chunxiao^{1,2}

¹ Frontiers Science Center for Deep Ocean Multispheres and Earth System, Key Lab of Submarine Geosciences and Prospecting Techniques, MOE and College of Marine Geosciences, Ocean University of China, Qingdao, 266100, China.

² Laboratory for Marine Mineral Resources, Qingdao National Laboratory for Marine Science and Technology, Qingdao, 266237, China.

Decades of exploration practice around the world has proved the great potential of deep oil and gas reservoirs. At present, more than 70 countries have carried out oil and gas drilling in strata with a depth of more than 4000 m, and achieved good exploration and development results. Bohai Bay basin is a Mesozoic Cenozoic basin on the eastern block of the North China Craton where the lithosphere has experienced regional-scale Indosinian (mainly in the Late Triassic), Yanshanian (mainly from the Middle Jurassic to the Cretaceous) and Himalayan (in the Cenozoic) movements successively since the very beginning of the Mesozoic.

As the main battlefield of energy exploration in eastern China, it is rich in oil and gas resources. In 2016, Bozhong 19-6, the world's largest metamorphic condensate gas field, was discovered in Bozhong sag, Bohai Bay Basin, China. This achievement is a major breakthrough in deep buried hill exploration. The buried-hill reservoirs in the Bozhong 19-6 anticline range in burial depth from 4,500 to 5,500 m, indicating an ultra-deep gneiss buried hill. The Archean buried hill in Bozhong sag is affected by multiple stages of tectonism, and its tectonic deformation dynamic background can be roughly summarized as follows: S-N-trending compression during the Indosinian, NW-trending compression during the early Yanshanian, extension during the late Yanshanian and dextral

extension-related shearing during the Himalayan. The multi-stage tectonic transformation makes the metamorphic rock reservoir have the characteristics of strong heterogeneity and complex genetic mechanism.

Combined with the compressive and tensile tectonic stress field experienced in Bozhong sag, this paper takes monzogranite, gneissic granite and amphibolite and carries out petrophysical experiments under compressive and tensile conditions. Acoustic emission measuring is used to monitor the number accumulation and temporal and spatial distribution of rock micro fractures during the experiment. Results of acoustic emission mechanical testing indicate that the three rock reservoirs have a certain scale of micro fractures under tensile stress and compressive stress, but the accumulation and temporal and spatial distribution of micro fractures are obviously different under the same stress condition. The internal fractures of monzogranite is more than that of gneiss granite and amphibolite. Mineral micro fractures will occur around the pre-existing early-stage fractures. The study shows that the reconstruction and activation of pre-existing early-stage fractures by the tectonic movement (Indosinian compression, Yanshanian extension and Yanshanian and Himalayan reactivation) is the key to favoured the development of ultra-deep metamorphic rock buried-hill reservoirs.

Zircon U-Pb ages of paragneisses in the Grove Mountains, East Antarctica: evidence for poly-metamorphic events and tectonic implications for supercontinent assembly

Laixi Tong^{1*}, Xiaohan Liu², Chao Li¹, Zhao Liu¹

¹ State Key Laboratory of Continental Dynamics, Department of Geology, Northwest University, Xi'an 710069, China

² Institute of Tibetan Plateau, Chinese Academy of Sciences, Beijing 100085, China

*Email: tonglx@nwu.edu.cn

The Grove Mountains have been considered as an inland extension of the Prydz Belt, East Antarctica, and to represent a single Pan-African metamorphic terrane consisting mostly of Early Neoproterozoic (910-920 Ma) orthogneisses and minor paragneisses. However, the paragneisses are still less studied. Here four paragneisses are collected from the study area for LA-ICP-MS zircon U-Pb age dating in order to better understand their tectono-metamorphic evolutionary history. The dating results show that three samples contain apparent Pan-African metamorphic zircon growths with mean ²⁰⁶Pb-²³⁸U ages of 534±12 Ma, 538±85 Ma and 553±51 Ma, respectively, suggesting an important effect of Pan-African metamorphic event. The three samples also contain Early Neoproterozoic metamorphic zircons with mean U-Pb ages of 943±23 Ma and 955±36 Ma, suggesting record of Grenvillian metamorphic event, and Late Mesoproterozoic inherited zircons with mean U-Pb ages of 1049±34 Ma, 1068±110 Ma and 1357±85 Ma. Moreover, the fourth sample contains apparent Early

Neoproterozoic metamorphic zircon growths with weighted ²⁰⁶Pb-²³⁸U mean age of 964±29 Ma, suggesting an important effect of Grenvillian metamorphic event, and Late Mesoproterozoic inherited zircons with mean U-Pb ages of 1114±28 Ma and 1235±81 Ma. Thus, the Grove Mountains region might actually represent a poly-metamorphic terrane involved in both the Rayner and Prydz orogeny rather than a single Pan-African terrane as previously thought, and hence the early Rayner orogeny likely associated with the Rodinian supercontinent assembly and the late overprinting Pan-African orogeny related to the Gondwana continent assembly.

Acknowledgements

We thank the 32nd CHINARE for the logistic support during the 2015-2016 Antarctic summer fieldwork in the Grove Mountains area. This research has been supported by the NSFC projects (41972050, 41530209).

Early Paleozoic low pressure-high temperature metamorphism and tectonic implications: insights from garnet-amphibolite and meta-sediments in the northern Yili Block (NW China)

Bo Wang, Ju Deng

State Key Laboratory for Mineral Deposits Research, School of Earth Sciences and Engineering, Nanjing University, Nanjing 210023, China

The Yili Block is one of the continental constituents of the Central Asian Orogenic belt (CAOB), its continental evolution recorded Paleozoic accretionary processes of the CAOB. The northern Yili Block is characterized by occurrence of its Precambrian basement known as the Wenquan metamorphic complex (WMC). Recent studies indicated that the WMC is actually composed of Neoproterozoic crystalline/metamorphic basement and early Paleozoic arc-type intrusions, but the timing and setting of high-grade metamorphism were poorly constrained. Based on field structural investigations, we recognized that a series of garnet amphibolites developed as tectonic lenses or ribbons within garnet-bearing micaschists and gneisses along several E-W-striking ductile shear zones. Geometry and structural features of the mylonitic foliations and stretching lineation indicate a strike-slip shearing, and kinematics suggest a dextral sense of movement. Microscopic and TIMA analysis indicate three types of mineral assemblages, including a prograde association of Qtz+Ttn+Ilm+Ep, a peak association of Grt+Amp+Pl+Qtz+Ilm+Rt, and a retrograde

association of Amp+Pl+Qtz+Ttn+Ep+Bt+Chl. Mineral chemistry and coupled traditional P-T estimation and Perple_X calculation obtained comparable conditions for the peak metamorphism at 750-770°C and 8-10 Kbar, and 500-600°C and 3-6 Kbar for retrograde metamorphism. The Sm-Nd isochron dating for garnet amphibolite and garnet-micaschist provided consistent age of 445 ± 11 Ma and 445.9 ± 4.5 Ma, respectively. Monazite and zircon U-Pb analyses yielded younger ages of 436-442 Ma and 440-420 Ma. Combined with the geochemical data on the amphibolites, and previously published data, it is suggested that a high-temperature and low pressure metamorphism occurred in latest Ordovician to earliest Silurian time, associated with arc-type but high temperature magmatism. This event is most likely corresponding to the initial subduction of the Junggar Ocean beneath the Kazakhstan-Yili microcontinent. The post-orogenic strike-slip faulting induced by oblique convergence reworked and exhumed the metamorphic belt during late Paleozoic.

Response characteristics of basins on both sides of the Yangjiang-Yitong'ansha Fault Zone to the Huizhou Movement and their genesis mechanism

Guangzeng Wang^{1,2*}, Sanzhong Li^{1,2}, Xinying Liu¹, Yue Yang¹, Huawang Zhan¹, Haiyang Yu¹, Xiaoqian Ma¹, Haohao Cheng¹

¹ Key Lab of Submarine Geosciences and Prospecting Techniques, MOE and College of Marine Geosciences, Ocean University of China, Qingdao 266100, Shandong, China

² Laboratory for Marine Mineral Resources, Qingdao National Laboratory for Marine Science and Technology, Qingdao 266100, Shandong, China

*Email: guangzengwang@gmail.com

The Huizhou Movement is a tectonic movement occurring to the Pearl River Mouth Basin (PPMB) during the early-late Wenchang transitional period in the Eocene. Basins on both sides of the Yangjiang-Yitong'ansha Fault Zone (YYFZ) show various responses to the Huizhou Movement, but their similarities and differences as well as genesis mechanism are not clear, because those basins were separated then. In this paper, various characteristics of the Zhu I Depression and the Zhu III Depression to the east and west sides of the YYFZ before and after the Huizhou Movement were studied. The results show that the Huizhou Movement caused not only uplift, denudation and magmatic diapir of/in the lower Wenchang Formation of both Zhu I and Zhu III depressions, but also clockwise rotation of the stress field (from NW to nearly S-N), change of dominated fault system (from the NE-NEE-trending extensional faults to both E-W-NWW- and NE-NEE-trending transtensional ones) and migration of the fault activity and sedimentation center (from south to north and then east to west) there. However, although the above characteristics of those basins were basically the same before and after the Huizhou Movement, their tectonic cycle and stratum thickness were not consistent. The basin to east of the YYFZ (Zhu I Depression) show one complete rifting cycle in both early and late Wenchang depositional stages, while the basin to the west of the

YYFZ (Zhu III Depression) show only one rifting cycle in the whole Wenchang depositional stage with a rifting stage in the early Wenchang period and a rift shrinking stage in the late Wenchang period. In terms of stratum thickness, the Wenchang Formation of the Zhu I Depression is thick with similar distribution and thickness of its upper and lower parts, while that of the Zhu III Depression is thinner with more limited distribution and thinner thickness of upper part compared to its lower part. We think the Eocene evolution and development of basins on both sides of the YYFZ are controlled mainly by regional tectonic movement and pre-existing weakness/fabrics. The former (the Huizhou Movement) is an important reason of common evolution of those basins, while the latter is the basis for their differential evolution with the YYFZ as an accommodation belt. The results of this study not only provide a basis for the cross-basin correlation of the isolated Wenchang Formation on both sides of the YYFZ, but also bear important significance for the whole basin analysis of the Pearl River Mouth Basin in the early Cenozoic.

Keywords: the Huizhou Movement; early-late Wenchang transitional stage; the Yangjiang-Yitong'ansha Fault Zone; the Zhu I Depression; the Zhu III Depression; the Pearl River Mouth Basin

3D Geological Model for Active Tectonics: from North China Area to Japan Subduction Zone

Jianchao Wang¹, Yuyang Tan^{1,3}, Zongwei Jin¹, Shuo Pang^{1,3}, Huilin Xing^{1,2,3}

¹ Frontiers Science Center for Deep Ocean Multispheres and Earth System, Key Lab of Submarine Geosciences and Prospecting Techniques, MOE and College of Marine Geosciences, Ocean University of China, Qingdao 266100, China

² Laboratory for Marine Mineral Resources, Qingdao National Laboratory for Marine Science and Technology, Qingdao 266100, China

³ International Center for Submarine Geosciences and Geoengineering Computing (iGeoComp), Ocean University of China, Shandong Qingdao 266100, China

The subduction, retention and roll-back of the western Pacific subduction plate have a significant impact on the tectonic stress background in North China area and play an important role in active tectonics and the mechanism of mineralization. We integrate the regional tomographic imaging data of the West Pacific subduction zone and the data of main fault system in North China Craton and surrounding area, combined with the plate tectonic boundary, regional topography and seismic activity distribution, establish the 3-D geological model from the Japan subduction zone to the North China fault system based on the GOCAD software platform. The model

visually shows the three-dimensional structure of the Western Pacific subduction plate, and depicts the distribution characteristics and variation laws of the main faults/fault zones in North China Craton and its surrounding areas. The establishment of the geological model is helpful for us to understand the effects of plate subduction and the retention of subduction plate in the mantle transition zone on the evolution of regional fault systems. At the same time, it provides geological input for simulation of regional tectonic evolution.

Keywords: 3D structural model, west Pacific subduction plate, fault systems, tectonic evolution

Weak linkage between subduction initiation and plateau collision at the Ontong-Java Plateau and the Solomon Island Arc

Liangliang Wang^{1,2}, Liming Dai^{1,2*}, Wei Gong^{1,2}, Sanzhong Li^{1,2*}, Xiaodian Jiang^{1,2}, Gillian Foulger⁴, Hao Dong^{1,2} & Zhonghai Li³

¹ Frontiers Science Center for Deep Ocean Multispheres and Earth System, Key Lab of Submarine Geosciences and Prospecting Techniques, MOE and College of Marine Geosciences, Ocean University of China, Qingdao 266100, China

² Laboratory for Marine Mineral Resources, Qingdao National Laboratory for Marine Science and Technology, Qingdao 266100, China

³ Key Laboratory of Computational Geodynamics, College of Earth and Planetary Sciences, University of Chinese Academy of Sciences, Beijing, China

⁴ Department of Earth Sciences, Durham University, Science Laboratories, South Rd. DH1 3LE, UK

*E-mail: dailm@ouc.edu.cn; sanzong@ouc.edu.cn

Subduction initiation is a fundamental aspect of plate tectonics theory. The collision of the Ontong-Java Plateau (OJP) with the Solomon Island Arc (SIA) is often touted as the most critical factor driving the subduction initiation of the Solomon Sea Basin (SSB). However, previous studies have shown that the onset of the subduction initiation actually predates the "hard docking" event between the OJP and the SIA; thus, the OJP-SIA collision may not be directly responsible for a subduction initiation of the SSB under the collisional setting. In this study, we examine the relationship between the collision of the OJP and the subduction initiation of the SSB using a series of numerical thermal-mechanical models. In our models, subduction initiation began to develop during the "soft docking" stage, prior to the time when the main OJP reached the subduction zone. In the "hard docking" stage, the main OJP collides with the SIA, resulting in a significant accretion and compressive deformation of the OJP. By varying the amount of plateau lithospheric depletion in our models, we find that the

depletion of lithospheric mantle in the oceanic plateau has a greater influence on the development direction of the high conjugate shear strain rate zone after the subduction initiation, and then lead to various tectonic outcomes, including double subduction and mantle detachment. Different from the previous views, the OJP, like a "wall", blocks the obduction and causes the uplift of the SIA, and then affected the evolution of subduction patterns. In addition, the models show that there is a weak linkage between the intra-oceanic subduction initiation and oceanic plateau collision. Our analyses find that the correlation between subduction initiation and the properties of the island arc and the back-arc basin (e.g., the width and thickness of the island arc and the lithospheric thickness of the back-arc basin) is much stronger than the correlation between the onset of subduction initiation and the properties of the OJP (e.g., the width of the OJP and the amount of lithospheric mantle depletion).

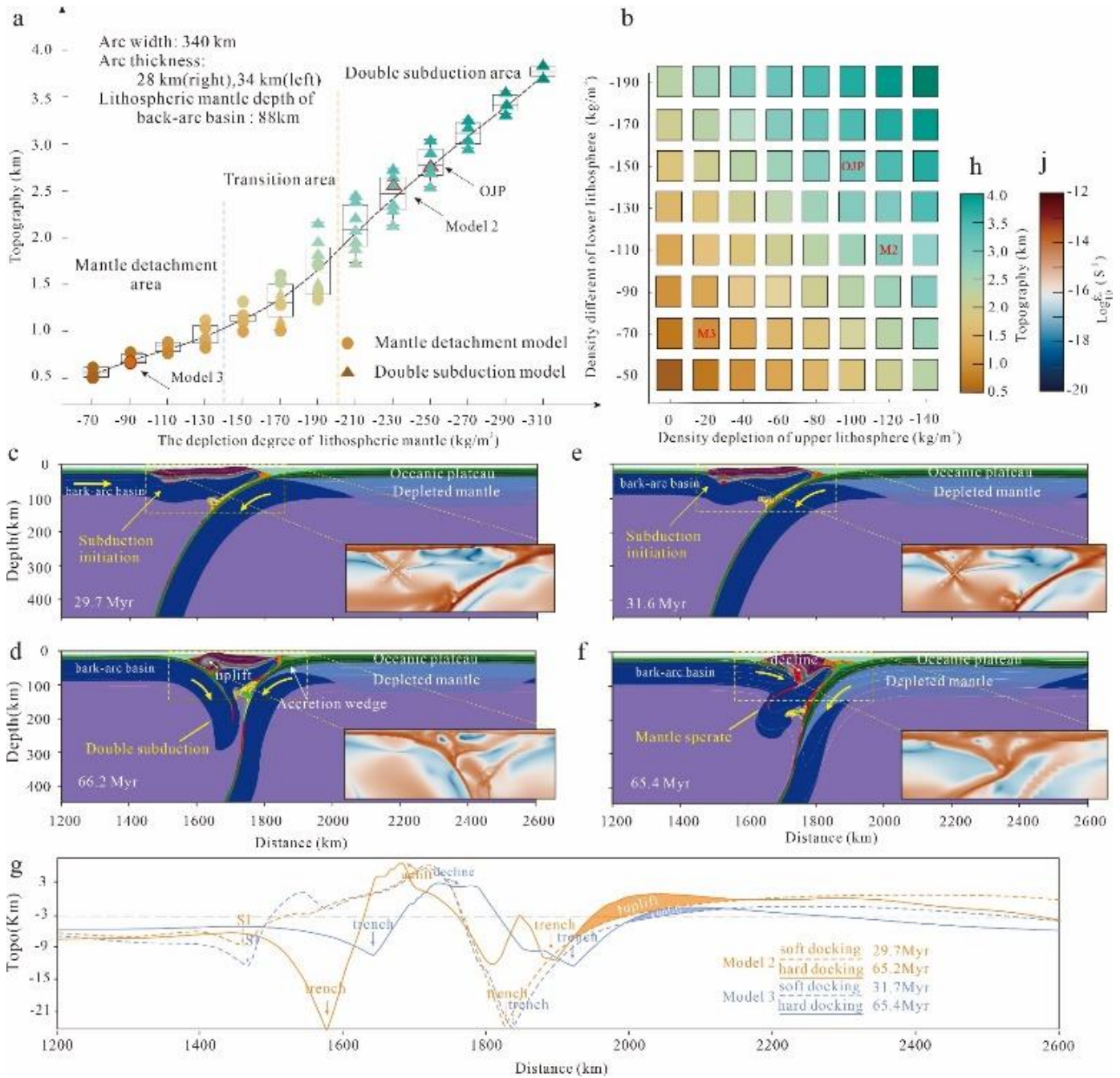


Figure 1 Summary of model results with varying degree of depletion in the lithospheric mantle of the OJP.

a The topography uplift caused by the OJP mantle depletion. Circles represent models that developed mantle detachments and triangles represent models that developed double subduction zones. Topographic uplift is relative to the initial seafloor level (17 km). Phase diagram with variable depletion degrees of the upper and lower parts of the lithospheric mantle are shown in Panel (b). **b** Phase diagram with variable depletion degrees of the upper and lower parts of the lithospheric mantle. Note, the density variation in the lithospheric mantle is relative to the normal density (3300 kg/m^3). The color bar of terrain uplift is shown in Panel (h) **c-f** The evolution of double subduction models (after **c** 29.7 Myr, **d** 66.2 Myr) and the mantle detachment (after **e** 31.6 Myr, **f** 65.4 Myr) have elapsed. The insert in the lower right of each panel represents the second invariant of strain rate. The color bar of strain rate is shown in panel (j) **g** Four topographical cross-sections corresponding to the four time periods shown in panels **c-f**. The orange lines represent topography results from Model 2 (the double subduction model in **c-d**), and the blue lines represent topography results from Model 3 (the mantle detachment model in **e-f**). The orange and blue areas represent plateau uplift in Models 2 and 3, respectively.

Structural, kinematic analysis in the northern margin of the South China Sea

Pengcheng Wang^{1,2*}, Sanzhong Li^{1,2}, Yanhui Suo^{1,2}, Lingli Guo^{1,2}, Guangzeng Wang^{1,2}, Jie Zhou^{1,2}, Suhua Jiang^{1,2}, Ze Liu^{1,2}

¹ Key Lab of Submarine Geosciences and Prospecting Techniques, MOE and College of Marine Geosciences, Ocean University of China, Qingdao 266100, Shandong, China

² Laboratory for Marine Mineral Resources, Qingdao National Laboratory for Marine Science and Technology, Qingdao 266100, Shandong, China

*Email: pengchengwang@ouc.edu.cn

The tectonic evolution history of the South China Sea (SCS) is important for understanding the interaction between the Pacific Tectonic Domain and the Tethyan Tectonic Domain. The spatial and temporal interaction between these two dynamic domains induced a dextral trans-tensional stress field, generating nearly several Cenozoic rift basins and marginal seas in the East Asia. Among these, the evolution of the SCS and its northern margin are of prime interest because of their spectacular magnetic lineations and strong rifting. Here we perform a comprehensive analysis of the spatial-temporal migration of the fault architecture and unconformities to unravel the Cenozoic tectonic evolution of the northern margin of the SCS. Based on detailed structural analysis of the geometry and kinematics, we confirm that the NE-striking onshore boundary faults propagated into the northern margin of the SCS. Combining the fault slip rate, fault combination, and a comparison of the unconformities in different basins, we identify two-stage NE-striking rifting events in the northern margin of the SCS: an early-stage rifting (from the Paleocene to the Early Oligocene) and a late-stage rifting (from the Late Eocene to the beginning of the Miocene). Temporally, the early-

stage rifting can be subdivided into three phases which show an eastward migration, resulting in the same trend of the primary unconformities. The late-stage rifting is subdivided into two phases, which took place simultaneously in different basins. The first and second phase of the early-stage rifting is related to back-arc extension of the Pacific subduction retreat system. The third phase of the early-stage rifting resulted from the joint effect of slab-pull force due to southward subduction of the proto-SCS and the back-arc extension of the Pacific subduction retreat system. In addition, the first phase of the late-stage faulting corresponds with the combined effect of the post-collision extension along the Red River Fault and slab-pull force of the proto-SCS subduction. The second phase of the late-stage faulting fits well with the sinistral faulting of the Red River Fault in response to the Indochina Block escape tectonics and the slab-pull force of the proto-SCS.

Keywords: Dextral strike-slipping; NE-striking faults; northern continental margin; South China Sea; Pacific Plate; Indo-Eurasian collision.

Zircon geochronology and Hf isotopes of dacite from Hezhou, northeastern Guangxi and its geological significance

Yong-Qiang Wang^{1,2}, Yu Shi^{1,2,3*}, Xiu-Mian Hu³, Xi-Jun Liu^{1,2}, Yuan-Lan Tang^{1,2}, Yi-Rong Sun^{1,2}

Key Laboratory of Marine Hydrocarbon Resources and Environmental Geology, Ministry of Land and Resources, Qingdao Institute of Marine Geology, Qingdao, 266071

¹ Guangxi Key Laboratory of Hidden Metal Mineral Exploration, Guilin University of Technology, Guilin 541004, China

² Collaborative Innovation Center for Exploration of Nonferrous Metal Deposits and Efficient Utilization of Resources, Guilin University of Technology, Guilin 541004, China

³ State Key Laboratory for Mineral Deposits Research, School of Earth Sciences and Engineering, Nanjing University, Nanjing 210093, China

*Email: shiyu_61@163.com

It is widely agreed that the tectonic stress field of the South China Block (SCB) has changed from compressional to extensional system in the Mesozoic, while the SCB changed from being influenced by the Tethyan tectonics to being influenced by the Pacific tectonics during the Mesozoic (Zhou et al., 2006; Shu et al., 2009; Wang et al., 2013; Mao et al., 2014). However, the duration of extension in the transition of tectonic framework and the timing of the transition from the Tethyan regime to the Pacific regime is still unclear. Take, for example, Dong et al. (2007) and Mao et al. (2014) presented a 'multi-directional convergence' tectonic framework, which has undergone three stages of strong compressional of intra-continental orogeny, extensional lithospheric thinning, and weak compressional deformation in the Mesozoic. The transition timing from the Tethyan to the Pacific regime of the SCB was considered to be in T3 (Wang et al., 2013), J1 (Zhou et al., 2006), J1-J2 (Shu et al., 2009), J2-J3 (Zhang et al., 2009), J3 (Xing et al., 2008), J3-K1 (Li, 2009) or K1 (Jia et al., 2004).

The research area in this study is located at the junction of Hunan and Guangxi Provinces, the convergence zone of the Yangtze plate and Cathaysia plates, and the western margin of Nanling metallogenic belt, which belongs to Kaishan Town, Hezhou City, Guangxi Province (Fig. 1). The samples were collected from 18 layers and the lithology was amphibolite (GPS: N24°42'37.64", E111°27'6.72"), with a variegated porphyritic structure, and the phenocrysts are altered

plagioclase (15%), altered dark mineral (5%) and quartz (5%). The matrix may be composed of plagioclase, dark minerals, quartz, magnetite, vitreous, etc., which has been strongly altered to sericite, chlorite, limonite (about 60%), microcrystalline cryptoquartz (15%), etc. The rocks have undergone strong alteration, metamorphism and weathering.

Cathodoluminescence (CL) images show obvious oscillating zoning, which is typical of magmatic zircons. The formation age of dacite sample is 157.1 ± 0.9 Ma. It is consistent with the age of the surrounding granites and ore deposits and is consistent with the episodic extension of the lithosphere in the region. $\epsilon_{\text{Hf}}(t)$ values were all smaller than 0 (-5.68~-0.97). The second-stage Hf model age (T_{DM2}) was concentrated at 1.26~1.54 Ga, with an average of 1.38 Ga. The Nanling Phanerozoic granites are all derived from the Mesoproterozoic (~1380 Ma) ancient basement.

The source region of the dacites is mainly the ancient crust of Mesoproterozoic, and the dacite is mainly derived from the crust material of Mesoproterozoic crystalline basement. The formation of dacite might be related to the intraplate extension and thinning of the Early Yanshanian lithosphere in the SCB.

Acknowledgements

This research was jointly supported by National Science Foundations of China (Grant Nos. 41862003, 41562005,

92055208); Guangxi Natural Science Foundations of China for Distinguished Yong Scholars (Grant Nos. 2019GXNSFFA245005 and 2018GXNSFFA281009).

References

Dong, S.W., Zhang, Y.Q., Chen, X.H., et al., 2007. The formation and deformational characteristics of East Asia multi-direction convergent tectonic system in Late Jurassic. *Acta Geoscientica Sinica* 29, 306-317 (in Chinese with English abstract).

Jia, D.C., Hu, R.Z., Lu, Y., et al., 2004. Characteristics of the mantle source region of sodium lamprophyres and petrogenetic tectonic setting in northeastern Hunan, China. *Science in China (Ser. D) Earth Sciences* 47, 559-569.

Li, X.H., 2000. Cretaceous magmatism and lithospheric extension in SE-China. *Journal of Asian Earth Sciences* 18, 293-305.

Mao, J.R., Li, Z.L., Ye, H.L., 2014. Mesozoic tectono-magmatic activities in South China: Retrospect and prospect. *Science in China (Ser. D)* 57, 2853-2877.

Shu, L.S., Zhou, X.M., Deng, P., et al., 2009. Mesozoic tectonic evolution of the southeast China block: New insights from basin analysis. *Journal of Asian Earth Sciences* 34, 376-391.

Wang, Y.J., Fan, W.M., Zhang, G.W., et al., 2013. Phanerozoic tectonics of the South China Block: Key observations and controversies. *Gondwana Research* 23, 1273-1305.

Xing, G.F., Lu, Q.D., Chen, R., et al., 2008. Study on the ending time of Late Mesozoic tectonic regime transition in South China-comparing to the Yanshan Area in North China. *Acta Geologica Sinica* 82, 451-463 (in Chinese with English abstract).

Zhang, Y.Q., Xu, X.B., Jia, D., et al., 2009. Deformation record of the change from Indosinian collision-related tectonic system to Yanshanian subduction-related tectonic system in South China during the Early Mesozoic. *Earth Science Frontiers* 16, 234-247.

Zhou, X.M., Shen, W.Z., Shu, L.S., et al., 2006. Petrogenesis of mesozoic granitoids and volcanic rocks in south china: a response to tectonic evolution. *Episodes* 29, 26-33.

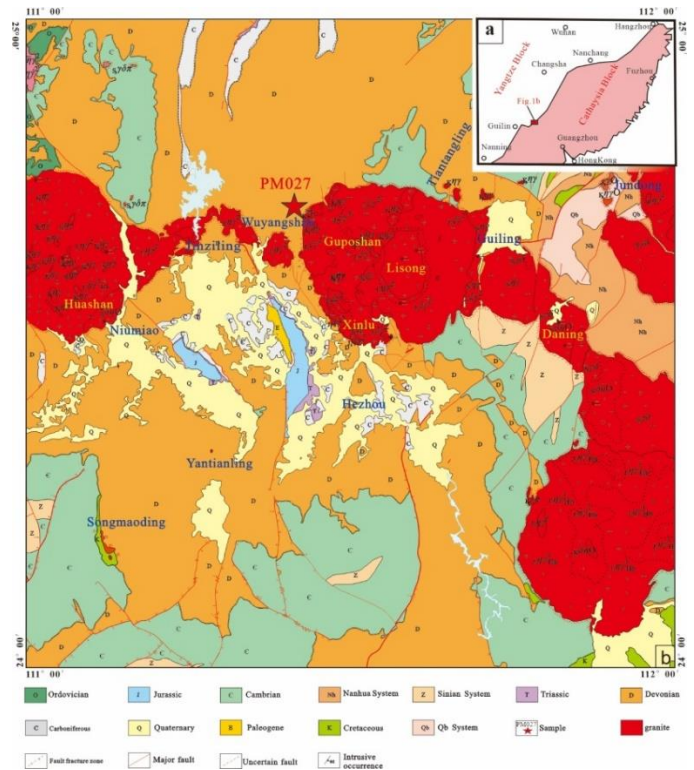


Figure 1 Geological map and sampling location of Northeastern Guangxi

Tectonic coupling between the Dabie Orogen and the Hefei Basin

Yongsheng Wang, Qiao Bai, Cong Jiang, Juanhao Yang

School of Resources and Environmental Engineering, Hefei University of Technology, Hefei, China

Orogenic belt and basin, as two basic tectonic units of continental lithosphere, are usually closely related and formed under the same tectonic framework and dynamic system. Basins develop on both sides of an orogenic belt in response to the flexure of continental lithosphere that takes place during continent–continent collision (Jordan, 1981; DeCelles and Giles, 1996; Naylor and Sinclair, 2008). The hinterland basin (also called the retro-foreland basin) is situated in the overriding plate that is being overthrust, and records relatively little accretion (Willett et al., 1993; DeCelles and Giles, 1996). Usually, the nonmarine hinterland basin is a key recorder of the history of uplift and erosion of the adjacent mountain range (Carter and Bristow, 2003; Perez and Horton, 2014). Therefore, study of the sediments in the hinterland basin is critical for understanding the mechanisms of the orogeny, including the processes of exhumation and erosion.

The Hong'an–Dabie–Sulu Orogen in China hosts the largest province of ultrahigh-pressure (UHP) rocks in the world, and formed during the Triassic continent–continent collision of the North China Block (NCB) and the South China Block (SCB) (Mattauer et al., 1985; Yin and Nie, 1993; Zhang et al., 1996). The Hefei Basin, in the hinterland region of the Dabie Orogen, was generated in response to uplift of the Dabie Orogen, and was filled with clastic material from the eroding mountain range (Liu et al., 2003; Li et al., 2005; Wan et al., 2005; Meng et al., 2007; Zhu et al., 2017). Although post-collisional large-scale extension and denudation resulted in the removal of large volumes of high-pressure (HP) and UHP rocks from the Dabie Orogen, many records of the tectonic evolution of the orogen can be obtained from the Hefei Basin. For example, the presence of Triassic coesite-bearing detrital zircons in the Lower Jurassic sediments clearly documents the exhumation of the UHP rocks of the Dabie Orogen to the surface as early as the Early Jurassic (Li et al., 2005). Detailed dating of detrital zircons in the Silurian to Cretaceous sandstones along the southern margin of the basin indicates that a ribbon-shaped microcontinent, along the entire Qinling–Tongbai–Hong'an–

Dabie Orogen, was present between the NCB and the SCB prior to the middle Paleozoic (Zhu et al., 2017).

However, the Lower Cretaceous Fenghuangtai Formation along the southern margin of the Hefei Basin lack detrital zircons with the age-frequencies that typify the nearby Paleozoic metasediments of the Foziling Group (Wan et al., 2005; Zhu et al., 2017), although the Foziling Group is now exposed along the southern flank of the Hefei Basin. The existing evolution model of the Dabie Orogen cannot explain the existence of this phenomenon, so there should be a tectonic evolution process that we do not understand in the tectonic evolution process. Therefore, we present details of our new field observations as well as the results of the dating of detrital zircons in the sedimentary rocks, from the Jurassic to the Cretaceous, of the Hefei Basin to help understanding the tectonic evolution of the Dabie Orogen.

The provenance of the Jurassic Fanghushan Formation was a mixture of the HP–UHP eclogite unit, the HP greenschist–amphibolite facies unit, and the early Paleozoic arc-magmatic rocks. The Middle Jurassic Sanjianpu Formation, the Lower Cretaceous Fenghuangtai and Zhougongshan Formations are characterized by the Triassic and middle Neoproterozoic zircon age clusters, while the Lower Cretaceous Heishidu and Xiaotian Formations are mainly characterized by the Early Cretaceous age clusters. The change of age cluster in these strata shows the change of source materials. According to the material distribution and zircon age characteristics in different units of the Dabie Orogen, it can be inferred that the source materials in the southern Hefei Basin mainly came from the HP–UHP metamorphic rocks from the Middle Jurassic to the Early Cretaceous, and transformed into the North Dabie unit mainly exposing migmatites and magmatic rocks developed during the earlier Early Cretaceous. The transformation of provenance in this period corresponds to the rapid uplift in the post-collisional extension of the Dabie Orogen in the Early Cretaceous. None of the sediments in the Hefei Basin contains a detrital zircon age population that corresponds to that found in the nearby

metasediments of the Paleozoic Foziling Group, which could not, therefore, have been the source of the sediments. It is deduced that the Foziling Group was covered and protected from erosion.

The exhumed HP-UHP rocks are represented by detrital zircons in the deposits of the Hefei Basin, but not in the Huangshi Basin to the south of the orogen and basins immediately to the east of the Dabie Orogen. This may be related to existence of a drainage divide in the orogen. The HP-UHP rocks just exposed north of the drainage divide and the Susong Complex unit cropped out both sides of the drainage divide. This is a good proof that the HP-UHP rocks were distributed locally and were only exposed in the north of the orogen during the Early-Middle Jurassic, while the Susong Complex unit is widely distributed in whole of the Dabie Orogen.

References

- Carter, A., Bristow, C.S., 2003. Linking hinterland evolution and continental basin sedimentation by using detrital zircon thermochronology: a study of the Khorat Plateau Basin, eastern Thailand. *Basin Research* 15, 271–285.
- DeCelles, P.G., Giles, K.A., 1996. Foreland basin systems. *Basin Research* 8, 105–123.
- Jordan, T.E., 1981. Thrust loads and foreland basin evolution, Cretaceous, western United States. *AAPG Bulletin* 65, 2506–2520.
- Li, R.W., Wan, Y.S., Cheng, Z.Y., Zhou, J.X., Li, S.Y., Jin, F.Q., Meng, Q.R., Li, Z., Jiang, M.S., 2005. Provenance of Jurassic sediments in the Hefei Basin, east-central China and the contribution of high-pressure and ultrahigh-pressure metamorphic rocks from the Dabie Shan. *Earth and Planetary Science Letters* 231, 279–294.
- Li, S.G., Jagoutz, E., Chen, Y.Z., Li, Q.L., 2000. Sm-Nd and Rb-Sr isotopic chronology and cooling history of ultrahigh pressure metamorphic rocks and their country rocks at Shuanghe in the Dabie Mountains, Central China. *Geochimica et Cosmochimica Acta* 64, 1077–1093.
- Liu, S.F., Zhang, G.W., Ritts, B.D., Zhang, H.P., Gao, M.X., Qian, C.C., 2010. Tracing exhumation of the Dabie Shan ultrahigh-pressure metamorphic complex using the sedimentary record in the Hefei Basin, China. *Geological Society of America Bulletin* 122(1/2), 198–218.
- Mattauer, M., Matte, P., Malavieille, J., Tapponnier, P., Maluski, H., Xu, Z.Q., Tang, Y.Q., 1985. Tectonics of the Qinling belt: Build-up and evolution of eastern Asia. *Nature* 317, 496–500.
- Meng, Q.R., Li, S.Y., Li, R.W., 2007. Mesozoic evolution of the Hefei Basin in eastern China: sedimentary response to deformations in the adjacent Dabieshan and along the Tanlu fault. *Geological Society of America Bulletin* 119(7/8), 897–916.
- Naylor, M., Sinclair, H.D., 2008. Pro- vs. retro-foreland basins. *Basin Research* 20, 285–303.
- Perez, N.D., Horton, B.K., 2014. Oligocene-Miocene deformational and depositional history of the Andean hinterland basin in the northern Altiplano plateau, southern Peru. *Tectonics* 33, 1819–1847.
- Ratschbacher, L., Hacker, B.R., Webb, L.E., McWilliams, M., Ireland, T., Dong, S.W., Calvert, A., Chateigner, D., Wenk, H.R., 2000. Exhumation of the ultrahigh-pressure continental crust in east central China: Cretaceous and Cenozoic unroofing and the Tan-Lu fault zone. *Journal of Geophysical Research* 105, 13303–13338.
- Wan, Y.S., Li, R.W., Wilde, S.A., Liu, D.Y., Chen, Z.Y., Yan, L., Song, T.R., Yin, X.Y., 2005. UHP metamorphism and exhumation of the Dabie Orogen: Evidence from SHRIMP dating of zircon and monazite from a UHP granitic gneiss cobble from the Hefei Basin. *Geochimica et Cosmochimica Acta* 69(17), 4333–4348.
- Willett, S., Beaumont, C., Fullsack, P., 1993. Mechanical model for the tectonics of doubly vergent compressional orogens. *Geology* 21: 371–374.
- Yin, A., Nie, S., 1993. An indentation model for the North and South China collision and the development of the Tan-Lu and Honan fault systems: East Asia. *Tectonics* 12, 801–813.
- Zhang, G.W., Meng, Q.G., Yu, Z.P., Sun, Y., Zhou, D.W., Guo, A.L., 1996. Orogenesis and dynamics of the Qinling orogen. *Science in China Series D: Earth Sciences* 39, 225–234.
- Zheng, Y.F., Zhao, Z.F., Wu, Y.B., Zhang, S.B., Liu, X.M., Wu, F.Y., 2006. Zircon U-Pb age, Hf and O isotope constraints on protolith origin of ultrahigh-pressure eclogite and gneiss in the Dabie orogen. *Chemical Geology* 231, 135–158.
- Zhu, G., Wang, Y.S., Wang, W., Zhang, S., Liu, C., Gu, C.C., Li, Y.J., 2017. An accreted micro-continent in the north of the Dabie Orogen, East China: Evidence from dating results of detrital zircons. *Tectonophysics* 698, 47–64.

Eocene thickening without extra heat in a collisional orogenic belt: A record from the Eocene metamorphism in mafic dike swarms within the Tethyan Himalaya, southern Tibet

Yuhua Wang^{1,2*}

¹ Key Lab of Submarine Geosciences and Prospecting Techniques, MOE and College of Marine Geosciences, Ocean University of China, Qingdao 266100, Shandong, China

² Laboratory for Marine Mineral Resources, Qingdao National Laboratory for Marine Science and Technology, Qingdao 266100, Shandong, China

*Email: wyh@ouc.edu.cn

Knowledge of the nature of the earliest metamorphism experienced by collisional orogenic belts is essential for reconstruction of tectonic processes for building high mountain chains and their environmental consequences. The metamorphic nature of Eohimalayan-phase orogeny of the Himalayan orogen, one of the typical examples of orogenic belts worldwide could provide some important constraints to test different tectonic models (shallow continental subduction vs slab breakoff) for the early phases of the development of large scale orogenic belts. As exhumed middle to lower crustal rocks in the Kangmar Gneiss Dome, the garnet amphibolites with a protolith age of 176.4 ± 3.6 Ma, experienced a phase of metamorphism at 47.2

± 1.8 Ma with an increase in pressure as well as temperature from 3-5 kbar/550-600 °C to over ~ 11 kbar/650 °C. This suggests that the middle to lower crustal rocks experienced a heating at least by ~ 50 °C while it underwent a compression and thickening. Heat flow estimation further demonstrates that the self-produced heat is high enough to achieve the observed P-T conditions recorded by the garnet amphibolite. Therefore, an additional heat supply is not required during early Eocene. A breakoff of the leading part of the subducting Indian continental slab, if occurred, should be younger than ~ 47 Ma.

Keywords: Eocene thickening; Collisional orogenic belts; high-grade metamorphism; Himalaya; Tibet

Linking ~1.4-0.8 Ga volcanic-sedimentary records in eastern Central Asian Orogenic Belt with southern Laurentia in supercontinent cycles

Zhiwei Wang^{1,2*}, Jia Peng^{1,2}, Zhihui Wang^{1,2}, Yanjie Zhang^{1,2}, Bei Xu^{1,2,3}, Yingjie Tian^{1,2}

¹ Hebei Key Laboratory of Strategic Critical Mineral Resources, Hebei GEO University, Shijiazhuang 050031, China

² College of Earth Sciences, Hebei GEO University, Shijiazhuang, 050031, China

³ Key Laboratory of Orogenic Belts and Crustal Evolution, Peking University, Beijing 100871, China

*Email: wangzw14@mails.jlu.edu.cn

The ~1.5-0.8 Ga period followed the long-lived Nuna to Rodinia supercontinent cycle. The record of Meso- to Neoproterozoic magmatism and sedimentation from western Xing'an-Airgin Sum Block (XAB), eastern Central Asian Orogenic Belt (CAOB), suggests that the XAB shared similar Meso- to early Neoproterozoic magmatic and sedimentary records to the southern Laurentia, and provides the first key evidence for the linkage with the Nuna to Rodinia supercontinent cycles. The ~1.5-1.3 Ga granite-rhyolite association within the western XAB was remarkably similar to the coeval Granite-Rhyolite Province on the southern Laurentia margin, which were probably the products of extension on a long-lived convergent plate margin, during the Columbia breakup. Siliciclastic, mixed clastic and carbonate sequences of the Airgin Sum Group accumulated on the western XAB during two stages at 1.00-0.92 and 0.87-0.75 Ga, which were comparable with the syn- to post-orogenic successions on the southern Laurentia margin representing two dominant phases of the Grenville orogenic cycle in Rodinia assembly. The well

preserved 1.7-0.8 Ga detrital zircons in the western XAB and their systemic variations of Ti-in-zircon thermometry, trace elements and Hf isotopes over time likely provide good correlations with the long-lived (1.7-1.2 Ga) subduction along the edge of Nuna, and 1.10-0.98 Ga collisional assembly of Rodinia followed by 0.9-0.8 Ga collisional collapse extension. The increasing new discovery of predominant 1.5-1.3, 0.9-0.8 Ga detrital zircon age peaks and coeval magmatism corresponding to valleys in previously global database, widely distributed in Nuna and Rodinia, further suggesting their volume mass was underestimated before and that they recorded much more intense magmatic activity, exhumation and deposition than previously thought. Juvenile continental crust growth underestimated in the previous researches, largely occurred in blocks within the CAOB and Nuna at ~1.5-1.3 Ga, and crust reworking significantly dominated the crustal evolution during the Rodinia assembly in 1.1-0.8 Ga interval.

Distribution of Mesozoic-Cenozoic magmatic arc in East Asian Continental Margin and their response to the Paleo-Pacific Plate subduction evidence from gravity and magnetic anomalies

Dong Wei^{1,2}, Suhua Jiang^{1,2*}, Sanzhong Li^{1,2*}, Jianli Zhang^{1,2}, Xueting Guan^{1,2}, Yanhui Suo^{1,2}

¹ Frontiers Science Center for Deep Ocean Multispheres and Earth System, Key Lab of Submarine Geosciences and Prospecting Techniques, MOE, College of Marine Geosciences, Ocean University of China, Qingdao 266100, China

² Laboratory for Marine Mineral Resources, Qingdao National Laboratory for Marine Science and Technology, Qingdao 266237, China

*Email: sanzong@ouc.edu.cn

In order to reveal the relationship between Mesozoic-Cenozoic magmatic arc and the Paleo-Pacific Plate subduction in East Asian Continental Margin, the distribution of Mesozoic-Cenozoic magmatic arc in East Asian Continental Margin is deeply studied, based on new gravity and magnetic anomalies evidence, obtained by the latest gravity and magnetic processing techniques, such as wavelet multi-scale analysis, upward continuation, directional derivative and residual gravity anomaly. Further combined with regional geological data, the distribution of Mesozoic-Cenozoic magmatic arc in East Asian Continental Margin and their response to the Paleo-Pacific subduction are discussed, and the following research results are obtained.

(1) In the free air gravity anomaly field, the continental margin magmatic arc shows an obviously high value anomaly. Taking the Sikhote Alin orogenic belt as an example, the eastern part of the orogenic belt is the late Cretaceous continental margin volcanic arc, and its free air gravity anomaly is mainly distributed between 60 ~ 100 mGal, which change slowly and gradually, related to the continuous and slow retreat of the Paleo-Pacific Plate in the late Cretaceous.

(2) In the crustal residual gravity anomaly field, the continental margin magmatic arc shows an obvious positive anomaly zone. Taking the Mesozoic Magmatic arc on the continental margin of the South China block as an example, the

location where the Jurassic magma arc developed appears to be relatively high in the crustal residual gravity anomaly field, reflecting a thinner crust, related to the thinning of the crust caused by the transition from Cretaceous to continental margin rift basins.

(3) In the wavelet multi-order detail and approximation field, the epicontinental volcanic arc surface is related to its crustal extension. Taking the Sikhote Alin orogenic belt as an example, in the fourth-order detail field, the continental margin volcanic arc mainly develops some arc-shaped anomaly axes, which are arranged in overlapping steps, showing the details of basement structure, corresponding to the tectonic evolution process of Mesozoic continental margin strike slip collage.

(4) In the magnetic anomaly field, the Mesozoic-Cenozoic continental margin magmatic arc shows strong magnetic anomaly or high anomaly. Taking the Okhotsk Chukotka volcanic arc as an example, it demonstrated as a strong magnetic anomaly zone.

This study not only reveal the distribution of Mesozoic-Cenozoic magmatic arc in East Asian Continental Margin, but also provides a geophysical basis for understanding the subduction evolution of the Paleo-Pacific Plate.

Keywords: East Asian Continental Margin; Mesozoic-Cenozoic; Magmatic arc; Gravity and magnetic anomalies; Paleo-Pacific Plate; Plate Subduction response

Environmental controllings on coral reefs in the Yongxing Island, Xuande Atoll, Xisha, South China Sea – the evidence from rare earth elements

Haotian Wei^{1,2}, Yanyan Zhao^{1,2,3}, Jun Yang^{1,2}, Haiyan Long², Sanzhong Li^{1,2,3}, Naishuang Bi²

¹ Key Laboratory of Submarine Geosciences and Prospecting Technique, Ministry of Education; Institute for Advanced Ocean Study, Ocean University of China, Qingdao 266100, China

² College of Marine Geosciences, Ocean University of China, Qingdao 266100, China

³ Laboratory for Marine Geology, Qingdao National Laboratory for Marine Science and Technology, Qingdao 266061, China

The corals of South China Sea mainly composed of aragonite and calcite. Although the corals have been experienced diagenetic alteration, the rare earth elements (REYs) in corals may still faithfully record the geochemical characteristics of the environments. In this study, the REYs of coral reefs of the Yongxing Island in Xisha Islands from 142 to 84 ka were analyzed. The results show that, since 142 ka, most of the coral reefs in the Yongxing Island have a normal seawater-like REY pattern, characterized by LREE depletion, negative Ce anomalies and high Y/Ho ratios. This indicates that coral in the Yongxing Island of Xisha Islands lived in the open shallow sea. In contrast, the coral skeletons of 114 ka have similar LREE

depletion, negative Ce anomalies and high Y/Ho ratios to the others, except Eu, which are characterized by positive anomalies. The REY features of ancient and modern carbonate show that the positive Eu anomalies are related to the hydrothermal fluids. In this way, the hydrothermal fluid may be input in the surround environment during the growth of corals. Based on the model calculations, at least 0.1% of hydrothermal fluid was added to the open seawater during that time. The hydrothermal fluids may be related to the volcanic activities at Gaojianshi island or Hainan island.

Keywords: coral; rare earth element; Eu anomaly; hydrothermal solution; South China Sea

Nature and evolution of the northern margin of the Tarim Craton and its adjacent block in NW China during the Neoproterozoic: A review and new perspective

Hongxiang Wu^{1,2}, Fengqi Zhang^{1,2*}, Caiyun Wang^{1,2}, Yildirim Dilek³, Kongyang Zhu¹, Xiubin Lin^{1,2}, Xiaogan Cheng^{1,2}, Hanlin Chen^{1,2}

¹ Key Laboratory of Geoscience Big Data and Deep Resource of Zhejiang Province, School of Earth Sciences, Zhejiang University, Hangzhou 310027, China.

² Research Center for Structural Analysis of Petroliferous Basins, Ministry of Education, Hangzhou 310027, China.

³ Department of Geology & Environmental Earth Science, Miami University, Oxford, OH 45056, USA.

*Email: zhangfq78@zju.edu.cn

Abundant Neoproterozoic tectono-magmatic records indicated that the Tarim Craton and other Central Asian blocks could have participated in the evolution of Rodinia supercontinent. However, whether the Tarim is located on the outer margin or inside of the supercontinent remains controversial. This study summarizes the progress of Neoproterozoic stratigraphy, magmatism, metamorphism, basin sedimentation and filling and clastic provenance in the northern margin of the Tarim and Central Tianshan-Yili Block, and provides a new constraint on the age of the metamorphism of the Aksu Group.

The early Neoproterozoic in the northern Tarim mainly was featured by the deposition of clastic rock to carbonate, indicating that this area was generally under stable and passive continental margin environment during 1800-860 Ma. Significantly different from the northern margin of Tarim, the early Neoproterozoic (960-860 Ma) of the Central Tianshan-Yili Block were mainly manifested by a large number of granitic magmatism, indicating an arc setting related to subduction. Based on the newly identified zircon U-Pb chronology of acidic dykes in bimodal dykes, it is believed that the metamorphic age of the Aksu Group should be older than 780 Ma. Based on previous studies, it is proposed that there was a metamorphic orogenic event with a short duration (ca. 830-780 Ma) in the mid-Neoproterozoic in the northern margin of Tarim, while the Central Tianshan-Yili Block mainly showed regional

unconformities and lacked stratigraphic records. In the late Neoproterozoic (780-560 Ma), the tectonic-stratigraphic and magmatism of the northern Tarim Craton and the Central Tianshan-Yili Block were very similar, including intrusions of 780-760 Ma aged basic and bimodal dike swarms, Nanhua and Sinian deposits interlayered with glacial diamictites during the Cryogenian and Ediacaran, and multiple-stages of A-type granitic intrusions and volcanic eruptions. The comprehensive provenance and protolith studies on the Aksu Group, Nanhua and Sinian systems in the Aksu area showed that the protolith of the Aksu Group was complex including allochthonous MORB, terrestrial deposits derived from the Paleoproterozoic (1800-2000 Ma), Archean (~2200-2700 Ma) crystalline rocks, and a large number of igneous rocks with ages of 950-860 Ma. It is speculated that the former two is mainly from the Precambrian basements of the Tarim, while the latter was mainly derived from the Central Tianshan-Yili Block based on the zircon Hf isotope data; and detrital zircons aged 840- 600 Ma shows the characteristics of a mixed magmatic source of the above two blocks. Although the arc-type volcanic- intrusive rocks of 900 Ma in age were sporadically exposed in the Aksu area, they were not the evidence of the active continental margin in the northern Tarim, but the nappe which was thrust into the northern Tarim during the mid-Neoproterozoic orogenic period.

Finally, an alternative new tectonic evolution model is proposed: (1) In the early Neoproterozoic period (960-860 Ma),

the northern Tarim was a typical passive continental margin. The ocean basin between the Tarim and the Central Tianshan - Yili Block subducted toward the latter, and a long-lived magma arc developed on the the Tianshan-Yili Block. (2) In the mid-Neoproterozoic (830-780 Ma), the ocean basin closed, and the Tarim collided with the Central Tianshan-Yili Block. A short-lived peripheral foreland basin developed. As the orogeny continued, both the accretionary complex at the southern margin of the Central Tianshan-Yili Block and the peripheral foreland basin sediments suffered metamorphism and formed the Aksu Group. (3) The 780-760ma orogeny ended and entered the stage of tectonic extension, with a large number of basic and bimodal dyke swarms developed. (4) During the period of 760-600 Ma, probably due to the deep mantle plume, the Tarim and its surrounding block experienced strong tectonic extension, featured by the development of a large number of rift basins and contemporaneous emplacement of volcanic-intrusive rocks. (5) The northern of Tarim Craton was finally separated from the Central Tianshan-Ili Block and became a new passive continental margin since ca. 600 Ma. Combined with the spatio-

temporal correlation of tectonic stratigraphic magmatic events in different blocks of Rodinia supercontinent, it is proposed that the Tarim Craton and the Central Tianshan-Yili Block are located in the interior of the supercontinent, playing a new "missing link" model of the supercontinent, that is, the southern Tarim is generally connected with the southeastern Australia and the East Antarctica blocks, The mid-Neoproterozoic orogeny of Tarim and Central Tianshan-Yili Block was caused by continental collision rather than subduction, which marked the final amalgamation of Rodinia supercontinent, and then entered into the complete fragmentation of supercontinent.

Acknowledgement

We are grateful to post-graduates of Xiao-Xin Cheng, Pan Li and Qi-Ye Lu of Zhejiang University and Zi-Yuan Yi of Peking University for their assistances in the field investigations. We thank Miss Su-Wen Qiu for her considerable help during the zircon U-Pb dating. This study was supported by the National Natural Science Foundation of China (Grant No. 42077223).

Complex strata architectures of the Luzon forearc basin constrained by arc–continent collision process

Shumei Xu^{1, 2*}, Pengcheng Shu^{2, 1}, Sanzhong Li^{1, 2}

Department of Earth Sciences, The University of Hong Kong, Pokfulam Road, Hong Kong

¹ Key Lab of Submarine Geosciences and Prospecting Techniques, Ministry of Education, Qingdao 266100, China

² College of Marine Geosciences, Ocean University of China, Qingdao 266100, China

*E-mail: xsm@ouc.edu.cn

The Luzon forearc basin formed during the South China Sea oceanic lithosphere subducted eastward beneath Philippine Sea Plate since the Early Miocene (~18 Ma), with basement of Eocene or older. Sediment accumulation rates are significantly greater in the forearc basin, which consists of oceanic volcanic and *mélange*, unconformably overlain by Pliocene–Pleistocene deep-sea turbidites, occasionally carbonate atolls formed around the Miocene volcanic island. Convergent basins are typified by rapid uplift, differential subsidence, steep and short river catchments and elevated sedimentation rates. The Lichi *Mélange* (Miocene) formed from forearc oceanic crust spreading, and shows a block-in-matrix feature. The exotic blocks in the Lichi *Mélange* are grouped into: (1) andesitic volcanics originated from the arc to the east; (2) well-lithified sandstones of Miocene abyssal turbidites; and (3) fragmented ophiolitic rocks from forearc oceanic crust spreading. Unmetamorphic forearc-derived Lichi *Mélange* formed during deep basal accretion, and juxtaposed to the high-pressure rocks of the Yuli Belt. Giant tuff blocks for several hundred meters in width and length are found in the eastern part of the remnant forearc trough, represented the true olistolith derived from the

volcanic arc transporting into the remnant forearc trough by slumping processes. Deep-sea fan deposition of volcanic conglomerates presented in the basin. The limestone blocks contain larger foraminifera and corals around the Miocene volcanic island when the basin underfilled. Coherent flysch sequences formed in the remnant forearc basin during shallow basal accretion and front accretion, including the Paliwan and Fanshuliao formations (Late Miocene). The depocenter firstly formed near the back of wedge and migrated eastward from accreted wedge to Luzon Arc. But not all the depocenter migrated toward arc. The volcanic and *mélange* formed near wedge-ward depocenter caused by deep basal accretion and basal décollement. Abyssal turbidites and flysch sequences deposited when depocenter migrated arc-ward the during frontal and shallow basal accretions.

This study was financially supported by the NSFC (grant No. 91958109 and 91958214).

Keywords: The strata architectures; The Lichi *Mélange*; the Luzon forearc basin; Subduction and collision process; Taiwan orogen

Genesis of the compositional diversity in composite batholith: a case study in the Laiyuan granitoid complex, central NCC

Fei Xue^{1,2*}, M. Santosh³

¹ School of Earth Sciences and Engineering, Hohai University, Nanjing 210098, China

² Graduate School of Life and Environmental Sciences, University of Tsukuba, Ibaraki 305-8572, Japan

³ School of Earth Sciences and Resources, China University of Geosciences Beijing, Beijing 100083, China

*Email: fei.xue@hhu.edu.cn

The compositional diversity of shallow granitoid intrusions can serve as a critical window to understand the deep Earth geodynamic process. The key is to constrain the complex magmatic process and evaluate their influence on the compositional diversity. The Early Cretaceous Laiyuan granitoid complex located within the intra-domain of the North China Craton recorded strong crust-mantle interaction with marked compositional diversity, the mechanism and genesis of which have not been well constrained. Here we investigate the granitoid suite from the Laiyuan complex in the central NCC to constrain the magmatic evolution and petrogenetic linkages and to gain insights into the common mechanism of the compositional diversity of granitoid batholith.

The Laiyuan granitoid complex comprises syenogranite, monzogranite, quartz monzonite and monzonite with mafic magmatic enclaves (MMEs). The granitoids were formed during the Early Cretaceous (137-128 Ma) with $\epsilon_{\text{HI}}(t)$ values and T_{DM}^{C} ages ranging from -21.8 to -16.8 and 2564 to 2255 Ma, respectively. The compositional variations of the different rock types suggest distinct magmatic evolution and petrogenesis. Geochemical and isotopic data indicate that the enriched lithospheric mantle-derived mafic magmas underwent early-stage plagioclase-dominated and late-stage hornblende-dominated fractional crystallization to form the monzonites and quartz monzonites. Geochemical modeling results suggest that the magma of the MMEs originated through mixing between lithospheric mantle-derived mafic magma and crust-derived felsic magma with post-injection hybridization to generate

MMEs with variable compositions. The monzogranites are classified as high-K calc-alkaline I-type granites with higher SiO_2 contents (69-71 wt. %) and lower $\text{Mg}^{\#}$ (41-44) than intermediate rocks. They were generated by partial melting of the basaltic lower crust, with the addition of mafic magma from an enriched mantle. The highly fractionated syenogranites with lower $\text{Mg}^{\#}$ (18-27) were evolved from the monzogranitic magma through plagioclase-dominated crystal removal. The adakitic affinities of the monzonites and monzogranites were generated by crystallization of mantle-derived magmas and partial melting of continental crust of normal thickness (~40 km), respectively. The bottom-up crust-mantle interaction accounts for the compositional diversity of the Laiyuan granitoids, and suggests that thermo-mechanical destruction played a dominant role in the destruction of the central NCC as compared with the continental delamination process in the eastern NCC.

Acknowledgement

This project was jointly supported by the Fundamental Research Funds for the Central Universities (Grant Nos. B210201004, LZUJBKY-2020-38) of Hohai University and Lanzhou University and the KIGAM Consignment Project of "Construction of the occurrence map of mantle and lower crust-related rocks in the central Korean Peninsula and their tectonic implications" (S.W. Kim, M. Santosh).

Multiple enrichment of subcontinental lithospheric mantle with Archean to Mesozoic components: Evidence from the Chicheng ultramafic complex, North China Craton

Fan Yang

Key Laboratory of Mineral Resources in Western China (Gansu Province), School of Earth Sciences, Lanzhou University, Lanzhou 730000, China Email: fanyang@lzu.edu.cn

Numerous Late Paleozoic to Early Mesozoic mafic-ultramafic intrusions occur along the northern margin of the North China Craton (NCC). The timing, magma source, genetic types and tectonic evolution of these intrusions still remain controversial. We conduct a systematic petrological, mineral chemical, whole-rock geochemical, isotopic (zircon Lu-Hf and whole-rock Sr-Nd isotopes) and geochronological study on representative samples from the Chicheng ultramafic complex, and our results provide new insights into multiple melt-fluid interactions in the subcontinental lithospheric mantle through time. Zircon U-Pb data from the ultramafic rocks (pyroxenite and serpentized dunite) show a wide range of ages (2721-129 Ma), indicating zircon growth within an evolving and metasomatized mantle wedge during multi-stage melt-fluid interactions. The youngest zircon population (145-129 Ma) possibly marks the timing of formation of the Chicheng ultramafic complex at the Early Cretaceous. Moreover, these ultramafic rocks also witnessed tectonic transition from Paleo-Asian Ocean to Paleo-Pacific Plate subduction during the Paleozoic to Early Mesozoic and subsequent progressive lithospheric thinning and craton destruction at the northern margin of the NCC, which is also attested by the newly discovered diorite porphyry dyke from this complex reported in

this study with zircon U-Pb ages in the range of 447 to 128 Ma. Zircon Lu-Hf isotopic data show $\epsilon_{\text{Hf}}(t)$ values in the range of -19.9 to +15.4 with T_{DM} of 219-3012 Ma and T_{DM}^{C} of 240-3650 Ma. Whole-rock Sr-Nd isotopic data display $\epsilon_{\text{Nd}}(t)$ values ranging from -12.3 to -1.6, indicating heterogeneous sources involving both depleted mantle and reworked ancient crustal components. Whole-rock geochemical data display enrichment in LILEs (Rb, Sr, Ba, Pb) and depletion in HFSEs (Nb, Ta, Ti), with positive anomalies at Ba, K, Pb and Nd and strongly negative Zr and Ti anomalies, suggesting geochemical affinities related to subduction-related island arc setting within an active continental margin. Mineral chemical data on clinopyroxenes do not correspond to "Alaskan-type" affinities. Integrating geochemical, geochronological and isotopic studies from this study and those from previous studies related to the mafic-ultramafic complexes in the northern Hebei Province along the northern margin of the NCC, we propose that these complexes might be composite plutons formed during the Early Cretaceous, which were derived from the interaction of melts and fluids released from subducted slab with metasomatized mantle peridotite, triggering different degree of partial melting of mantle wedge.

Controlling mechanisms of sea surface salinity in the Central South China Sea over the last 12.6ka

Jun Yang^{1,2}, Yanyan Zhao^{1,2,3}, Haotian Wei^{1,2}, Haiyan Long², Sanzhong Li^{1,2,3},
Naishuang Bi²

¹ Key Laboratory of Submarine Geosciences and Prospecting Technique, Ministry of Education; Institute for Advanced Ocean Study, Ocean University of China, Qingdao 266100, China

² College of Marine Geosciences, Ocean University of China, Qingdao 266100, China

³ Laboratory for Marine Geology, Qingdao National Laboratory for Marine Science and Technology, Qingdao 266061, China

The South China Sea (SCS) is one of the most important forcing engines of the earth climatic system. In this study, the short-term SSS and SST variations of 12.6~2.3ka in the central SCS are analysed. The Mg/Ca ratios, $\delta^{18}\text{O}$ and $\delta^{13}\text{C}$ values of *Globigerinoides ruber* indicate that the variations of SST since 12.6ka is consistent with those of other stations in the SCS and stalagmite records in Chinese cave. This proves that the SST even in the deep sea area of the SCS during the Holocene was variable, rather than a single rise. The records suggest that the variations of surface conditions in the central SCS were mainly controlled by the East Asian monsoon (EAM). From south to north SCS, there are large differences in SSS and SST, which may be contributed to the intensity of El Niño–Southern Oscillation (ENSO), the change of sea level and latitude. The

two stages of SSS variations can be distinguished: lower salinity at 12.6~9.1ka (average 32.7psu) and relatively higher salinity at 9.1~2.3ka (average 33.7psu). In detail, at lower salinity stage, the SSS in the Younger Dryas (YD) period (12.6~11.8ka) is higher than that in the early Holocene (11.8~9.1ka). This is mainly due to the abrupt intensity changes of the East Asian Summer Monsoon (EASM) and East Asian Winter Monsoon (EAWM). At higher salinity stage, the changes of SSS were mainly controlled by EASM. The decrease of SSS at 3~4ka and 5.3~6.3ka may be attributed to the sudden decrease of EAWM intensity and the cold phase of ENSO (La Niña).

Keywords: central SCS; planktonic foraminifera; Mg/Ca ratios; oxygen isotope; sea surface salinity

Student Himalayan Exercise Program 9 years

Masaru Yoshida¹ and Student Himalayan Exercise Project²

¹ Gondwana Institute for Geology and Environment, Hashimoto (GIGE), Japan

² Conveners of the Project include M. Yoshida, K. Arita, T. Sakai and B.N. Upreti.

A student who visits the Himalaya feels the movement of the crust, and understands the principal importance of studying geology and geomorphology in the field.

The Student Himalayan Exercise Project¹ has been conducting a two weeks (depart from and return to Japan) Student Himalayan Exercise Tour (SHET) in the Himalayan Orogen with its full traverse from the north to the south in every March since 2012, nominally sponsored by 6 academic societies of Japan and Nepal including IAGR. The exercise tour covers the Tethys Himalayan, Higher Himalayan, Lesser Himalayan, Sub Himalayan and the Gangetic Alluvial zones, observing important geologies of all the geologic zones and boundary major faults. The tour starts from northernmost Muktinath (3800m asl), the world's very holy temple of Hinduism, passing through Pokhara city, the central of the Himalayan sightseeing and Tansen city, a traditional capital town of old Palpa kingdom, and ends at Lumbini (150m asl), the world's most holy place of Buddhism as the birth place of Buddha, traversing from the tundra zone to subtropical zone within its 250km length of the tour route. The changing climatic zones reflects dramatic changes of vegetations as well as living styles of human beings. Thus the tour includes a variety of interests apart from geology as well.

Before the start and after the end of the tour, a pre-tour seminar and a summary seminar have been organized, held at the Department of Geology, Tri-Chandra Campus, Tribhuvan University (DGTU), Kathmandu, and after the seminars, the

participants of the SHET have been escorted to city tours by students of the DGTU. Participants of the SHET submit a report of the tour and the tour leader assembles all the reports and tour data and forms a book titled *Traversing the Himalayan Orogen 2012* (2013 and so on), and the project has published the book every year². All 144 participants of the tour of 9 years evaluated not only the great geology and beauty of the Himalaya but also friendship interaction among participants as well as with students of the DGTU.

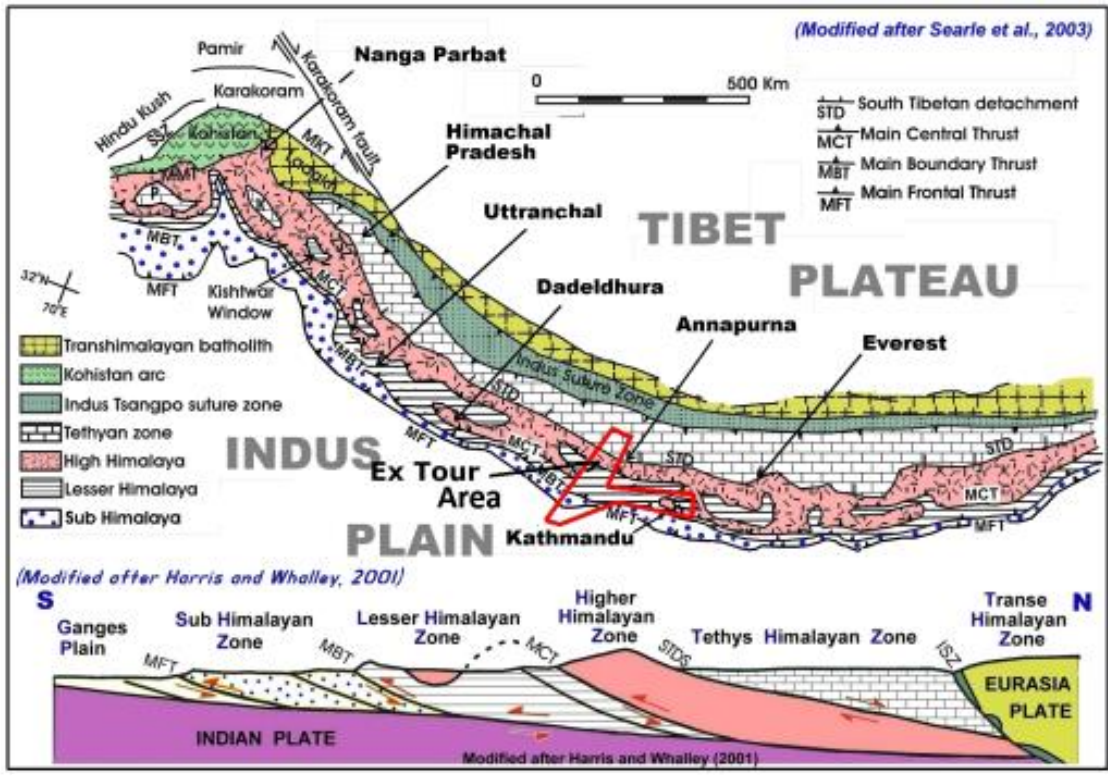
The voluntary leaders and teachers of the exercise tours have included retired and/or active university teachers and office engineers who are experienced in the Himalayan geology as well as field geology. The Gondwana Institute for Geology and Environment (Hashimoto, Japan) has mainly been conducting the organization of the exercise tour, in collaboration with the DGTU.

The total number of Participants of the 1st to 9th SHET included 113 students from 25 Japanese universities and 20 students of Nepalese, Indian and Chinese universities, and 11 citizens of Japan and Nepal. Participation fee for a Japanese student including the airfare ranged from 139000--190000 JPY with the average of about 165000 JPY. At the poster presentation, highlights of the exercise tours of past 9 years, along with details of participants and account summaries. A recruit for the 10th SHET to be held in next March will also be delivered.

¹ SHET-HP:

http://www.gondwanainst.org/Studentfieldex_index.htm

² *Traversing the Himalayan Orogen 2020 - A Record of the Ninth Student Himalayan Field Exercise Tour in March 2020* (Field Science Publishers, 193 pages) is the most recent publication.



Himalayan geologic outline and the exercise tour area



The SHET-7 team with the Dhaulagiri range on the back sight (March 2018)

Multistage anatexis during tectonic evolution from oceanic subduction to continental collision: A review of the North Qaidam UHP Belt, NW China

Shengyao Yu^{1,2*}, Sanzhong Li^{1,2}, Yongjiang Liu^{1,2}, Jianxin Zhang³, Yinbiao Peng¹

¹ Key Lab of Submarine Geosciences and Prospecting Techniques, MOE and College of Marine Geosciences, Ocean University of China, Qingdao 266100, China

² Laboratory for Marine Geology, Qingdao National Laboratory for Marine Science and Technology, Qingdao 266061, China

³ Institute of Geology, Chinese Academy of Geological Sciences, Beijing 100037, China

*Email: yushengyao@ouc.edu.cn

The North Qaidam ultra-high pressure (UHP) metamorphic belt in the northern Tibetan Plateau is considered as a typical Alpine-type UHP metamorphic belt due to the Early Paleozoic subduction of the Qaidam Block beneath the Qilian Block. The well-preserved Paleozoic metatexite migmatite, diatexite migmatite, felsic sheet/dyke and anatectic granite in the North Qaidam UHP metamorphic belt provide us with an excellent opportunity to study the generation, transport and final fate of crustal melt and geodynamic processes associated with orogenesis. Based on structural relationships, petrology, geochronology, whole-rock geochemistry and Sr-Nd isotope data, the Early Paleozoic anatexis during oceanic subduction to continental collision in the North Qaidam UHP metamorphic belt can be further divided into three stages of development ~470 Ma, 446-428 Ma and 432-420 Ma. The first-stage granitic leucosomes are rich in K, poor in Na with low Sr/Y and enrichment of large ion lithophile elements (LILEs), which were probably derived from partial melting of ancient felsic gneiss in continental arc circumstances during oceanic subduction.

The second-stage Na-rich leucosomes and tonalite plutons are characterized by high Na, Sr, Sr/Y and La/Yb and low heavy rare earth elements (HREEs), with positive $\epsilon_{Nd}(t)$ values of 0.1~4.3 and zircon $\epsilon_{Hf}(t)$ values of 8.3-10.2, similar to typical tonalite-trondhjemite-granodiorites (TTGs). These TTG-like magmas were produced through partial melting of newly emplaced gabbroic rocks with arc affinity under high-pressure (HP) granulite-facies conditions in a thickened lower crust during continental collision. The volumetrically significant

migrated plutons evolved from TTG-like melt will become segments of continental crust and contribute to crustal growth, with partial residual products of HP granulite and/or garnet pyroxenite to the mantle by delamination. The third stage of anatexis was preserved in both migmatitic UHP gneiss and eclogite in the Xitieshan and Luliangshan terranes. The Kfs-rich felsic leucosomes inside UHP gneisses in the third stage are characterized by high alkali contents and low mafic component with $FeO_T + MgO + TiO_2$ less than 2%. In trace element distribution diagrams, these Kfs-rich leucosomes exhibit parallel patterns to their host gneisses but lower element contents and slightly positive Eu and Sr anomalies. The Pl-rich leucosomes within the retrograde eclogite have geochemical features as follows: (1) rich in CaO, Na₂O and poor in K₂O, with Na₂O/K₂O ratios greater than 2.0; (2) high La/Yb and Sr/Y, and low Y and HREEs; (3) high Al₂O₃ and low Mg# values; and (4) enriched in LILEs (e.g., Rb, Ba, K, Sr, Pb) and poor in high field strength elements (HFSEs). Partial melting of UHP eclogite and felsic gneiss during the initial retrogression stage with Pl-rich and Kfs-rich leucosome formation was triggered by dehydration melting involving predominant zoisite and muscovite.

The anatectic melts from partial melting of deeply subducted UHP gneiss have accumulated and migrated outside the deeply subducted crustal slice in the form of syn-collisional plutons. The melt evolution from the leucosomes produced at the early exhumation stage to syn-collisional granitoids produced at the late exhumation, might contribute greatly to the exhumation of the North Qaidam UHP metamorphic belt from mantle depths to the lower crustal levels.

Paleozoic, Oceanic subduction, Continental collision

Keywords: North Qaidam UHP belt, Multiple anatexis, Early

Mafic–ultramafic rocks in the Buqingshan Complex of the East Kunlun Orogen, northern Tibetan Plateau: Remnants of the Paleo-Tethys Ocean

Yuangang Yue¹, Yunpeng Dong^{1,2}, Shengsi Sun¹, Dengfeng He¹, Bo Hui¹, Xiang Ren¹, Bin Zhang¹, Weidong He¹

¹ State Key Laboratory of Continental Dynamics, Department of Geology, Northwest University, Northern Taibai Str. 229, Xi'an 710069, China

² Collaborative Innovation Centre of Continental Tectonics, Northwest University, Northern Taibai Str. 229, Xi'an 710069, China

*Email: dongyp@nwu.edu.cn (Y. Dong)

The Buqingshan Complex, located in the eastern part of the Muztagh–Buqingshan–Anemaqen ophiolitic mélangé zone, preserves abundant information on the evolution of the Paleo-Tethys Ocean. Field investigations reveal that the mafic–ultramafic rocks of the Buqingshan Complex consist mainly of serpentinite, diabase, massive basalt, and pillow basalt. The serpentinites show similar geochemical characteristics to abyssal peridotites, which is probably the residual part of depleted upper mantle after melt extraction. The mafic rocks have geochemical affinities similar to both normal mid-ocean ridge basalt (N-MORB) and oceanic island basalt (OIB). The rocks with N-MORB features include diabases, massive basalts, and pillow basalts, which occur in association with serpentinites and cherts. They are depleted in Th, Nb, Ta, and LREEs [(La/Yb)_N=0.36–0.63], which may be derived from a depleted mantle source and probably erupted in a mid-oceanic ridge setting. The OIB-type pillow basalts are enriched in Th, U, Nb,

Ta, and LREEs [(La/Sm)_N=2.00–2.37] and have differentiated HREEs [(Gd/Yb)_N=1.69–1.87]. They are associated with bioclastic limestones, carbonate breccias, and carbonate-volcanogenic clastic rocks, resembling a typical sequence of a seamount. Zircon U–Pb dating of the diabases yield a Latest Carboniferous age at 303 ± 3 Ma. The reported biostratigraphic age data from the overlying limestone suggest the formation age of the basalt basement to be the Late Carboniferous–Early Permian. Combining geochemical data, lithological assemblages, and geological relationships, the N-MORB- and OIB-type assemblages most likely represent a fragment of the oceanic lithosphere of mid-ocean ridge origin and a dismantled seamount, respectively. This provides powerful evidence for the existence of the mature Paleo-Tethys Ocean with mantle plume-related magmas erupted in the ocean basin during the latest Paleozoic time in the East Kunlun Orogen.

Petrological and geochemical constrains for carbon bearing fluid evolutions and its implications for geological CO₂ capture in sandstone aquifers, Yinggehai Basin, South China Sea

Lei Yu^{1,2}, Sanzhong Li^{1,2}, Keqiang Wu³, Yanyan Zhao^{1,2}, Li Liu⁴, Na Liu⁴, Kun Pang⁵

¹ Frontiers Science Center for Deep Ocean Multispheres and Earth System, Key Lab of Submarine Geosciences and Prospecting Techniques, MOE and College of Marine Geosciences, Ocean University of China, Qingdao 266100, China

² Laboratory for Marine Mineral Resources, Qingdao National Laboratory for Marine Science and Technology, Qingdao 266237, China

³ China National Offshore Oil Corporation (CNOOC) Research Institute Co., Ltd., Beijing 100028, China

⁴ College of Earth Sciences, Jilin University, Changchun 130061, China

⁵ School of Materials Science and Engineering, Ocean University of China, Qingdao 266100, China

Large quantity of anthropogenic CO₂ generated from industry activities and released into atmosphere has been a major factor for global warming. Up to date, more and more researchers have demonstrated that mineral carbonation in geological formations is the safest way to reduce the rising CO₂ concentration in the atmosphere. Sandstone aquifers with impermeable cap-rocks can function as carbon reservoirs due to their adequate permeability, pore space, and wide distribution in the subsurface. The natural gas reservoirs of Yinggehai (YGH) basin in the South China Sea (SCS) are enriched in CO₂ and natural gas. A lot of CO₂- or hydrocarbon gas-rich reservoirs have been discovered during natural gas explorations in recent decades. According to the geochemistry and fluid inclusions results, we could know there are at least 3 major episodes of gas emplacement have been proposed. at least 3 generations They provide an excellent opportunity for us to study the petrographic and geochemical changes before and after CO₂ injections and accumulations.

Here, we conducted petrological, isotopic, and numerical modelling analyses to constrain the changes during the injection and accumulation of high-concentrated CO₂. The sandstone types are dominated by Quartz arenite and Sublitharenite in the reservoirs of DFX1 and LDY1 structures, whose detrital minerals are composed a large amount quartz, feldspar, mudstone matrix, rock debris and a little biological debris according to the optical observations by polarizing microscope and SEM. The authigenic minerals in the sandstone are mainly

composed of quartz, pyrite, two generations siderite, dolomite, dawsonite, ankerite and clay minerals. The paragenetic sequences from early to late are during diagenesis progress are: clay rims, pyrite, siderite I, quartz overgrowth, dolomite, microcrystalline quartz, kaolinite, dawsonite, siderite II and ankerite, respectively. In order to clear the carbon bearing fluid evolutionary characters in the reservoirs here, we take 16 sandstone samples to measure the carbon and oxygen isotopes for the authigenic carbonates. We found that the $\delta^{13}\text{C}$ values of ankerite and dawsonite are from -4.7 to -0.6‰ and from -4.3 to -0.8‰, respectively, which indicate that their carbon sources are dominantly related to the inorganic CO₂. The dolomite $\delta^{13}\text{C}$ values are relatively lower, from -6.8 to -3.3‰, implying the addition of ¹³C-depleted organic carbon. The siderite $\delta^{13}\text{C}$ values are in a range from -6.3 to -0.5‰, however, suggesting the mixed carbon sources. Comparing to those CO₂-poor formations, most of the reservoirs with high CO₂ concentrations are significantly enriched in kaolinite in YGH basin. Numerical modelling results proved that kaolinite, quartz, ankerite, and siderite are the dominated minerals during the fluid-rock reactions when CO₂ injected into the sandstone reservoirs. Here, we propose that the enrichment of kaolinite and ankerite can be used as alternative indicators for the CO₂-rich reservoirs in YGH basin when dawsonite is absent. Kaolinite formation under high CO₂ concentrations could lead to the dissolution of the mineral precursors, such as feldspars and clay minerals etc., and releasing divalent metal ions into pore waters. The CO₂

injection and accumulation can promote the formation of micro-crystalline quartz, kaolinite, siderite II, dawsonite, and ankerite, which can benefit carbon capture and storage.

Keywords: kaolinite enrichment; authigenic carbonates; carbon and oxygen isotopes; carbon capture and storage; Yinggehai basin

Formation of the wide rift system at the northern South China Sea: insight from architecture and nature of basement

Cuimei Zhang^{1,2}, Zhen Sun^{1,2}, Minghui Zhao^{1,2}, Xiong Pang^{3,4}, Gianreto Manatschal⁵

¹ Key Laboratory of Ocean and Marginal Sea Geology, South China Sea Institute of Oceanology, Chinese Academy of Sciences, Guangzhou, 510301, China.

² Southern Marine Science and Engineering Guangdong Laboratory, Guangzhou 511458, China

³ CNOOC Ltd.-Shenzhen, Shenzhen, 518054, China.

⁴ CNOOC Ltd.-Deepwater, Shenzhen, 518054, China.

⁵ Université de Strasbourg, CNRS, ITES UMR 7063, Strasbourg F-67084, France

Wide rift as an important mode of extension has been extensively studied for decades. However, it remains enigmatic how the crust is deforming during wide rifting, what is the mechanical behavior of the lithosphere, how the strain localizes and rift system evolves. A requisite to answer these questions is to map the basement and deformation based on a more in detail evaluation of a complete high-resolution seismic data set and drill holes. In this study, we develop a method to investigate the nature of acoustic (top) basement in the northern South China Sea and to provide insight into extension mechanism of the wide rift system.

The result shows that two types of basement can be identified including remnants of upper crustal allochthones and windows of exhumed deep crust. The nature of (top) basement repeatedly shifts in between, indicating that the original top of pre-rift basement was highly fragmented and locally separated by the detachment faults. The common exhumation of the deep crust, combined with the updoming basement, coincident topographic high and ubiquitous magmatic-related structures, are

reminiscent of metamorphic core complexes (MCCs) formation. MCCs are more widely distributed from the eastern Baiyun Subbasin to the ocean-continent transition. Almost all MCCs initiated coevally at early rifting when the strain was distributed basin wide. Each MCC was observed to propagate in kinematic transport direction once they nucleated. The magma intruded before, during and after MCC formation. The feedback between extension and decompression melting kept weakening the crust outboard and facilitated the ductile flow of the mid-lower crust. The high thermal gradient, the substantial ductile flow and the delocalized strain during rifting finally lead to the formation of an extremely wide rift system prior to final breakup.

This study was financially supported by K.C. Wong Education Foundation (GJTD-2018-13), Key Program of NSFC (41730532), and Key Special Project for Introduced Talents Team of Southern Marine Science and Engineering Guangdong Laboratory (Guangzhou) (GML2019ZD0205).

Key words: Detachment; metamorphic core complexes; nature of basement; wide rift; South China Sea

The northern boundary of the Proto-Tethys Ocean: Constraints from early Paleozoic deformation and detrital zircon geochronology of the North Qinling Terrane and Qinling-Qilian connection zone

Shujuan Zhao ^{1,2}, Sanzhong Li ^{1,2}, Huahua Cao ^{1,2}, Li Xiyao ^{1,2}

¹ Frontiers Science Center for Deep Ocean Multispheres and Earth System, Key Lab of Submarine Geosciences and Prospecting Techniques, MOE and College of Marine Geosciences, Ocean University of China, Qingdao 266100, China

² Laboratory for Marine Mineral Resources, Qingdao National Laboratory for Marine Science and Technology, Qingdao 266237, China

The North Qinling Terrane (NQT) is located in the northern part of the Qinling Orogenic Belt which formed through the collision between the North China Block (NCB) and the South China Block (SCB). The Qinling-Qilian connection zone (QQCZ), located in the middle-north segment of the Central China Orogen (CCO), links the west part of the North Qinling Orogen to the east part of the North Qilian Orogen. These areas are key to reveal the relationship between the two orogens and to reconstruct the evolutionary tectonic model of the CCO.

In order to evaluate the deformation and thermal histories of the NQT and the QQCZ, we report a large amount of new structural data based on detailed structural analyses in the field and detrital zircon U-Pb ages (Zhao et al., 2015, 2020). Our results provide important insights on the evolution of the study area during the Neoproterozoic to early Paleozoic interval and offer better constraints on the tectonic framework of the northern boundary of the Proto-Tethys Ocean.

Three episodes of deformation (D_1 , D_2 and D_3) are recognized in the NQT and the QQCZ. The D_1 deformation is characterized by NNE-dipping and SSW-dipping penetrative foliations (S_1). The S_1 foliations are mainly marked by a strong preferred orientation of hornblende crystals, and they were subsequently overprinted by the D_2 deformation. The D_2 deformation is marked by tight asymmetric folds with NNE-dipping and SSW-dipping axial plane foliations (S_2). We propose that the D_1 and D_2 deformations mainly occurred during ~440-400 Ma after the peak ultra-high pressure metamorphic event (~520-480 Ma). And these two deformation events could constrain the collision

and exhumation processes of the NQT, which probably indicates the closure of the Kuanping Ocean located between the NQT and the NCB in the early Paleozoic. These two deformations are overprinted by the D_3 deformation characterized by ENE-trending upright open folds.

Two detrital zircon age spectra for the Kuanping Group with the youngest zircon of ~640 Ma and ~510 Ma, respectively, are different from those recorded for the North China Block, which may reveal the continuous southward subduction of the Kuanping Ocean during the Neoproterozoic to early Paleozoic interval. We propose that the Kuanping Ocean marks the northern boundary of the Proto-Tethys Ocean in the study area.

The similarity of the detrital zircon age spectra of the Huluhe Group in the North Qilian Orogen and the Erlangping Group in the North Qinling Orogen suggests that the two groups have similar provenance, which may indicate that the North Qilian Orogen corresponded to the North Qinling Orogen in a regional tectonic framework. In addition, the remarkable age peak at ~435 Ma of the detrital zircon age spectrum of the Duanjiaxia Formation in the southwestern NCB indicates that this formation obtained the provenance of the North Qilian and North Qinling orogens, which may be generated by the collage of the southwestern NCB and the QQCZ during the Late Ordovician-Early Silurian. Based on structural, detrital zircon and metamorphic data, we suggest that the North Qilian and North Qinling orogens underwent similar evolution during the early Paleozoic due to the close of the North Qilian and the Kuanping oceans which located at the northern boundary of the

Proto-Tethys Ocean.

References

Zhao, S.J., Li, S.Z., Cao, H.H., Li, X.Y., Liu, X., Yu, S.Y., Guo, X.Y. 2020. A missing link of the Proto-Tethys Ocean between

the Qinling and Qilian orogens, China: Insights from geochronology and structural geology. *Geoscience Frontiers* 11, 1495-1509.

Zhao, S.J., Li, S.Z., Li, X.Y., Somerville, I., Cao, H.H., Liu, X., Wang, P.C. 2017. Orogen and its implications for the evolution of the Proto-Tethys Ocean. *Geological Journal* 52, 202-214.

Petrogenesis and geodynamic implications of collisional granitoid from the northern Qinghai-Tibet Plateau

Shihua Zhong^{1,2}, Sanzhong Li^{1,2}, Hongying Qu³, Shuyue He⁴, Guoyan Liu⁴, Zhiqing Lai¹

¹Frontiers Science Center for Deep Ocean Multispheres and Earth System, Key Lab of Submarine Geosciences and Prospecting Techniques, MOE and College of Marine Geosciences, Ocean University of China, Qingdao 266100, China

²Laboratory for Marine Mineral Resources, Qingdao National Laboratory for Marine Science and Technology, Qingdao 266237, China

³MLR Key Laboratory of Metallogeny and Mineral Assessment, Institute of Mineral Resources, Chinese Academy of Geological Sciences, Beijing 100037, China

⁴The Third Institution of Qinghai Geological Mineral Prospecting, Xining 810012, China

*Email: Shihua Zhong (zhongshihua@ouc.edu.cn)

The recent discovery of numerous large porphyry Cu deposits in the southern Qinghai-Tibet Plateau shows that porphyry Cu deposits can be hosted in magmatic suites in collisional settings. To reveal the nature and origin of the collisional magmatic rocks from the northern Qinghai-Tibet Plateau as well as their fertility in terms of Cu mineralization, collision-related intrusions from the Qimantagh Metallogenic Belt (QMB) are examined. Based on previous studies, two volumetrically dominant intrusive suites are identified: 435-370 Ma granitoids (Suite I) and 245-196 Ma granitoids (Suite II). They formed during syn- to post-collisional stages of the Caledonian and Hercynian-Indosinian Orogenies, respectively. In contrast, arc magmatic rocks are relatively scarce. Both Suites I and II are characterized by low zircon Ce/Ce* and Eu/Eu* values, low whole-rock Sr/Y and Eu/Eu* values with arc-like features (e.g., depletion of Nb and Ta). Furthermore, both suites display some evolved Sr-Nd-Hf isotopic values (e.g., $\epsilon_{\text{Nd}} = -8.1$ to 0.1), with the majority of samples characterized by Paleo- to Meso-Proterozoic two-stage Nd and Hf model ages. These features suggest that the parental magmas of the two suites were probably derived from subduction fluid-modified mantle sources which underwent significant crustal AFC processes during magma ascent.

Combined with published studies, we propose a conceptual geodynamic model for the QMB as follows (Zhong et al., 2021).

1. During Early Cambrian, a branch of the Proto-Tethys Ocean had existed in the northern QTP, which was probably

related to the breakup of the supercontinent Rodinia (Li et al., 2018). The North Kunlun Terrane (the main part of the QMB) was as an accretionary wedge along the convergent margin at this time, which is considered as the western extension of the Kuanping Proto-Tethys Ocean to the east (Li et al., 2016). At the same time, the Central Kunlun Terrane was possibly as a part of the northern margin of the Gondwana.

2. During ca. 520-436 Ma, the Qimantagh Proto-Tethys Ocean (also known as the Kuanping Ocean) developed a southward flat-slab subduction system beneath the northern margin of the Gondwana. Because of the relatively shallow angle of subduction, the asthenospheric mantle wedge was of small size. The slab progressively dehydrated during subduction, with the released fluids metasomatizing the base of the Qimantagh crust root and subcontinental lithosphere mantle, which served as the source for subsequent collisional magmas. The majority of, if not all, sediments covering the oceanic crust were accreted into the wedge and were not subducted into the mantle. This gave rise to subduction of a relatively “dry” lithospheric slab, which inhibited significant arc magmatism. No porphyry and skarn deposits formed in this stage, probably due to the low magmatic water content, sulfur content and/or metal content of those arc magmas.

3. During ca. 435 Ma, the Qimantagh Proto-Tethys Ocean closed, and the Tarim-Qaidam-Alxa Block (?) was probably welded to the North Kunlun Terrane along the

North Kunlun Suture (Li et al., 2016; 2018). The Central Kunlun Terrane and the North Kunlun Terrane were also linked together along the Nalingguole River Fault. The North Kunlun Terrane and the northern part of the Central Kunlun Terrane collectively constitute the current architecture of the QMB. After a short syn-collisional period, the QMB evolved into the post-collisional extension stage since ca. 432 Ma which might have lasted to 370 Ma. The increased tensile stress within the subducted slab finally triggered slab breakoff.

4. The slab breakoff resulted in the upwelling of the asthenosphere mantle, which in turn induced partial melting at shallow depths within the mechanical boundary layer of overlying lithosphere. This gave rise to strong magmatism which formed the Suite I and some mafic rocks. The Suite I was derived from hybrid sources comprising mantle and crustal components. The mantle components were derived from either the asthenospheric mantle that upwelled through an opening slab window, or the Qimantagh subcontinental lithospheric mantle, or both. The crustal components probably came from slab dehydration-derived fluids, plus variable degrees of AFC processes within the overlying lithosphere. The relatively low magmatic oxidation state and especially the low magmatic water content inhibited formation of large porphyry Cu systems.

5. After ca. 370 Ma, the North Kunlun Terrane, accompanying the Central Kunlun Terrane, was torn away from the northern Gondwana margin. Between the Central Kunlun Terrane and the newly born northern margin of the Gondwana the South Kunlun Ocean (as the western extension of Shangdan Ocean) formed, which had the Paleo-Tethys Ocean affinity. The QMB was probably in a within-plate environment at this period, marking the beginning of the Hercynian-Indosinian Orogenic Cycle.

6. The South Kunlun Ocean might have begun to subduct northward before 306 Ma. Despite the different subduction polarity from the Caledonian Orogeny, this Hercynian-Indosinian Orogeny in the QMB was also characterized by a low-angle oceanic slab subduction, which hindered extensive arc magmatism. Only minor arc magmatic rocks formed in the Central Kunlun Terrane and the southern North Kunlun Terrane.

7. From ca. 245 Ma, the QMB, following the closure of the South Kunlun Ocean and the Mianlue Ocean (also called the Anyuqin Ocean here), entered into another collisional stage.

Similar to the collisional stage in the Caledonian Orogeny, slab breakoff triggered asthenosphere upwelling during collision, which generated voluminous collisional magmatic rocks (including the Suite II granitoids) in the QMB. The post-collisional extension might have lasted to 370 Ma. The Suite II magmas were also derived from an evolved mantle source (which had been contaminated by pre-collisional slab-derived fluids) and experienced different degrees of crustal AFC processes during ascending. Only a couple of small porphyry Cu-Mo and some skarn deposits are discovered, and no large porphyry Cu deposits occur, which mainly resulted from low magmatic water content.

Compared to previously proposed models, this model pays particular attention to the relative scarcity of arc mechanism in the QMB and the contrasting fertility of collision-related granitoids compared to the GMB. It emphasizes that the Caledonian and Hercynian-Indosinian orogenies in the QMB share similar features, which can be consistently explained by a pre-collisional flat subduction process (despite of the opposite subduction polarities) and slab breakoff-deduced collisional magmatism. The magmatic Suites I and II did not have the potential to form large porphyry Cu systems during their evolution mainly due to low magmatic oxidation state and water content.

References:

- Li, S.Z., Yang, Z., Zhao, S.J., Li, X.Y., Suo, Y.H., Guo, L.L., Yu, S., Dai, L.M., Li, S.J., Mu, D.L., 2016. Global early paleozoic orogens (II), subduction-accretionary-type orogeny. *Journal of Jilin University (Earth Science Edition)*, 46 (4): 968–1004 (in Chinese with English abstract).
- Li, S.Z., Zhao, S.J., Liu, X., Cao, H.H., Yu, S.Y., Li, X.Y., Somerville, I., Yu, S. and Suo, Y.H., 2018. Closure of the Proto-Tethys Ocean and Early Paleozoic amalgamation of microcontinental blocks in East Asia. *Earth-Science Reviews*, 186: 37-75.
- Zhong, S., Li, S., Feng, C., Liu, Y., Santosh, M., He, S., Qu, H., Liu, G., Seltmann, R., Lai, Z., Wang, X., Song, Y. and Zhou, J., 2021. Porphyry copper and skarn fertility of the northern Qinghai-Tibet Plateau collisional granitoids. *Earth-Science Reviews*, 214: 103524.

Does U-Pb signatures of river sediment represent the age distributions in the catchments? A study of variegated catchments along the eastern border of the Songliao Basin, NE China

Jianping Zhou^{1, 2, 3*}, István Dunkl¹, Yongjiang Liu^{2, 3}, Sanzhong Li^{2, 3}, Weimin Li⁴, Hilmar von Eynatten¹

¹ University of Göttingen, Geoscience Center, Department of Sedimentology and Environmental Geology, Goldschmidtstrasse 3, Göttingen, D-37077, Germany

² Frontiers Science Center for Deep Ocean Multispheres and Earth System, Key Lab of Submarine Geoscience and Prospecting Techniques, College of Marine Geosciences, Ocean University of China, Qingdao 266100, China.

³ Laboratory for Marine Mineral Resources, Qingdao National Laboratory for Marine Science and Technology, Qingdao, 266237, China.

⁴ College of Earth Sciences, Jilin University, Jianshe Str. 2199, Changchun 130061, Jilin, China

*Email: jzhou1@uni-goettingen.de (J.P. Zhou)

We studied five modern river catchments of variable size (~500 to ~40,000 km²), dominated by Carboniferous to Jurassic granitoids, Proterozoic to Early Paleozoic siliciclastic (meta-)sediments and Jurassic to Cenozoic volcanic rocks in northeastern China. The Songliao Basin, its eastern "satellite" basins and the associated sediment-supplying basement highs form an excellent natural laboratory for detrital zircon U-Pb studies as the currently exhumed basement areas are composed mostly of zircon-bearing igneous formations having highly variable emplacement ages. This contrast in the sources generates highly informative detrital age patterns. Our results show strong contrasts between the proportions of the zircon U-Pb age components in the river sands and the areal proportions of the potential source units in the catchments. The limited range of zirconium content of the granitoids does not support high variations in zircon fertility between the magmatic suites having different emplacement ages. The detected mismatch between the obtained and the expected ages can be best explained by re-considering emplacement ages of some igneous suites of the region. We suggest that most of the granitoids mapped as Permo-Carboniferous are actually belonging to the

Jurassic igneous suites. Some metasedimentary units with assumed Proterozoic protolith age have probably much younger, Paleozoic sedimentation age. Despite the proportional contrast between detrital age components and spatial coverage, the mean ages of the age components in the modern sand samples and the age components of the published basement U-Pb data show excellent agreement. The zircon U-Pb age distributions from modern sands thus provide useful hints to detect, verify or re-classify the ages of the zircon-bearing units in the catchment. This approach can be especially helpful at a reconnaissance prospecting on areas that are covered by imprecise large-scale geological maps only.

The detrital age distributions in modern sediments also serve diagnostic information for the provenance analysis of ancient sedimentary formations in the same areas, better than the simple map-based evaluation of the areal proportions of basement units. In our case, combining the zircon U-Pb age patterns of the studied modern catchments and the region-wide compilation of the basement ages allows for refining the Cretaceous provenance history of the Songliao Basin and its strongly inverted eastern satellite basins.

The strike-slip structural model and dynamics concerning middle section of Pearl River Mouth Basin in north margin of South China Sea

Jie Zhou^{1, 2*}, Sanzhong Li^{1, 2}, Yanhui Suo^{1, 2}

State Key Laboratory of Lithospheric Evolution, Institute of Geology and Geophysics, Chinese Academy of Sciences, Beijing 100029, China

¹ Frontiers Science Center for Deep Ocean Multispheres and Earth System, Key Lab of Submarine Geosciences and Prospecting Techniques, MOE and College of Marine Geosciences, Ocean University of China, Qingdao 266100, China

² Laboratory for Marine Mineral Resources, Qingdao National Laboratory for Marine Science and Technology, Qingdao 266237, China

E-mail: zj888@ouc.edu.cn

The tectonic position of Pearl River Mouth Basin (PRMB) is very special, and it is generally believed that the present complex tectonic features are formed under the joint action of the collision system of Indo-Australia Plate and Eurasian plate and the subduction system of Pacific Plate (Philippine Sea Plate). The northern margin basement of the South China Sea is the basement of the South China Block, which has experienced multi-stage tectonic events. The type, tectonic stage and dynamic mechanism of the PRMB have always been controversial. Based on the structural style changes according to seismic data interpretation and taking Xijiang, Baiyun and Liwan sags as examples, we conclude that the sub-basins of the PRMB are transtensional basins, which have features of both classic rift and pull-apart basins. The PRMB can be divided into five structural layers from bottom to top: Indosinian ramp-flat thrust, Yanshanian high-angle thrust, early Cenozoic graben rift, mid-Cenozoic half-graben rift, and late Cenozoic depression. During the Indosinian period, the paleotethyan Ocean closed,

and four strongly deformed thrust nappe belts with NEE strike consistent with Qiongnan Suture were formed in the Pearl River Mouth Basin. In the middle-late Yanshanian period, the paleo-Pacific Plate subducted NW forward, and forming NE trending high angle thrust faults, broad folds and large basement lenses. In the early Cenozoic (~ 55-45 Ma), the Izanagi-Pacific mid-ocean ridge subducted beneath the East Asian continental margin, and the study area entered the NNW-SSE diffusion extension stage, forming the NEE-trending wide rift. In the middle Cenozoic (45-25Ma), the paleo-Pacific Plate subducted from NNW to NWW under the East Asian continental margin, and the Mesozoic structure was activated, showing NE-NNE-trending dextral strike-slip. In the late Cenozoic (since 25 Ma), the Philippines Sea Plate NWW wedged in, and the South China Sea began to subduct under it. Combined with the extrusion of the Indosinian Block, the regional stress field was dominated by the NNE-SSW extension, and the NW-trending sinistral strike-slip structures developed.

Characteristics and Environmental Significance of Late Carboniferous Brachiopods within the Qijiagou Area, Southern Margin of the Junggar Basin

Xiaohu Zhou¹, Jiyuan You²

¹ State Key Laboratory of continental dynamics, Northwest University, Department of geology, Xi'an 710069, China

² College of energy engineering, Yulin University, Yulin, 719000, China

1. Introduction

Brachiopods are common fossils in Carboniferous strata and are marine benthic invertebrates. Their living environments include significant characteristics and are relatively sensitive to environmental conditions such as water depth, temperature, salinity, seabed topography, and hydrodynamic changes, exhibiting strong geographic differentiation. Brachiopods live in groups and as solitary individuals, and are of great significance in determining geological ages and sedimentary environments as well as in palaeobiogeographic analysis.

On the basis of the 1:50,000 regional geological survey of Xinjiang in 2019, our research team studied the Late Carboniferous stratigraphic section in the Qijiagou area at the southern margin of the Junggar Basin. This section mainly comprises bioclastic, sandy and calcareous limestone. The Upper Carboniferous–Lower Permian strata in the Qijiagou area are well developed, with continuous exposure and a complete sedimentary sequence. The brachiopod fossils in these strata are abundant and relatively well preserved. It is therefore easy to identify taxa and perform regional comparisons; thus, this area is ideal for biostratigraphic work. This article analyses the Late Carboniferous sedimentary environment of the area through the Upper Carboniferous lithological assemblage and the brachiopod fossils in the Qijiagou section of this area. This research is of great significance for regional comparative analysis of the Carboniferous strata at the southern margin of the Junggar Basin, and for division of the Carboniferous and Permian strata.

2 Characteristics and Environmental Significance

2.1 Burial characteristics

On the basis of brachiopod fossil data for the study area, combined with the other types of fossils present, the characteristics of the surrounding rocks, and the distribution of fossils, it is believed that the palaeobiological assemblage is a benthic community dominated by brachiopods. This community is mainly distributed in the Qijiagou Sa area on the southern margin of the Junggar Basin. The representative section is the Qijiagou section of the Upper Carboniferous. The fossils are present in bioclastic limestone and mudstone. The degree of preservation is good, the shell ornamentation is clear, and there are no obvious signs of later destruction. In addition to complete fossils, some separated shell valves were roughly matched with dorsal and abdominal shells, which were poorly sorted and likely buried in different places.

Brachiopod fossils collected in the research area were buried in different places. The reasons for this inference are as follows. (1) Many fossils were obviously damaged. However, damage alone is not enough to indicate that they were transported, because the impact of water flow can also cause fossil damage. (2) The fossils are severely worn. Under normal circumstances, water flow can only cause the fragmentation of fossils, but cannot cause wear on fossils, because wear requires friction with the substrate or carried objects, and thus implies a certain distance of transport. However, it is also necessary to eliminate the influence of weathering, because weathering may also cause the appearance of surface wear. Most of the fossils collected from the study area are preserved in fresh rocks; thus, the interference of weathering can be eliminated. (3) The distribution of fossils is relatively scattered, with different orientations, and the preservation direction presents an obvious

angle of intersection with the plane. The micrographs indicate that the fossils have different orientations. If it is preserved in situ, the shell should have the same orientation. The combination of these three points indicates that the brachiopod fossils in the study area were transported for some distance.

2.2 Biopalaeogeographic attribution

Historical studies on the biopalaeogeography of brachiopods known from the Late Palaeozoic of the Junggar block always started from the Permian, and the content of earlier periods was not involved. What kind of biopalaeogeography should be included for the current brachiopods of the Junggar block? Based on the extensive comparative analysis of brachiopods from the same period, the author believes that this geographic area belongs to the northern edge of the Chinese part of the Tethys Bioregion, named the Tianshan–Liaoji Brachiopod Biogeographic Division. From the end of the Early Carboniferous to the Late Carboniferous, the Bashkirian brachiopod division basically inherited the early characteristics. Between Siberia and the Tarim platform is a vast and large-scale geotrough sea area. Roughly taking the Tianshan–Yinshan–Changbai Mountains as the boundary, China is divided into the southern brachiopod biogeographic area and the northern brachiopod biogeographic area.

The similar brachiopod fauna represented by *Gigantoproductus* in the Datang Period shows connection of the waters of western China. At that time, the Tarim platform and the North China platform were roughly at the same latitude, forming the main barrier blocking the connection between the northern and southern brachiopod areas in China. However, there are brachiopods similar to those of the Tianshan Mountains in Xinjiang in the Beishan Mountains, the southern foot of the Qilian Mountains, the Qilian Trough, and the Kunlun Mountains in the west. These areas may represent the passage of the north–south bioregions; that is, they may have connected through the Qilian Trough, the West Kunlun area, and the northern margin of Qaidam. From the end of the Early Carboniferous to the Bashkirian Stage, the distribution of brachiopods in China was inherited, and local passages emerged. The western Kunlun Mountains and the northern Qilian Trough are mainly characterised by a set of light green quartz conglomerates, coarse sandstones (medium-grained sandstones), and sandstones. The geographical ties of the northern and southern brachiopod regions were blocked. It has been speculated that a narrow sea area formed along the Tianshan Mountains, Yinshan Mountains, and the northern margin of North China during this period; that is, north of the Tianshan

Mountains and south of the Junggar–Xing'an region.

2.3 Depositional environments of brachiopod fossils

Outcrops and petrological investigations show that the Qijiagou Formation formed in a variety of intermediate continental shelf environments, mainly from lagoons to deltas. Based on microfacies data, the sediments of the Qijiagou Formation are divided into three different facies belts, including lagoons, end intermediate facies, and distal intermediate facies. However, in general, the facies attributes show a sedimentary environment dominated by deltas. The lowest parts of some rock units, mainly mudstone microfacies, were deposited in lagoon environments. Lagoon-like sedimentary deposits were gradually replaced by siliciclastic and bioclastic microfacies in the upper part of the distal middle shelf. This sedimentary zone has been identified in all research sections. However, in each part, the distribution and thickness changes of siliciclastics, bioclastics, and calcium rock microfacies are recorded. In addition, the carbonate content, including skeletal and non-skeletal components, dominates in the lower part, whereas the upper part is mainly characterised by source flux. In the middle part of the proximal end, bioclastic microfacies were deposited.

3. Conclusion

(1) The outcrop observations presented here show that unit thicknesses in different areas of the Upper Carboniferous Qijiagou Formation at the southern margin of the Junggar Basin vary laterally, consisting of thick layers of fossil-bearing, channelised, sandy and calcareous limestones. The lower section of the profile comprises relatively coarse carbonate rock, while the upper section is clastic rock with finer carbonate rock. The Qijiagou area is dominated by bioclastic limestone, with sandy mudstone and tuffaceous mudstone locally.

(2) The detailed petrology of rock units revealed four microfacies, showing an intermediate continental shelf setting dominated by different lagoons in the delta. The microfacies evolved upward from carbonate to sandy carbonate. We identified 15 species of brachiopod fossils in 11 genera, which belong to the orders Spiriferida Waagen, Productida Sarycheva et Sokolskaya, and Strophomenida Öpik. Thus.

(3) In the Late Carboniferous, the Qijiagou area on the southern margin of the Junggar Basin existed in a relatively warm carbonate platform sedimentary environment with turbulent and shallow water bodies, and two regressions occurred.

Global large-magnitude oceanic intraplate seismicity: Implications for lithosphere evolution

Junjiang Zhu ^{1,2}, Sanzhong Li ^{1,2}, Huilin Xing ^{1,2}, Zhongjia Jia ^{1,2}, Xiaolin Ou ^{1,2},
Shaoyu Zhang ^{1,2}, Ruixue Chen^{1,2}, Xianzhi Cao ^{1,2}

¹ Frontiers Science Center for Deep Ocean Multispheres and Earth System, Key Lab of Submarine Geosciences and Prospecting Techniques, MOE and College of Marine Geosciences, Ocean University of China, Qingdao 266100, China

² Laboratory for Marine Mineral Resources, Qingdao National Laboratory for Marine Science and Technology, Qingdao 266100, China

In this paper, we consider 37 large oceanic intraplate earthquakes ($M \geq 6$). The larger ($M \geq 7$) events are mainly concentrated under the Indian Ocean. Moderate events ($6 \leq M < 7$) are sparsely distributed under the Indian Ocean and other oceans where lithospheric ages are between 20 m.y. and 90 m.y. old. Oceanic intraplate events related to mantle plumes or hot spot are rare though low-velocity anomalies beneath hot spots are common feature. Tomographic cross-sections for Indian Ocean areas with large intraplate earthquakes indicate strong

heterogeneity in the mantle. Large oceanic intraplate earthquakes beneath the Indian Ocean are explained by shallow stress variations caused by a combination of tectonic forces including slab-pull, ridge-push, drag by mantle flow, plume-push and buoyant forces as a consequence of low-velocity anomalies in the mantle. Oceanic intraplate seismicity in the Indian Ocean is related to large-scale, low-velocity anomaly structure around the Ninety East Ridge.

Study on the characteristics of horizontal zoning of fluorite orebody: A case of Wushan fluorite deposit in Zhejiang

Hao Zou^{1,2*}, Min Li¹, Liming Yu¹, Bin Xiao¹, Huidong Yu¹

School of Earth and Space Science, Peking University, Beijing 100871, China

¹ State Key Laboratory of Oil and Gas Reservoir Geology and Exploitation, Chengdu University of Technology, 610059, China

² Key Laboratory of Tectonic Controls on Mineralization and Hydrocarbon Accumulation of Ministry of Land and Resources, Chengdu University of Technology, Chengdu, Sichuan 610059, China

E-mail: zouhao21@gmail.com

Most hydrothermal fluorite deposits are filled by deposition of ore-bearing fracture control and are affected by structure-formation-time-space factors during the mineralization process of crystallization. Hydrothermal crystallization is a complex physicochemical process (Ehya, 2012). However, fluorite orebody horizontal zoning characteristics and variation regularity are important for study of hydrothermal crystallization. The ore bodies of Wushan fluorite deposit are strictly controlled by NW trending faults in the South China, which vary in size (Yu, 1987). Fluorite veins have obvious lateral zoning characteristics (Fig. 1): from the edge to the middle, there are veinlets-stockwork-mineralized zone lumpy brecciated ore belt, banded ore belt, pure banded ore and lump ore belt (Zhang et al., 1997).

This study revealed the lateral zonation characteristics of the fluorite ore and the crystallization sequence variation regularity through vein shape, ore texture and structure, mineral assemblage, homogenization temperature, density, salinity of fluid inclusions and fluid composition of the Wushan deposit.

In combining with previous research and the results of this research, we draw the following conclusions:

1. The ore body of the Wushan fluorite deposit is characterized by significant lateral variation. The lateral zonation of the ore fabric exhibits a certain regularity from the edge to the middle, which can be divided into fine vein-stockwork-mineralized zone lumpy brecciated ore belt, positive banded ore belt, pure strip banded ore belt and lump ore belt.

2. Ore-forming fluids of the Wushan fluorite deposit have low temperature, low salinity and low density. The temperature and salinity of the ore-forming fluid are relatively high and the density is relatively low at the edge of the ore body. However, the temperature and salinity of the ore-forming fluid are

relatively low and the density is relatively high in the middle of the ore body. In the middle of the ore body, H₂ is presents in the fluid inclusions, which indicates reducing conditions of the central fluid environment, while the environment of edge forming fluids is mainly oxidizing.

3. In the northwestern part of the study area, homogenization temperature and salinity of the samples are relatively high, while homogenization temperature and salinity of the samples of the southeastern part are relatively low. Intermediate homogenization temperature and salinity values were observed between the two parts, which is related to the side-volt direction of the ore body and has been confirmed by the geological survey and exploration drilling.

Keyword: Wushan fluorite deposit; ore body; horizontal zoning; fluid inclusion

References

Ehya, F., 2012. Variation of mineralizing fluids and fractionation of REE during the emplacement of the vein-type fluorite deposit at Bozijan, Markazi Province, Iran. *Journal of Geochemical Exploration* (112) 93–106.

Yu, G.H., 1986. *Rock Formation in Zhejiang Province*. Beijing: China University of Geosciences press 24-68. (in Chinese)

Zhang, S.T., Li, Z.Q., Xu Z.Z., 1997. The Vertical zonality of Fluorite ore body in the middle part of the Wu Yi basin, Zhejiang Province. *Journal of southwest industry (Chengdu University of Technology)*, 12(4):52–58. (in Chinese with English abstract)

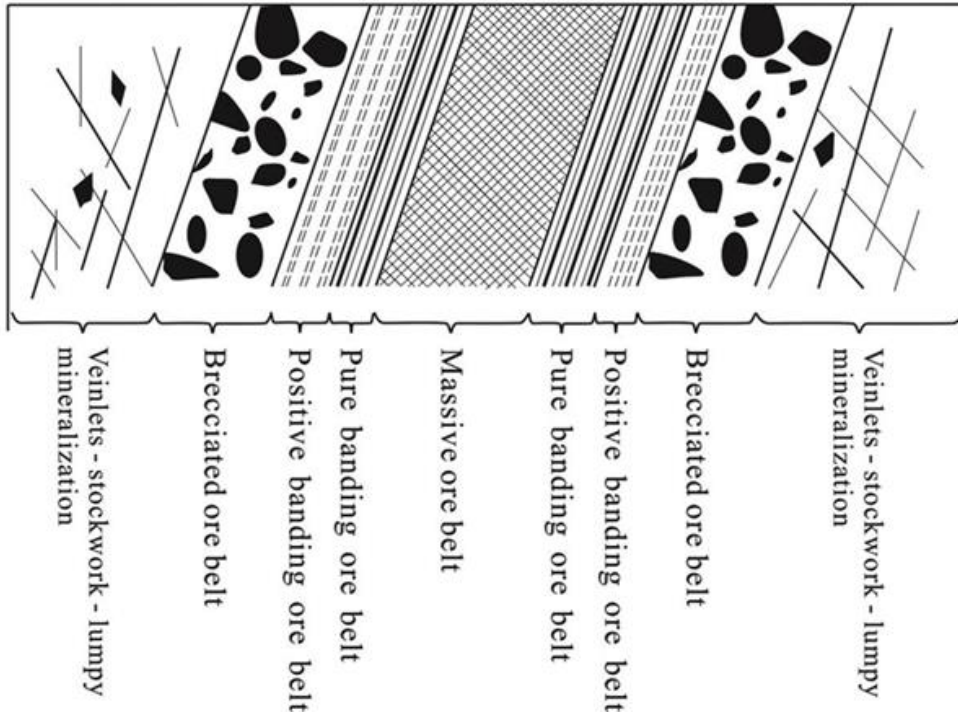


Fig. 1. Sketch of the ideal mode of the ore mineral central structure with horizontal zoning in fluorite ore-bodies